Localization and Possible Function of Glutamate, AMPA and Kainate Receptor Subunits in the Developing Mouse Optic Pathway

CHENG, Xiaojing

A Thesis Submitted in Partial Fulfillment

of the Requirements for the Degree of

Doctor of Philosophy

in

Anatomy

The Chinese University of Hong Kong

November 2010

Thesis/Assessment Committee

Professor CHAN Wood Yee (Chair)

Professor CHAN Sun On (Thesis Supervisor)

Professor CHO Yu Pang. Eric (Committee Member)

Professor YUNG Kin Lam. Ken (External Examiner)

Abstract of thesis entitled:

Localization and possible function of glutamate, AMPA and kainate receptor subunits in the developing mouse optic pathway

Submitted by Cheng, Xiaojing

for the degree of Doctor of Philosophy

at The Chinese University of Hong Kong in October 2010

Abstract

Glutamate is the dominant amino acid neurotransmitter in the central nervous system naturally occurring in the L-form. Glutamate ionotropic receptors can be further divided into three types by their ligand specificities: α-amino-3-hydroxy-5-methyl-4-isoxazole-propionate (AMPA, GluR1-4), N-methyl-D-aspartate (NMDA, NR1-3) and kainate (KA, GluR5-7 and KA1-2) receptors, which function as ligand-gated ion channels. In this study, we focus on the AMPARs and KARs which are expressed in the developing brain.

Here, we used semi-quantitative RT-PCR to analyze mRNA expression levels of AMPAR and KAR subunits in the mouse retina and ventral diencephalons at different developmental stages, and in adult retina. The results show that both AMPAR and KAR subunits can be detected in retina and ventral diencephalon at as early as E13. We also used specific antibodies to investigate glutamate, AMPAR and KAR subunit expression in the mouse retinofugal pathway. We found that: 1) Glutamate is expressed at as early as E13. In retina, it tends to localize in retinal ganglion cells (RGCs) and their axons; in ventral diencephalon, it is most intense in optic stalk, optic chiasm and optic tract. It is also localized with chiasmatic neurons, which are related to the formation of optic chiasm. 2) For the individual AMPAR and KAR subunits, all of them are expressed at as early as E13. The immunoreactive

GluR1 and GluR5/6/7 are distributed preferentially in the RGCs and their axons; the staining of GluR2/3 and GluR4 are largely found in RGCs and the supporting cells around the pathway, but for GluR4, its staining is weakly detected in optic fibers and strongly in the midline of chiasm. Although the staining patterns of these specific subunits are different, they are all localized in chiasmatic neurons in diencephalon.

Furthermore, for the function of glutamate, AMPARs and KARs in the optic chiasm formation, we did retinal explant culture experiment at E14 in vitro, with application of different concentration of L-glutamate (500μM -1mM), AMPAR antagonists: CP465022 hydrochloride (2-20μM) and GYKI5466 dihydrochloride (25-150μM), and KAR antagonists: CNQX (50-500μM) and UBP301 (5-25μM). The results show that L-glutamate promotes retinal axon outgrowth; AMPA receptor antagonists inhibit that; and KAR antagonists have no effect on that. In the presence of different combinations of ionotropic receptor antagonists (including NMDAR antagonist), they suggest that the blockage of glutamate iontroptic receptors displays an obvious effect of inhibiting neurite outgrowth in E14 retinal explants. However, inhibiting kainate receptors show little effect on retinal neurite outgrowth which is different from that of blocking AMPARs. We also did E13 and E15 brain slice culture experiments, and found that blocking of glutamate ionotropic receptors affects crossed axon projection in the midline at early stage, but has no effect to the uncrossed one.

For glutamate and the developing optic pathway, glutamate and its ionotropic receptor subunits are expressed widely in retina and ventral diencephalon, and in cells that are related to the chiasm formation. These studies indicate that glutamate may act as a communicator or attractor to coordinate with other factors to affect the retinal axon pathfinding in the prenatal optic pathway.

論文摘要

谷氨酸是神經系統主要的神經遞質，在自然界以左旋的形式存在。按不同啟動劑，其離子型受體可以進一步分為： α -氨基- 3 -羥基- 5 -甲基- 4 -異惡唑丙酸受體受體（AMPA 受體; 包含四個亞基，GluR1-4）， N -甲基 D -天冬氨酸受體受體（NMDA 受體; 包含七個亞基, NR1-3）和紅藻氨酸鹽受體 (kainate 受體; 包含五個亞基, GluR5-7 和 KA1-2), 其功能為配體門控型離子通道。在這項研究中，我們將研究 AMPA 和 kainate 受體，它們均在大腦發育中明顯表達。

在這裡，我們利用半定量 RT - PCR 技術分析在小鼠胚胎不同階段視網膜和腹側間腦，成鼠視網膜的 AMPA 和 kainate 受體亞基基因表達水準，其結果顯示 AMPA 和 kainate 受體亞基可表達於 E13 天小鼠視網膜和腹側間腦。我們同時利用免疫組織化學法，研究谷氨酸和 AMPA 以及 kainate 受體在小鼠視神經通路中的表達。我們發現：1）谷氨酸在 E13 天小鼠表達。在視網膜中，它表達於視網膜神經層和神經節細胞層; 在腹側間腦，它表達於整個間腦，但集中於視柄，視交叉和視束。它同時表達于視交叉形成相關神經元。 2）對於 AMPA 和 kainate 受體亞基，其均表達於 E13 天小鼠。GluR1 和 GluR5/6/7 明顯表達於視網膜神經節細胞和視神經纖維; GluR2 / 3 和 GluR4 主要分佈於視網膜神經節細胞和視神經通路周圍的支持細胞，但是 GluR4 較弱表達於視神經，典型分佈於視交叉中部。儘管這些亞基在視神經通路中分佈不同，他們都表達於腹側間腦的視交叉形成相關神經元。

此外，為研究谷氨酸和 AMPA 以及 kainate 受體在視交叉形成期的作用，我們在體外培養 E14 天的視網膜塊，同時加入不同濃度的谷氨酸，AMPA 受體拮抗劑和 kainate 受體拮抗劑，其結果顯示谷氨酸可以促進視網膜軸突生長; AMPA

受體拮抗劑抑制軸突生長; kainate 受體拮抗劑幾乎不影響軸突生長，但是有一個趨勢即低濃度的 kainate 受體拮抗劑促進視網膜軸突增長，儘管該結果沒有統計學意義。我們同時加入不同組合的離子型受體拮抗劑，它表明同時阻斷 AMPA 和/或 NMDA 和 kainate 受體，可以明顯抑制視神經軸突生長；但是單獨阻斷 kainate 受體卻和阻斷 AMPA 受體不同，幾乎不影響軸突生長。我們同時做了 E13 和 E15 腦切片體外培養實驗，它們表明，谷氨酸離子型受體影響早期的交叉視神經投射，它們不影響非交叉視神經投射。

對於谷氨酸和發育期視神經通路，離子型谷氨酸以及其受體亞基廣泛地分佈於視網膜和腹側間腦，它們都表達于視交叉形成相關神經元；同時它們在視神經軸突生長上也發揮重要作用，這些研究表明，谷氨酸可以作為一種通訊者或吸引者同其它視神經發育影響因數一起，影響胚胎期視網膜軸突在視神經通路中的生長。

Acknowledgements

I would like to thank all people who work together with me in our daily life during these three years. Firstly, I want to show my gratitude to my respectful supervisor, Professor Sun-on Chan, by helping me out of difficulty. In his lectures, they give me a deep impression for his kindness; and I earnestly appreciate his knowledgeable in the neuroscience field. Under his guidance and help in the experiment, I could continue to explore my study when encountering confusion. I also earnestly thank to Professor Chan for his serious revision of my thesis and articles, and for the better English writing.

Secondly, I would like to show my grateful feeling to Professor Woody Chan, Professor Eric Cho, and Professor Zhao Hui, who are patient for instruction and suggestion in the experiment and the lab meeting. I also appreciate Peggy Leung and Anny Cheung for their helps and support in the daily lab experiment. I am deep thankful for the discussion in the project and help in the lab life from my lab mates: Wang Liqing, Li Jia, Jason Chan, Wong Yik Sung and Chen Tingting; and from other lab: Wong Wai Kai, Wang Xia, Bao Lihua, Zhou Rui, Richard and so on. Especially, I greatly appreciate the technical assistance in my study from Corinna Au, Jenny Hou, Jean Kung, Simon Tong, Samuel Wong; and I am thankful for Ching Pik Mei for her help in the experiment preparation.

Finally, I want to express my cordial appreciation for my family who supports and encourages me all along; and my remote friends who give me the nice recollection and kind help; all these accompany my growth.

Table of Abbreviations

AF488	Alexa Fluor 488
AGB	1-amino-4-guanidobutane
AMPA	α-amino-3-hydroxy-5-methyl-4-isoxazole-propionic acid
AMPAR	α-amino-3-hydroxy-5-methyl-4-isoxazole-propionic acid receptor
CMZ	Ciliary margin zone
CNQX	6-cyano-7-nitroquinoxaline-2, 3-Dione
CNS	Central nervous system
CREB	cAMP response element binding protein
Cy3	Cyanine 3
DEPC	Diethyl Pyrocarbonate
DiI	1, 1'-Dioctadecyl-3, 3, 3', 3'-tetramethylindo-carbocyanine perchlorate
DMSO	Dimethyl sulfoxide
DN	Dorsal nasal
E	Embryonic day
ECM	Extracellular matrix
FITC	Fluorescein isothiocyanate
GABA	γ-Aminobutyric acid
GCL	Ganglion cell layer
GFAP	Glial fibrillary acidic protein
GLAST	GLutamate ASpartate Transporter
GLT	Glutamate Transporter
GluR	Glutamate receptor
INL	Inner nuclear layer
IPL	Inner plexiform layer
IZ	Intermediate zone
NFL	Nerve fiber layer
NGFI-A	Nerve growth factor inducible factor A

NMDA	N-methyl-D-aspartate
NMDAR/NR	N-methyl-D-aspartate receptor
OC	Optic chiasm
OD	Optic disk
ONL	Outer nuclear layer
OPL	Outer plexiform layer
OS	Optic stalk
OT	Optic tract
PB	Phosphate buffer
PBS	Phosphate buffered saline
PVDF	Polyvinylidene fluoride
RGC	Retinal ganglion cell
RT-PCR	Reverse transcription-polymerase chain reaction
SSEA-1	Stage specific embryonic antigen 1
TARP	Transmembrane AMPAR regulatory proteins
TBS	Tris buffered saline
VT	Ventral temporal

Table of Contents

CHAPTER 1

General introduction

The role of glutamate and its ionotropic receptors in the developing retina and central nervous system

In the retina and central nervous system (CNS), glutamate is one of the excitatory neurotransmitters. It might guide axonal growth cones along their paths in the brain and mediate the long-range communication of cellular interactions (Behar et al., 1999; Komuro and Rakic, 1993; Zheng et al., 1994). It has been reported that glutamate and acetylcholine act as chemoattractants for growth cones from *Xenopus laevis* motoneurons (Zheng et al., 1994; Zheng et al., 1996). Activation of AMPARs/kainate receptors affects axonal filopodial motility in hippocampal neuronal culture and slices (Chang and De Camilli, 2001; Schenk et al., 2003; Tashiro et al., 2003). Activation of kainate receptors induces a fast and reversible growth cone stalling in hippocampal neurons (Ibarretxe et al., 2007). Glutamate can also be released by the growth cones of the developing hippocampus neurons, cortical cells, and tangential fibers (Herrmann, 1996; Soeda et al., 1997). Through

study of glutamate transporters GLAST and GLT1 double knockout mice, it indicates that glutamate is involved in several essential aspects of neuronal development, such as cell proliferation, radial migration, neuronal differentiation, and survival of subplate neurons. Extracellular glutamate environment is an important regulator in the maintenance of neuronal signal connections, modulation of cell proliferation and neuronal differentiation (Behar et al., 1999; LoTurco et al., 1995; Matsugami et al., 2006).

Although glutamate as a neurotransmitter is crucial to the developing CNS, others such as GABA, acetylcholine (Ach), and glycine can also depolarize embryonic cortical neurons (Ben-Ari, 2002; Gao and van den Pol, 2000). It may be useful to study effects of activation of individual neurotransmitter receptors when we want to analyze the direct functional role of these early appearing transmitters during development.

1. Basic structure and function of glutamate and its ionotropic receptors

Glutamate is one of the dominant excitatory neurotransmitters in the retina and other parts of the brain. Glutamate receptors are divided into metabotropic and ionotropic ones. The metabotropic receptors have eight subunits. The ionotropic receptors can be further divided into three kinds of receptors by their excitatory ligands: AMPA (α-amino-3-hydroxyl-5-methyl-4-isoxazole-propionate), NMDA (N-methyl-D-aspartic acid) and kainate receptors (Collingridge and Lester, 1989; Hollmann and Heinemann, 1994; Watkins and Evans, 1981).

AMPA receptors are encoded by four genes (*GluR1–4*), which play the critical role in rapid excitatory synaptic transmission (Geiger et al., 1995; Jonas and Spruston, 1994). Kainate receptors are encoded by three genes for 'low-affinity' subunits (*GluR5–7*) and two for 'high-affinity' subunits (*KA1* and *KA2*), which

participate in major modulation at both presynaptic and postsynaptic sites (Lerma, 2003), NMDA receptors are encoded by seven genes (*NR1*, *NR2A–D*, *NR3A* and *NR3B*), which act together to modulate synaptic plasticity and memory (Cull-Candy et al., 2001; Hollmann and Heinemann, 1994). In all, the family of the glutamate receptors has a large number of members, and these members were transcribed by a large number of genes, which are modified by alternative splicing and RNA editing, making it difficult to analyze their functions (Mayer, 2006).

Electrical activity exists in the developing neurons much earlier than the synaptic networks is fully established, it may regulate establishment of neural circuits (Zhang and Poo, 2001). As electrical activity is intermittent in the developing brain, and neurotransmitters are expected to act on a short timescale before they are eliminated; it may induce neurotransmitters to play a key role in the developing neural circuit formation (Ibarretxe et al., 2007; Zheng et al., 1996). Previous reports show that the axonal filopodial motility of hippocampal neurons in culture can be activated by stimulating AMPA/kainate receptors (Chang and De Camilli, 2001). Moreover, glutamate and GABA are released in the developing hippocampus and are detected in neurons before they bear synapses (Demarque et al., 2002). And transient activation of kainate receptors can induce a fast and reversible growth cone stalling (Ibarretxe et al., 2007). Therefore, glutamate may also regulate long-range interactions of cellular interactions by autocrine ways which transmit important signals to shape the early developing brain (Komuro and Rakic, 1993; Zheng et al., 1994).

Destroying glutamate homeostasis through GLAST/GLT1 double knockout mice shows that several aspects of neuronal development were impaired, such as: cell proliferation, radial migration and neuronal differentiation. GLAST and GLT1 are

glutamate transporters expressed in the embryonic mouse CNS. Other evidences show that NMDA receptors can regulate some early transiently expressed genes, which are over-expressed in regions of neuronal proliferation and migration in neonatal brain and dramatically down-regulated during early postnatal development (Sugiura et al., 2001). Loss of NMDA receptor functions during development increases neuronal cell death and prevents the formation of precise neural circuits (Deisseroth et al., 2004).

2. Glutamate and the developing retina

2.1. Glutamate functions in developing retina

How about the function of glutamate and its ionotropic receptors in the developing retina? Extracellular levels of endogenous glutamate are relatively high in the developing retina, which will support normal retinal development processes (Haberecht and Redburn, 1996). Application of high concentration of glutamate (5mM) to rat neonatal retinal ganglion cell cultures has been shown to be neurotrophic; which can regulate the survival of retinal ganglion cells cultured in serum free defined medium alone (Nichol et al., 1995). Other toxic study shows that application of glutamate analogs such as NMDA at postnatal day 1 into the rabbit retina leads to a disruption of the outer plexiform layer and cellular organization of the neuroblastic layers; and it is also shown that the toxic tolerance in neonatal retina is approximately 2 times greater than that in the adult retina (Haberecht et al., 1997). Application of glutamate or glutamate receptor antagonists induces a response by patch clamp recordings in E15 mouse retina, which demonstrates ligand-activated ion channels are expressed in the retinal ganglion cell layer, and may underlie the generation of spontaneous action potential (Rorig and Grantyn, 1994).

Interestingly, biochemically assays show that a significant proportion of

endogenous glutamate pools are found in rabbit retina at birth, and localized around cell bodies and growing processes of cones and ganglion cells; the extracellular concentration of glutamate will decrease to very low levels in the adult retina (Haberecht and Redburn, 1996). This high concentration of extracellular glutamate in neonatal retina may play an important role in a variety of developmental events such as the dendritic pruning, programmed cell death, neurite sprouting and may also regulate the retinal ganglion cell numbers during retinal ontogeny (Haberecht and Redburn, 1996; Nichol et al., 1995).

2.2. Glutamate ionotropic receptors express and function in adult retina and developing retina

Excitatory synaptic transmission in the adult retina is mediated mainly by glutamate neurotransmission. Cone photoreceptors release glutamate onto bipolar cells, activating either ionotropic or metabotropic receptors. This activation initiates parallel OFF and ON pathways (DeVries, 2000; Miller, 2008). Bipolar cells release glutamate onto both amacrine cells (interneurons) and ganglion cells (output neurons), which express various receptor types (Dumitrescu et al., 2006; Miller, 2008). Furthermore, ganglion cells can release glutamate, which may activate receptors on these cells by autocrine actions. AMPA and NMDA receptors play cooperative roles in ganglion cell synaptic transmission. NMDA receptors increase conductance with depolarization, offsetting the decreased function of AMPA receptors. Their combination can generate excitatory synaptic currents with amplitudes which are voltage independent (Dingledine et al., 1999). Moreover, AMPA receptors encode spontaneous, low-frequency presynaptic release, whereas NMDA receptors encode evoked, high frequency or multivesicular release (Chen and Diamond, 2002; Taylor et al., 1995). However, glutamate ionotropic receptors

expressed in the adult retina participate in the visual processes.

Like the adult retina, the prominent expression and function of glutamate in the developing retina suggests that glutamate may also play a key role in retinal ontogeny, in which the ionotropic receptors will be required (Brandstatter et al., 1998). Early study by immunohistochemistry in postnatal rabbit retina shows that there is a transient increase in AMPA receptor subunits in the outer plexiform layer during P2 to P6. In the inner plexiform layer they increase during the first week of postnatal stage reaches to the adult level after P10. Furthermore, through 1-amino-4-guanidobutane (AGB, a channel-permeant guanidinium analogue) entry secondary to agonist activation experiment, it shows that AMPA receptors are functional in the developing retina (Acosta et al., 2007; Chang and Chiao, 2008). This evidence supports that glutamate and its ionotropic receptors may play an important role in the retinal circuit formation and refinement during development (Wong et al., 2000a; Wong et al., 2000b).

For the prenatal mouse retina, previous studies by in situ hybridization have indicated that AMPA/kainate receptor subunits GluR1, GluR4, and KA2 start to express approximately E14, while other subunits of AMPA/kainate receptors are first detected at about E16 (Zhang et al., 1996). NMDA receptors subunits NR1 and NR2B are detected at as early as E15 (Watanabe et al., 1994). For the gene and protein expression examined by real-time PCR and immunohistochemistry, glutamate ionotropic receptors subunits GluR1, KA2, and NR1 are detected at the earliest E14 in the mouse retina (Martins et al., 2006). Although most of retina development focuses on postnatal period, the distribution of glutamate ionotropic receptor subunits in the prenatal period has suggested functions in the retinal progenitor cell proliferation and cell fate specification; and these effects are mediated

by activation of AMPA/kainate receptors (Martins et al., 2006).

As the glutamate ionotropic receptors appear throughout retinal development and their functions are reported preceding the establishment of synapses and plasticity of the retina (Kater and Lipton, 1995), it is possible that neurotransmitter receptors and voltage-gated ion channels have an earlier role in the differentiation and dispersion of the cells, prior to their role in establishing synaptic contacts (Rakic and Komuro, 1995). It has been shown that glutamate can be an endogenous anti-proliferative signal mediating normal cell cycle through post-transcriptional mechanisms (Martins et al., 2006).

3. Glutamate and the developing brain

3.1. Glutamate ionotropic receptors express and function in developing brain

Glutamate as the main excitatory neurotransmitter in adult brain is also found accumulating in embryonic cells and it is believed to mediate long-range interactions in the embryonic period (Behar et al., 1999). There are two ways affecting the cell-cell interaction during development. One is to act as non-diffusible signaling molecules by short-range communications, such as Ephrin/Eph receptor (Williams et al., 2003), Nogo/NgR (Wang et al., 2008) and extracellular matrix (ECM); the other is long-range communications, such as morphogens and Semaphorins (secreted) (Goldberg et al., 2004), and diffusible guidance molecules: netrin-1 (Shewan et al., 2002) and neurotransmitters.

Cryostat sections of E13 cortex are stained by anti-glutamate antibody. It stains the cortical cells and processes in the primordial plexiform layer (Behar et al., 1999). Through dissociated cell chemotaxis assays from E13 to E18, this studys show that glutamate can play as a chemoattractant to signal cells to migrate into the cortical plate by activating NMDA receptors. Patch-clamp recordings and neuroanatomical

techniques show that the intermediate zone (IZ) cells express calcium permeable AMPA receptors; and cortical fibers accumulating high concentration of glutamate that is released by their growth cones can activate the IZ cells (IZ is a region between the ventricular zone and the cortical plate) at E12.5. This evidence reveals that glutamate affects the cortical cell migration and cell fate by a short-range influence during development (Metin et al., 2000). Growing neurites of rat dorsal root ganglion neurons in culture can release glutamate from their growth cones, which can induce the inward currents of hippocampal neurons that contain glutamate receptors plated near these dorsal root ganglion neurons (Soeda et al., 1997). This supports that glutamate can be a short-range cue to affect the immature cells. From these reports, we propose that glutamate may participate in the embryonic development in different ways depending on its target cells or tissues.

Regardless which way glutamate selects, its final function depends on which receptors it activates. In rats, the GABA receptors promote cortical plate cell motility ($GABA_B$- and $GABA_C$-like) and arrest cortical plate cell movement ($GABA_A$-like) (Behar et al., 1998). The same mechanism may also exist in the glutamate ionotropic receptors, some receptors promote cell motility, then activate a second class of receptors to attenuate this. Glutamate may act as an attractor to some embryonic cells; then the high concentration of glutamate near the target activate other receptors, providing a stop signal to notify the cells when they approach their final positions (Behar et al., 1999; Metin et al., 2000).

3.2. Glutamate receptors mediate genetic changes in developing neurons and glia

Despite the importance of glutamate and its ionotropic receptors for brain development, knowledge of molecular mechanisms regulated by glutamate receptors

in developing neurons is rudimentary.

By using a unique combination of NMDAR1 knockout mice, a group of three NMDA receptor-regulated genes (*NARG1*, *NARG2* and *NARG3*) is discovered, which has the common striking regulatory features. In the brain-stem, *NARG*s are expressed at approximately 2-fold higher than normal in NMDAR1 knockout animals. In the adult, all three *NARG*s are expressed at low levels. But with the brain development, these genes reach their peak in expression around the time of birth. These results show that NMDA receptors can regulate some stage specific gene expressions which play a pivotal role for neuronal maturation during mammalian brain development (Sugiura et al., 2001).

Glutamate receptors can be activated to induce the cellular changes of Ca^{2+}, and affect gene transcription in glia through modulating the expression and activity of transcription factors (Eun et al., 2004; Gallo and Russell, 1995; Morgan and Curran, 1988). Agonists of both ionotropic and metabotropic glutamate receptors can stimulate changes of some immediate early response genes that include the *c-fos* and *c-jun* families in astrocytes and cells of the oligodendrocyte lineage in the hippocampus (Sonnenberg et al., 1989; Steinhauser and Gallo, 1996). Similar study demonstrates that electrical stimulation or glutamate activation of optic nerve axons can also elicit a Ca^{2+} response in the surrounding glial cells, which are accompanied by an increase in immunoreactive cells for c-fos, c-jun and nerve growth factor inducible factor A (NGFI-A) (Gudehithlu et al., 1993; Mack et al., 1994). Glutamate receptors mediated Ca^{2+} signaling activated by kainate is also involved in the phosphorylation and activation of cAMP response element binding protein (CREB) (De Cesare and Sassone-Corsi, 2000), a crucial mediator of gene expression in the nervous system. Previous evidence supports that kainate stimulates Ca^{2+}-dependent

phosphorylation of CREB in oligodendrocyte progenitor cells in rat at E20 (Pende et al., 1997). A common glutamate receptor mediated signal transduction pathway involving Ras and mitogen-activated protein (MAP) kinase has emerged in different glial cell types (Liu et al., 1999; Pende et al., 1997).

The neurotransmitters have the same function in the retina as that in the brain. Application of excitatory amino acids can increase both Fos- and Jun-related proteins in amacrine and ganglion cells. It suggests that these retinal cells activated by neurotransmitters can induce the increase of Fos- and Jun-related protein mediated responses (Yaqub et al., 1995). Light changes mediated by neurotransmitters receptors can also induce a transient increase of mRNA for the immediate-early genes *c-fos* and *NGFI-A* in the retina (Gudehithlu et al., 1993).

However, there may be other genes regulated by glutamate receptors in the developing neurons and glia. Electrical activity generated by neurotransmitters can also induce a series of gene changes among brain regions as well as during development.

3.3. Factors influence glutamate ionotropic receptors expression in cells at developing period

There is a traditional view of transmitter mediated signaling in the CNS, which is confined to communication between neurons mainly through synaptic specializations. Recently, it has become apparent that neurotransmitter mediated signaling can also take place along fiber tracts between axons and glia (Gallo and Ghiani, 2000). However, there are no synaptic specializations or gap junctions between axons and glia,suggesting that this may occur as a result of diffusion of chemical messengers (such as: neurotransmitters and Netrin-1) released from the active fibers (Metin et al., 2000). There are a number of candidates for this role, but previous evidence has

shown that glutamate may play a major role in this form of communication. It is reported that retinal ganglion cells use glutamate in neurotransmission, and direct application of glutamate produces activity dependent responses in glia similar to that seen when the nerve is stimulated (Chiu and Kriegler, 1994). Based upon these findings, Chiu and Kriegler have proposed a model for glutamate mediated axon-glia signaling in which glutamate is released along axons via a glutamate transporter coupled to sodium and potassium transmembrane gradients (Chiu and Kriegler, 1994). Although there is much evidence implicating glutamate mediated interactions between glia and optic nerve axons, the type of receptor that mediates this form of communication has not been identified (Mack et al., 1994). Consequently, it is not clear whether such receptors are present on all glial types, confined to a specific subtype or to glial cells in certain topographic regions. It is also possible that such receptors may be present on axons themselves, as suggested by Chiu and Kriegler. A description of the distribution of these receptors is critical if the functional relationship between axons and glia is to be unraveled.

Some growth factors (PDGF, bFGF) can control the proliferation and differentiation of glial cells (McKinnon et al., 1990). They also modulate the expression of glutamate receptor channels. In oligodendrocyte progenitor cells, basic fibroblast growth factor (bFGF) upregulates levels of the AMPA receptor subunits GluR1and GluR3 and the KA receptor subunits GluR7, KA1, and KA2. The combined treatment of oligodendrocyte progenitors with platelet-derived growth factor (PDGF) and bFGF, which maintains oligodendrocyte progenitor cells in an undifferentiated state, causes an increase in transcription of the gene encoding the AMPA receptor subunit GluR1 and in density of functional GluR1-containing channels by electrophysiology analysis of AMPA receptors (Chew et al., 1997).

These findings agree with the observation that GluR1 and GluR2 mRNA expression levels vary with different regions. GluR3 expression levels also show a difference in the hippocampus and frontal cortex of adult brain. Moreover, these subunits are regulated as a function of age in the postnatal period (Durand and Zukin, 1993). The extrinsic growth factors might play a critical role in shaping glutamate receptor subunits composition by changing their rate of gene transcription in glia or neurons at early developing stages or shaping synaptic transmission in the brain (Chew et al., 1997; Pellegrini-Giampietro et al., 1991). This is also attributable not only to heterogeneity of ionotropic receptor subunits in the brain but also to elucidate that different molecules coordinate together to participate in the neuronal complexity network at different developing stages.

3.4. Glutamate receptors connect neurons and glia

The excitatory neurotransmitter glutamate and its receptors are important molecular elements at the contacts between neurons and glia. Most areas of the brain are either innervated by or contain glutamate-containing neurons. Physiological, biochemical and molecular studies show that both ionotropic and metabotropic glutamate receptors are present on glial cells *in vivo* at a density similar to that found on neurons. Experiments *in vitro* demonstrate that glial cells release neuromodulators through Ca^{2+}-dependent and Ca^{2+}-independent mechanisms (Attwell et al., 1993; Bezzi et al., 1998). These active substances can either act on neuronal receptors directly to modulate synaptic transmission or activate receptors on other glial cells and influence neuronal activity indirectly (Gallo and Ghiani, 2000).

4. Glutamate and its ionotropic receptors is in relation to the mouse retinofugal pathway

4.1. The formation of mouse retinofugal pathway

Retinal axons from two eyes meet together at the optic chiasm, which is the major region of fiber reordering before retinal axons separate to form the optic tracts. The optic tracts will project further into targets in the thalamus and midbrain. In the mouse, retinal axons will divide into crossed and uncrossed axons in the optic chiasm; axons from the nasal retina will cross the midline and project to contralateral visual targets; axons from the temporal retina remain uncrossed in the chiasm and project to ipsilateral targets.

The retinal axon path-finding is related to a number of glial cells and early generated neurons that exist prior to the arrival of retinal axons. The glial cells are located near the ventricular zone at the midline. These cells and their processes span throughout the midline region and can be identified with RC2 antibody. All retinal growth cones make contact with these glial cells during the path-finding process. The other group of cells is the chiasmatic neurons (CD44/SSEA-1 positive neurons) that are located directly posterior to the position where the optic chiasm will later develop. These chiasmatic neurons are essential for axon crossing at the optic chiasm. Ablating these chiasmatic neurons before the retinal axons arrival to the diencephalon produces a failure of chiasm formation (Lin and Chan, 2003; Sretavan et al., 1995)

Beside these cells in the diencephalon, there are many molecules and genetic control that determine for the chiasm formation. These molecules are located on the retinal ganglion cells, glial cells in the retina or along the pathway, the chiasm, and the chiasmatic neurons in the diencephalon. The related molecules and genes are: Ephrin-B2/Eph-B1 (Williams et al., 2003), Nogo/NgR (Wang et al., 2008), Netin-1 (Shewan et al., 2002), Robo2 (Ringstedt et al., 2000), Slit 1/2 (Niclou et al., 2000), semaphorins (Goldberg et al., 2004) and *Pax6* (Marquardt et al., 2001), *Zic2*

(Rasband et al., 2003), and *Vax2* (Schulte et al., 1999).

4.2. Glutamate ionotropic receptors vary with the mouse retina

Recent studies have examined the time course of changes in ionotropic glutamate receptor expression throughout retinal development and identified that they are functional even before synaptic contacts are formed. The expression of ionotropic receptors since embryonic ages is supported by studies in rat neuroepithelial cells, in which functional AMPA/kainate receptors are seen as early as the time of terminal cell division and during the early commitment of cells (Maric et al., 2000). From embryonic to postnatal stages, glutamate and its ionotropic receptors are involved in the regulation of dendritic refinement and neuronal migration (Lujan et al., 2005). The temporal functionality of glutamate receptors combined with high levels of glutamate early in the development of the retina may be essential for differential activation and remodeling of neuronal precursor cells and neuroepithelial cells.

By in situ hybridization analysis, the expression level of AMPA and kainate receptor subunits was generally higher during retinal development than in the adult. During retinal development, the AMPA receptor subunits appeared to distribute in the ganglion cell layer (GCL) and inner nuclear layer (INL), but in the adult, its distribution is stronger in the INL than the GCL (Hamassaki-Britto et al., 1993). This difference in the expression of AMPA and kainate receptor subunits during development suggests a role for these receptors in retinal differentiation and synaptogenesis and possibly in controlling cell death (Young, 1984; Zhang et al., 1996). Recent research demonstrates that the glutamate receptors mediate excitotoxic cell death associated with brain insults (Gallo and Russell, 1995). In the developing retina they may play a role in remodeling of neuronal precursor cells and neuroepithelial cells of retina (Zhang et al., 1996).

5. Future directions

The optic fiber growth is very fascinating. The mouse optic pathway is a model for axon guidance and for analyzing how binocular vision is patterned. But what are the mechanisms that control optic pathway formation remain an unresolved question (Jeffery and Erskine, 2005).

Recent studies have identified several molecular players that influence the growth direction of the optic nerve, especially on the decision made at the optic chiasm. More and more efforts are being made currently to unravel the role of these guidance molecules in directing optic pathway development, especially the optic chiasm formation. Glutamate is well studied molecule, but it may have new function to be discovered of. Both mRNA and protein of distinct glutamate receptor subunits have been detected in neural progenitors of the embryonic mammalian nervous system (Gallo et al., 1995). AMPA and kainate receptor mRNAs are detected at E11 in rats (Gallo et al., 1995) and functional glutamate receptors have been identified in the CNS of rodent and human embryos (Bardoul et al., 1998a; Bardoul et al., 1998b).These receptors are also detected at E14 in mouse retina (Zhang et al., 1996).

From the above descriptions, we have an initial thought that glutamate receptors may play a crucial role in the embryonic periods, and different receptor subunits can induce distinct effect to axon growth. In the following studies, we aimed at characterizing expression of glutamate and its receptors in the mouse optic pathway, to determine possible function of glutamate signaling in guidance axon growth in the prenatal development of the brain.

CHAPTER 2

Localization and possible function of Glutamate in the developing mouse optic pathway

Introduction

Glutamate is a non-essential amino acid naturally occurring in the L-form, and it is the dominant amino acid neurotransmitter in the central nervous system (CNS). It binds to a large number of ionotropic and metabotropic receptors. There are three types of ionotropic glutamate receptors: α-amino-3-hydroxy-5-methyl-4-isoxazole-propionate (AMPA), kainate (KA) and N-methyl-D-aspartate (NMDA) receptors (Hollmann and Heinemann, 1994); in this study, we will focus on two ionotropic glutamate receptors, AMPARs and kainate receptors. AMPA receptors are heteromeric receptors composed of GluR1, GluR2, GluR3 and GluR4 subunits. Kainate receptors are formed by GluR5, GluR6 and GluR7 subunits, as well as KA1 and KA2 subunits (Dingledine et al., 1999); they are also named as: Grik1, Grik2, Grik3, Grik4 and Grik5 subunits. AMPARs and kainate receptors have been well studied in the mammalian retina. Zhang et al. show that the ionotropic glutamate receptor subunits are expressed as early as embryonic day (E) 14-18 through in situ hybridization study (Zhang et al., 1996). According to other

studies using immunocytochemistry and Western blots, some of these pharmacologically defined ionotropic glutamate receptors are found in adult and developing mouse retina (Liu et al., 2001; Sucher et al., 2003); and by using the agmatine (1-amino-4-guanidobutane; AGB) labeling technique, functional ionotropic glutamate receptors are identified in the developing mouse retina (Acosta et al., 2008; Acosta et al., 2007). The prominent expression of glutamate and its ionotropic receptors early in development suggests that glutamate also plays a key role in the ontogeny and early functionality of the retina.

Glutamate can be one of the neurotransmitters released by neuronal activity in the developing brain, when there is no synaptic connection. Neuronal activity plays an important role in the process of refining neural connection during development of the neuronal pathway (Cohen-Cory, 2002). The released neurotransmitter may have important communication and signaling roles in early events such as proliferation, migration, differentiation and survival of neurons (Behar et al., 1999; Komuro and Rakic, 1993; LoTurco et al., 1995; Nguyen et al., 2001). In mice with genetic deletion of glutamate transporters (GLAST/GLT mutants), they show multiple brain defects and die in utero around E17-18. Several critical aspects of neuronal development, for example stem cell proliferation, radial migration, neuronal differentiation is impaired (Matsugami et al., 2006). All these demonstrate to us that as one of the neurotransmitters, extracellular glutamate concentration is essential to maintain the cell microenvironment and moderate glutamate concentration is an indispensable factor in the early neuronal activity.

As glutamate might be an important factor in the retinal histogenesis and it also takes part in the neuronal activity to control the axon growth in the developing CNS, we want to further study the glutamate and its receptors in the mouse retinofugal

pathway, focusing at the stages from E13- to 15, which is an essential period for the retinal projection development at the chiasm and optic tract (Leung et al., 2004). Some molecules have been reported to participate in the retinal axon guidance and projection, such as Ephrin-B2 and its EphB1 receptor (Birgbauer et al., 2000; Birgbauer et al., 2001), Nogo (Wang et al., 2008), Sema5A (Goldberg et al., 2004; Oster et al., 2003), and Vax2 (Barbieri et al., 2002). However, the molecular basis of the axon growth mechanism in the chiasm needs further exploration. Retinal axons may recognize guidance cues expressed by cells along the path and in the intermediate targets. There are glial cells and neurons resident in one of these intermediate targets, the optic chiasm: (1) the retinal axons with their growth cones will contact with endfeet and processes of radial glial cells which make them pause during growth in the chiasm (Chan et al., 1998; Marcus et al., 1995; Marcus and Mason, 1995). Some reports show that the changes in growth direction of retinal axons are always associated with an alteration of glial environment in the chiasm (Guillery and Walsh, 1987; Reese et al., 1994). (2) The same with neurons at the chiasm, a group of SSEA-1 and CD44 immunopositive neurons, which form the posterior border and a rostral raphe at the midline of the chiasm, will contact with the retinal axons (Mason and Sretavan, 1997; Sretavan, 1990; Sretavan et al., 1994; Sretavan et al., 1995). These neurons will also present guidance cues to the retinal axons. Ablating the CD44 immunopositive neurons will render the retinal axons unable to grow into the chiasm (Sretavan et al., 1995). Specific antibodies to CD44 will induce dramatic defects in routing of the retinal axons which arrive early in the chiasm (Lin and Chan, 2003).

Recently, studies show that glutamate can control growth rate and branching of dopaminergic axons, all of its ionotropic receptors participate in these activities

(Schmitz et al., 2009). Studies through cultured hippocampal neurons show that high levels of glutamate, quisqualate (a AMPA/group I mGluR agonist) and kainate inhibit axonal growth (De Paola et al., 2003; Mattson et al., 1988; McKinney et al., 1999). However, it is also reported that some new-born neurites can turn toward a local gradient of glutamate in a concentration dependent manner (Zheng et al., 1994; Zheng et al., 1996). A large variety of extracellular local cues can guide axon growth; another study shows that transient activation of kainate receptors induces a fast and reversible growth cone stalling (Ibarretxe et al., 2007). So, there is increasing evidence indicating that glutamate as a neurotransmitter can play a role in shaping axonal structure.

Although glutamate can be a guidance cue for axon growth, its function in the optic pathway in vivo is unknown. In this study, we will examine the expression of glutamate in the mouse optic pathway in order to explore whether glutamate may contribute to the path-finding of optic axons.

Materials and Methods

Animal preparation

C57BL/6J mice were kept in a breeding colony at the Laboratory Animal Services Center of the Chinese University of Hong Kong. Embryonic day 0 (E0) was defined as midnight on the day a vaginal plug was found. Animals were treated according to procedures approved by the Laboratory Animal Services Center of the Chinese University of Hong Kong. The pregnant mice were killed by cervical dislocation. Embryos from E13 to E18 were taken out by Caesarean section and kept in cold Dulbecco's modified Eagle's medium (DMEM)/F12 (high glucose) medium containing penicillin (1000U/ml) and streptomycin (1000μg/ml).

Immunohistochemistry

Expression of L-glutamate was investigated in the developing mouse retinofugal pathway. The heads of E13- to E15 embryos were fixed with 4% paraformaldehyde (PFA) in 0.1M phosphate buffer (PB), pH7.4, and were stored overnight at 4°C. The tissues were processed according to the following procedures:

(1). Embeded in a gelatin-albumin mixture for vibratome sectioning; the sections were 100μm thickness. Serial horizontal or frontal sections of the retinofugal pathway from the eyes to the proximal parts of the optic tract were collected in 0.1M phosphate buffer saline (1xPBS), pH7.4. (2). Blocked sections with 10% normal goat serum in 1x PBS, pH 7.4, for 1 hr at room temperature (RT). (3). Incubated sections with primary antibody: anti-L-glutamate (1:500, mouse monoclonal IgM; Abcam; UK) in 1xPBS, pH7.4, containing 1% normal goat serum and 0.1% Triton X-100 at 4°C overnight. (4). Washed sections for 10 min three times with 1xPBS, pH7.4, and then incubated with AF488 conjugated goat anti-mouse IgM (1:200; Molecular Probes, USA) for 2 hr at RT. (5). After being washed for 10 min three times with

1xPBS, pH7.4, fluorescent signals on the sections were imaged using confocal microscopy (FV300, Olympus Co, Japan). (6). Controls were prepared with the same procedures but in the absence of the primary antibody.

Double staining with neuronal cell marker: TuJ-1 in the mouse retina

To identify the L-glutamate positive cells in the retina, TuJ-1 double staining experiment was performed on the retinal sections. Frontal or horizontal sections containing the retina and optic disk were collected in 1xPBS, pH7.4, and washed with 1xPBS, pH7.4, for three times. The procedures were:

(1). Sections were blocked with 10% normal goat serum in 1xPBS, pH7.4, for 1 hr at RT. (2). Incubated sections with the primary antibodies: anti-L-glutamate and TuJ-1 (1:500, mouse IgG2a; Abcam, UK) at 4°C overnight. (3). Washed sections for 10 min three times with 1xPBS, pH7.4; incubated sections with secondary antibodies at RT for 2 hr. The secondary antibodies for L-glutamate and TuJ-1 were AF488 conjugated goat anti-mouse IgM and AF568 conjugated goat anti-mouse IgG2a (1:200; Molecular Probes, USA). (4). After being washed for 10 min three times with 1xPBS, pH7.4, fluorescent signals on the sections were imaged using confocal microscopy (FV300, Olympus Co, Japan). (5). Controls were prepared with the same procedures but in the absence of the primary antibody.

Double staining with chiasmatic neuronal marker: CD44 in the mouse ventral diencephalon

To Identify the L-glutamate positive cells in the ventral diencephalon, CD44 (IM7) double staining experiment was performed on the horizontal sections. The procedures were:

(1). Sections were blocked with 10% normal goat serum in 1xPBS, pH7.4, for 1 hr at RT. (2). Incubated with primary antibodies: anti-L-glutamate and CD44 (IM7, rat

IgG2a, 1:100; BD, USA) in horizontal sections at 4 °C overnight. (3). Washed sections for 10 min three times with 1xPBS, pH7.4; incubated sections with secondary antibodies at room temperature for 2 hr. The secondary antibodies for L-glutamate and CD44 was AF488 conjugated goat anti-mouse IgM and AF568 conjugated goat anti-rat IgG2a (1:200; Molecular Probes, USA). (4). After being washed for 10 min three times with 1xPBS, pH7.4, fluorescent signals on the sections were imaged using confocal microscopy (FV300, Olympus Co, Japan). (5). Controls were prepared with the same procedures but in the absence of the primary antibody.

Preparation of retinal explants and L-glutamate treatments

Retinal explants culture was prepared as the early report from E14 mouse embryos (Chan et al., 2002). The eyes were dissected and removed into a culture dish with cold DMEM/F-12 medium. After removing the lens, vitreous and pigment epithelium, the retinas were cut into small pieces.

The retinal explants were plated on a laminin/Poly-L-Ornithine-coated coverslip and cultured in L-glutamate and L-glutamine free medium (Invitrogen Co, USA), supplemented with N1, 1% bovine serum albumin and 0.4% methylcellulose (all were bought from Sigma Co, USA) at 37 °C for about 20 hr. For the functional experiment, L-glutamate (500μM to 2mM) (RBI Co, USA) was added to the culture medium at the beginning of the retinal explants culture; the control culture group was added the same volume of 1xPBS, pH7.4.

Analysis of the retinal explant outgrowth

The controls of cultured retinal explants and L-glutamate treated retinal explants were fixed with 4% paraformaldehyde in 0.1M PB at pH 7.4 for 15 min at RT, then wash three times with 1xPBS, pH7.4,. The retinal outgrowth of these explants was

directly captured by the control software of a Spot digital camera (Diagnostic Instruments Inc., USA), which was connected to a Zeiss Axiovert 200 microscope (Germany). By using Photoshop 8.0 software (Adobe., USA), a series of images were assembled to give an image of the whole explants. The total neurite outgrowth was measured using the MetaMorph software (Universal Imaging Co., USA). Data of neurite outgrowth obtained in every drug treatment group was compared with those in the control group (treated without any drug but instead of the same volume of 1xPBS, pH7.4,) using Mann-Whitney nonparametric tests for analysis (GraphPad Inc., USA).

Results

1. Expression of L-glutamate in the optic pathway during embryonic development

1.1. Expression of L-glutamate in the mouse retina

1.1.1. Anti-L-glutamate was stained in the retina

Anti-L-glutamate is a mouse monoclonal antibody, used to stain L-glutamate in adult retina and the developing retina from E13 to E15. No staining was detected in the control section at E13 (Fig. 1A). There was obvious staining in adult retina (n=2), the staining was localized largely in nerve fiber layer (NFL), ganglion cell layer (GCL), and inner plexiform layer (IPL); and sporadic labels were observed in inner nuclear layer (INL) and outer plexiform layer (OPL). No obvious staining was detected in outer nuclear layer (ONL) (Fig. 1B). At E13 (n=6), there were some retinal axons forming the optic nerve and starting to enter the chiasm and the optic tract, positive L-glutamate staining was found in the whole retina, but was most intense in the inner regions of the retina and in the optic axons. In addition, strong staining of

L-glutamate was detected in the ciliary margin zone (CMZ), lens and blood vessels (Fig. 1C). At high magnification, most L-glutamate signals were obviously distributed on the cell bodies in the inner retinal layer, but weakly in the outer layers (Fig. 1D). At later stages, L-glutamate displayed a neuronal expression pattern more obviously than that at E13. At E14 (n=6), L-glutamate was expressed in the retinal axons extending to the optic disk (Fig. 1E). At E15, L-glutamate was also found in the inner retinal layer, the CMZ and the lens (Fig. 1F-G). At high magnification, the cells and axons in the inner layer of the retina were labeled intensively by L-glutamate antibody (Fig. 1H).

1.1.2. Double staining with anti-L-glutamate and TuJ-1 in the retina

To examine the identities of these L-glutamate-positive cells, the retina was doubly stained with antibodies against L-glutamate, and one of neuronal cell markers: TuJ-1, an antibody for beta III tubulin. It is a marker for retinal ganglion cells (RGCs), which are the first neuronal subtypes that are generated during retinal development (Brittis and Silver, 1994).

At E15, TuJ-1-positive neurons were confined to the inner layer and the axon layer of the central retina, which were also strongly labeled by anti-L-glutamate (n=5; Fig. 2A-G). Some TuJ-1 absent cells in the outer layers of retina were also stained (Fig. 2E, G). In high magnification, L-glutamate staining was concentrated in the inner layer and the axon layer of the retina; but in the optic disk, there still were some L-glutamate positive glial-like cells which could not be stained by TuJ-1 (Fig. 2B, D). Furthermore, L-glutamate positive staining was also found in the CMZ where TuJ-1 was nearly absent except in a few cells (Fig. 2A).

1.2. Expression of L-glutamate in the mouse ventral diencephalon

1.2.1. Anti-L-glutamate was stained in the ventral diencephalon

For the expression of L-glutamate, we stained the horizontal and frontal sections of the mouse ventral diencephalon from E13 to E15. L-glutamate was highly expressed in the optic chiasm (OC) and the chiasmatic neurons in E13 ventral diencephalon (n=8; Fig. 3A). At E14, there was strong labels of L-glutamate in the optic nerve, the optic stalk (OS) and the optic tract (OT) (n=10; Fig. 3B-D) However, a weak L-glutamate staining was also observed in the other regions of the ventral diencephalon, including some chiasmatic neurons (Fig. 3C). The staining of OC was also obviously found at E15 (n=4; Fig. 3E). Furthermore, in the frontal sections, L-glutamate was intensely labeled in the OC and OT (Fig. 3F-H, 4A-D). In addition, L-glutamate positive cell bodies were also arranged along the ventricular zone (Fig. 3H); it also was detected in some cells in the midline region along the axons in the OC (Fig. 3F-H, 4A).

1.2.2. Double staining with anti-L-glutamate and IM7 in the ventral diencephalon

To examine the identity of these L-glutamate-positive cells in the ventral diencephalon, horizontal sections were doubly stained with antibodies against L-glutamate, and one of markers for the chiasmatic neurons: CD44 (IM7), a membrane glycoprotein which is found in the chiasmatic neurons at the midline of the chiasm (Sretavan et al., 1994). These early generated neurons have been shown to be related to the chiasm formation (Sretavan et al., 1995).

At E14, L-glutamate was localized in CD44 positive neurons in the ventral diencephalon, which was shown in the low and high magnification images (Fig. 5A-G), indicating that part of the L-glutamate positive cells were chiasmatic neurons. However, there were other anti-L-glutamate positive cells that are negative to anti-CD44 (Fig. 5A, D, and G).

2. L-glutamate promoted retinal axon growth

For the function of L-glutamate on the retinal axons, we used L-glutamate free and L-glutamine free medium as controls to culture E14 retinal explants. In the control dish, neurites from the retinal explants were very sparsely distributed and grew only for a short distance (Fig. 6A), indicating that glutamate might be an essential component to support retinal axon growth; In the presence of 500μM, 1mM and 2mM L-glutamate (Haberecht and Redburn, 1996; Habercht et al., 1997; Nichol et al., 1995), neurites from the retinal explants were denser and longer when compared with the controls (Fig. 6B-D). Statistical data showed that there was significant difference between the L-glutamate treated groups and the control one ($P<0.01$ and $P<0.001$) (Fig. 6E), confirming that L-glutamate might act as a promoter to axon growth during the early prenatal periods of retinal pathway development.

We found several of explants grew better in the control dishes, and the ventrotemporal (VT) region of the retina was much narrow when compared with the dorsonasal (DN) region, so we further examined outgrowth from different regions of the retina in response to L-glutamate. For the DN and VT retina cultured in L-glutamate and L-glutamine free medium, neurites from the DN retina were significantly fewer compared with the ones from the VT retina (Fig. 7A, C). With 1mM L-glutamate, neurite outgrowth from the DN retina was significantly enhanced but not in VT neurites (Fig. 7B, D). The statistical data showed that there was significant difference between the DN retina groups and the 1mM L-glutamate treated DN retina ones; but there was no difference among VT retina groups and the 1mM L-glutamate treated VT retina ones (Fig. 7E). These results indicated that the neurite outgrowth from the DN retina is stimulated by L-glutamate and that stimulatory effect is not observed in VT neurites.

Discussion

Through this part of study, we investigate the expression pattern of L-glutamate in the mouse retinofugal pathway from E13 to E15, during which optic axons navigate through the chiasm and the optic tract to their subcortical targets (Chan et al., 1998). L-glutamate is the major excitatory neurotransmitter utilized by many different cell types, such as photoreceptor cells, bipolar cells and ganglion cells in the vertebrate retina (Barnstable, 1993; Massey and Miller, 1988). However, little knowledge is known for the L-glutamate expression and its function in the developing mouse retinofugal pathway. In this study, the results of L-glutamate staining show that it is expressed at as early as E13 and tends to localize in the retinal axon layer and ganglion cells layer. In the ventral diencephalon, L-glutamate is expressed in the whole diencephalon, but most intense in the optic stalk, optic chiasm and optic tract. These staining results suggest that L-glutamate might take part in the development of the retina and retinal axon patterning at the optic chiasm.

1. L-glutamate expresses in the mouse retinofugal pathway

1.1. L-glutamate expresses in the retina

In retinal histogenesis, there are two types of cells: one is the new-born RGCs, which are without axons and attain a radial configuration, anchoring at the inner and outer layers of the retinal neuroepithelium (Colello and Guillery, 1990). The other is the Müller glia, which have radial processes spanning through the inner and outer limiting membrane (Bhattacharjee and Sanyal, 1975). At E13, L-glutamate is localized largely in RGC layer; but a weak signal is detected on the neuroepthilial cells, which are radially arranged through the thickness of the retina. At this early

stage, the retinal axons are beginning to form, so the axon layer and RGC layer are very thin compared with the later stages.

At E14 and E15, the intense staining of L-glutamate is found in the RGC layer and their axon layer; and is weak in outer retinal regions. L-glutamate is clearly stained the retinal axons and some radial arranged glial-like cells at the optic disk. At the optic disk, there are also some molecules that guide the retinal axons towards the optic disk and enter the optic nerve. Netrin-1, Robo2 and Slit2 are the molecules affecting retinal axon path-finding into the optic nerve head (Goldberg et al., 2004; Livesey and Hunt, 1997; Plachez et al., 2008; Thompson et al., 2006). Whether L-glutamate plays a part at the optic disk to guide the retinal axon growth needs to further investigation.

1.2. L-glutamate expresses in the mouse ventral diencephalon

We find that L-glutamate is expressed extensively in the ventral diencephalon. It strongly localizes in the optic nerve, optic stalk, optic chiasm and optic tract. It is also found in some cells that are CD44 positive ones; CD44 is a marker specific for the chiasmatic neurons in the mouse embryos (Marcus and Mason, 1995; Sretavan et al., 1994). The identity of L-glutamate positive cells is confirmed by the co-localization with CD44 (IM7) in horizontal sections of the diencephalon. Retinal axons may recognize guidance cues which are expressed by these chiasmatic neurons, and these neurons have been shown to form the posterior border and a rostral raphe at the midline of the chiasm that affect bilateral path-finding of retinal axons. The presence of glutamate may suggest a possible role in this process.

L-glutamate is found most intensely in the optic axons along the pathway. At early embryonic stages, neurotransmitters are believed to mediate long-range interactions (Behar et al., 1996; Zheng et al., 1994; Zheng et al., 1996). Previous

studies report that L-glutamate accumulates in embryonic cortical cells and tangential fibers and can be released by growth cones (Herrmann, 1996; Soeda et al., 1997). The axonal experiment of L-glutamate may suggest a potential role to participate in axon growth in the optic pathway; and this role will be further investigated in the following chapters.

2. L-glutamate promotes the neurite outgrowth of the DN retina

From the retinal explants culture experiment at E14, we show that glutamate mediates retinal axon growth, with a promoting effect on the DN retinal neurites, but such effect is not obvious on the VT neurites. It suggests that axons from different regions of the retina respond differentially to glutamate.

It has been reported in the developing corticofugal pathway that the intermediate zone (IZ) cells expressing calcium-permeable AMPA receptors can be activated by millimolar concentration of glutamate (Clements et al., 1992; Hestrin, 1992); and glutamate released by growing corticofugal axons can reach high concentrations close to IZ cells and efficiently activates them to control the intracellular calcium in embryonic IZ cells, inducing the IZ cell migration (Metin et al., 2000). So through their experiment, we can hypothesis that the neurites of DN retina may be actually dependant the extracellular glutamate, however, those of VT retina might not need the extracellular glutamate. However, the mechanism of glutamate affecting the DN and the VT retina needs to further explore.

As the previous report shows that there is a local glutamatergic communication between the elongating cortical axons and IZ cells at the embryonic stages (Metin et al., 2000). Together with our observations, we might propose that: (1) the local glutamatergic communication might also occur in the mouse embryonic retina varying with different retinal region; (2) glutamate functions with the neurites of DN

retina might through the diffuse humoral effect (Mattson et al., 1988). All these need our future experiment support. Anyway, glutamate could be critical for the retina and ventral diencephalon development.

Figures

Figure 1. Immunostaining of retinal sections for anti-L-glutamate at different stages. No staining was detected in the control section at E13; L was for lens, R for retina (Fig. A). There was obvious staining in adult retina (n=2). The staining localized largely in nerve fiber layer (NFL), ganglion cell layer (GCL), and inner plexiform layer (IPL); and sporadic labels were observed in inner nuclear layer (INL) and outer plexiform layer (OPL). There was no obvious staining in outer nuclear layer (ONL) (Fig. B). At E13 (n=6), anti-L-glutamate stained preferentially in the inner regions of the retina and in the optic axons. In addition, strong staining of L-glutamate was detected in the ciliary marginal zone (CMZ) (asterisks), lens and blood vessels (arrows) (Fig. C). At high magnification, most L-glutamate signals were obviously distributed on the cell bodies in the inner retinal layer, but weakly in the outer layers (Fig. D). At E14 (n=6), L-glutamate was expressed in the retinal axons extending to the optic disk (OD) (Fig. E). At E15, L-glutamate was also found in the inner layer, the CMZ, the lens and the blood vessels (n=9; Fig. F-H). At high magnification, the cells and axons in the inner layer of the retina were labeled intensively by L-glutamate antibody (arrows) (Fig. H). Scale bars = 200μm in A (also applies to C, F-G); 100μm in B (also applies to D-E, H).

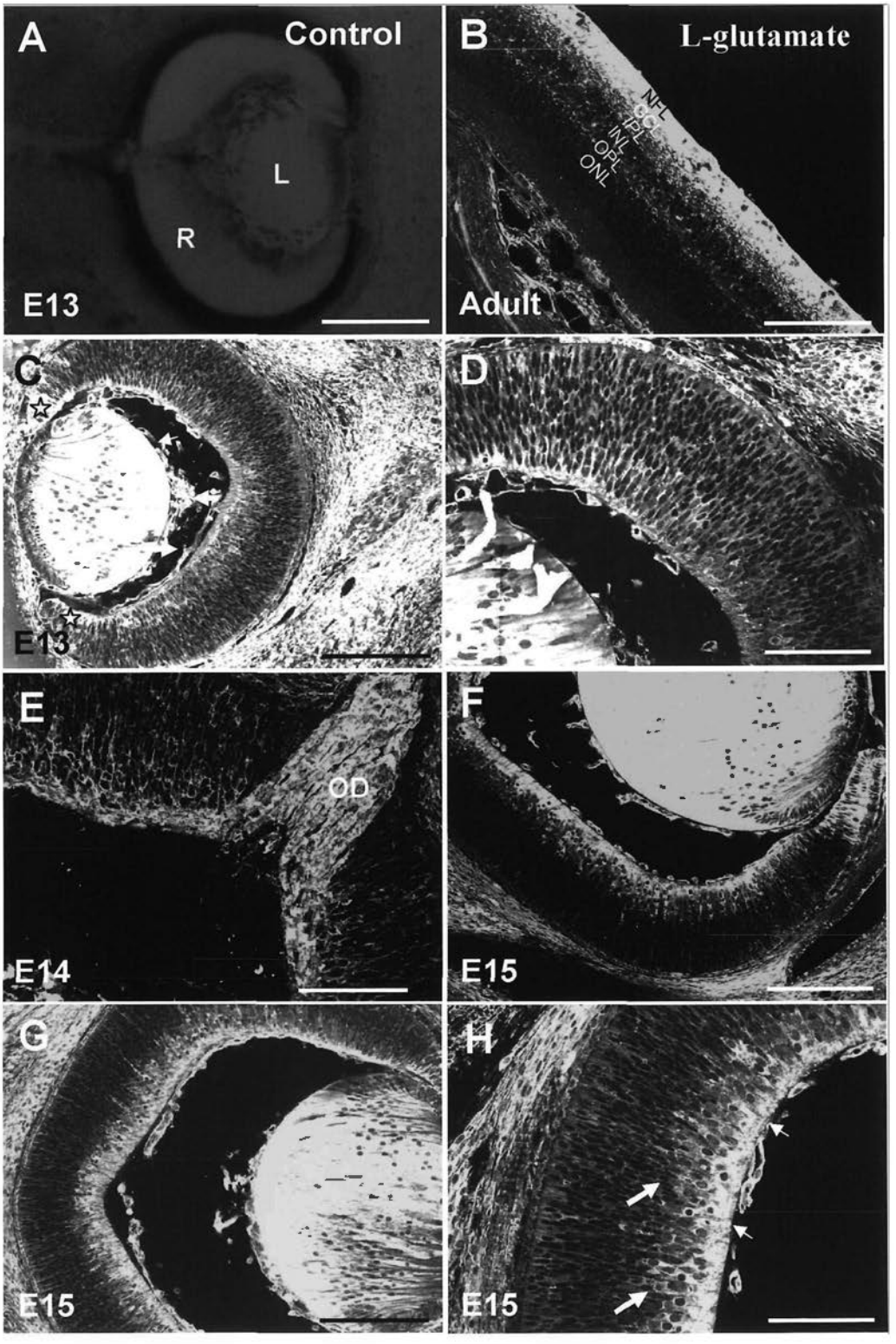
A
Control
L
R
E13
B
L-glutamate
NFL
GCL
IPL
INL
OPL
ONL
Adult
C
E13
D
E
OD
E14
F
E15
G
E15
H
E15

Figure 2. Immunostaining of retinal sections for anti-L-glutamate and TuJ-1 at E15. At low magnification, L-glutamate-positive staining was colocalized with TuJ-1-positive neurons except in the ciliary marginal zone (CMZ) where could not be stained by TuJ-1 at E15 (arrows) (n=5; Fig. A); and could also be merged together in the inner regions of the retina and in the optic axons including the optic disk (OD) (Fig. B-G). Anti-L-glutamate intensely labeled in the retinal axons and some radially arranged cells (arrows) in the OD (Fig. B and D); but TuJ-1 staining was localized in the retinal axons (Fig. 2C). In the merged image, it showed that the colocalization of these two antibodies was in the retinal axons (Fig. D). For the retina, the immunoreactive anti-L-glutamate was positively distributed in the inner layer and axon layer of the retina, other cells in the retinal outer layers (arrows) (Fig. E). TuJ-1 positive neurons were obviously labeled in the inner layer and axon layer of the retina; some new-born neurons were also stained in the outer layers of retina (Fig. F). The merged image showed that most of the anti-L-glutamate positive cells and axons could be colocalized with TuJ-1 staining; but other cells in the retinal outer layers could not be stained with TuJ-1 (arrows) (Fig. G). Scale bars = 200μm in A; 50μm in B (also applies to C-G).

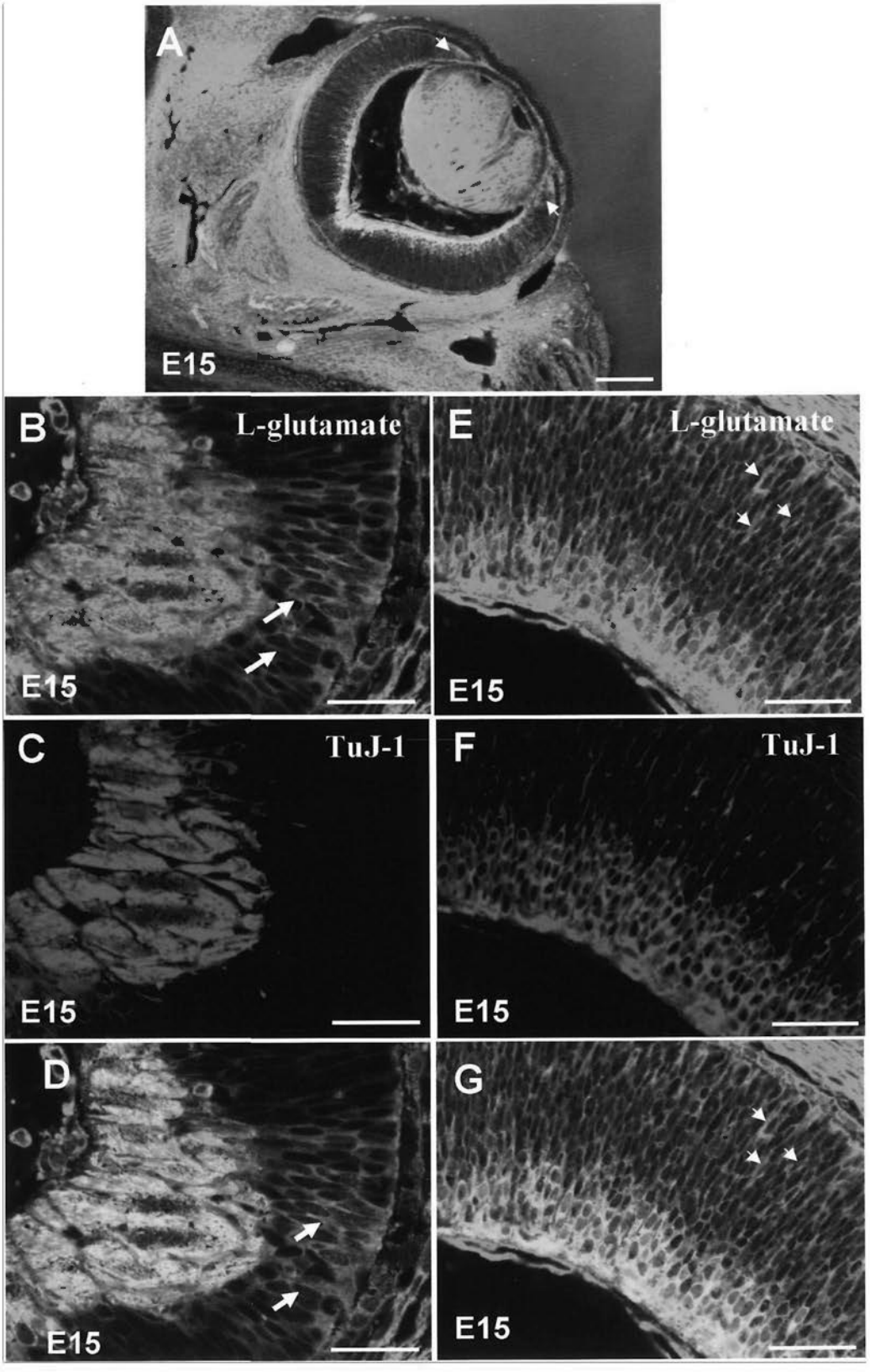
A
E15
B
L-glutamate
E15
E
L-glutamate
E15
C
TuJ-1
E15
F
TuJ-1
E15
D
E15
G
E15

Figure 3. Immunostaining of ventral diencephalic sections for anti-L-glutamate at different stages. These were the horizontal (Fig. A-E) and frontal sections (Fig. F-H); rostral and dorsal were to the top and the midline was indicated by arrows. L-glutamate was highly expressed in the optic chiasm (OC) and the cells were arranged in an inverted 'v' shape (arrows) at E13 (n=8; Fig. A). At E14, there was strong label of L-glutamate in the optic stalk (OS) (n=10; Fig. B). L-glutamate was strongly expressed in the OS and the OT; however, L-glutamate staining was also observed in the other regions of the ventral diencephalon (Fig. C). Further image showed the L-glutamate staining in the high magnification (Fig. D). There was strong staining in the OC at E15 (n=4; Fig. E). In the frontal sections, L-glutamate was strongly labeled in the OC and cell bodies (arrows and arrowheads) between the ventricular zone and the OC (Fig. F-H). Scale bars = 200μm in A (also applies to C, G); 100μm in B (also applies to D-F, H).

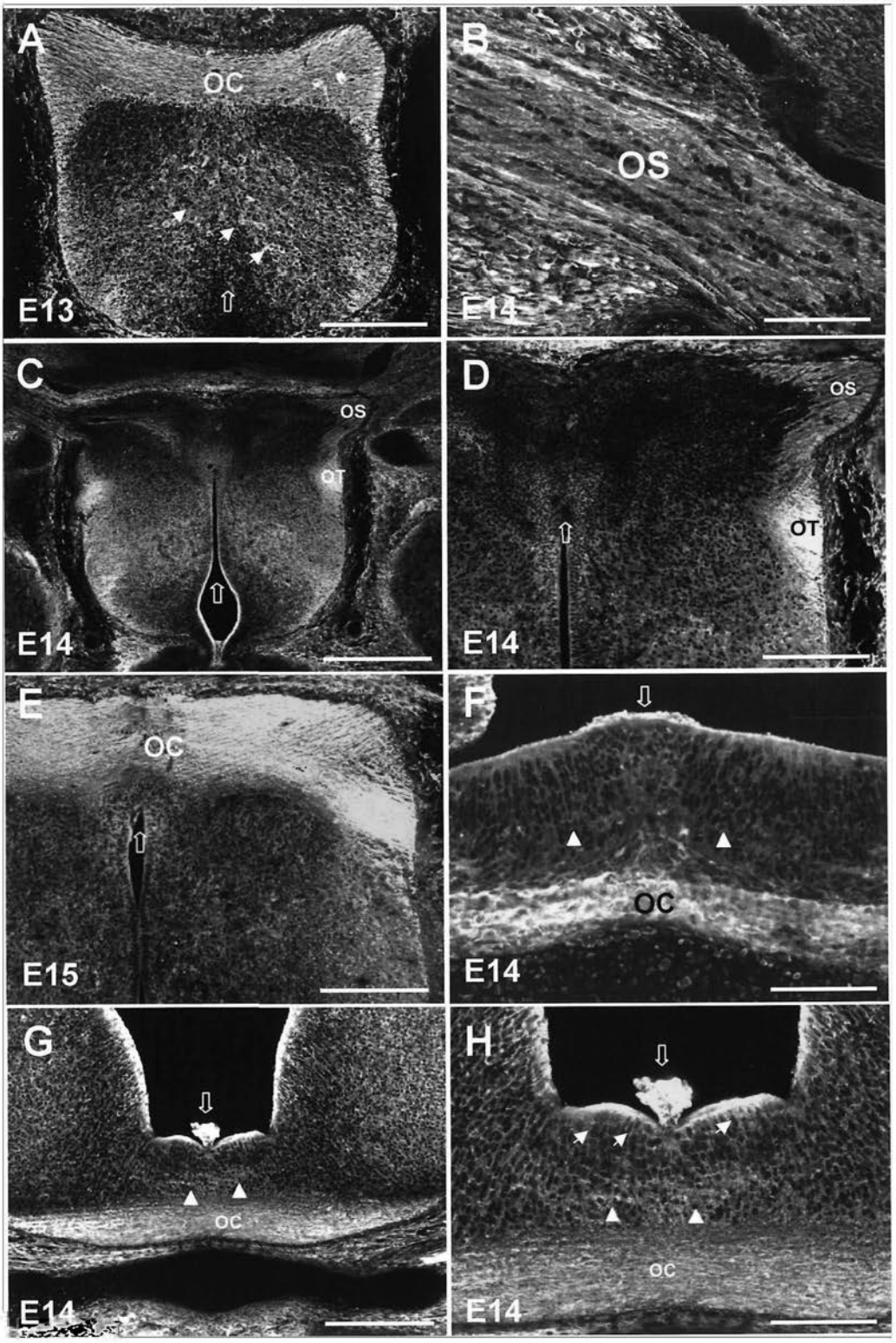
A
OC
E13
B
OS
E14
C
OS
OT
E14
D
OS
OT
E14
E
OC
E15
F
OC
E14
G
OC
E14
H
OC
E14

Figure 4. Immunostaining of including chiasm sections for anti-L-glutamate at E14. There were frontal sections; the arrow points to the midline of the brain, and rostral is up. L-glutamate was intensely localized in the retinal fibers in the beginning of the chiasm, glial-like cells in ventricular zone and some cells (arrowheads) in the midline region above axons in the optic chiasm (OC) (Fig. A). At the midlevel within the chiasm, the staining in the cells was the same with Fig. 4A and strong in the OC (Fig. B-C). L-glutamate was also intensely observed in the optic tract (OT) (Fig. D). Scale bars = 200μm in A (also applies to B-C); 100μm in D.

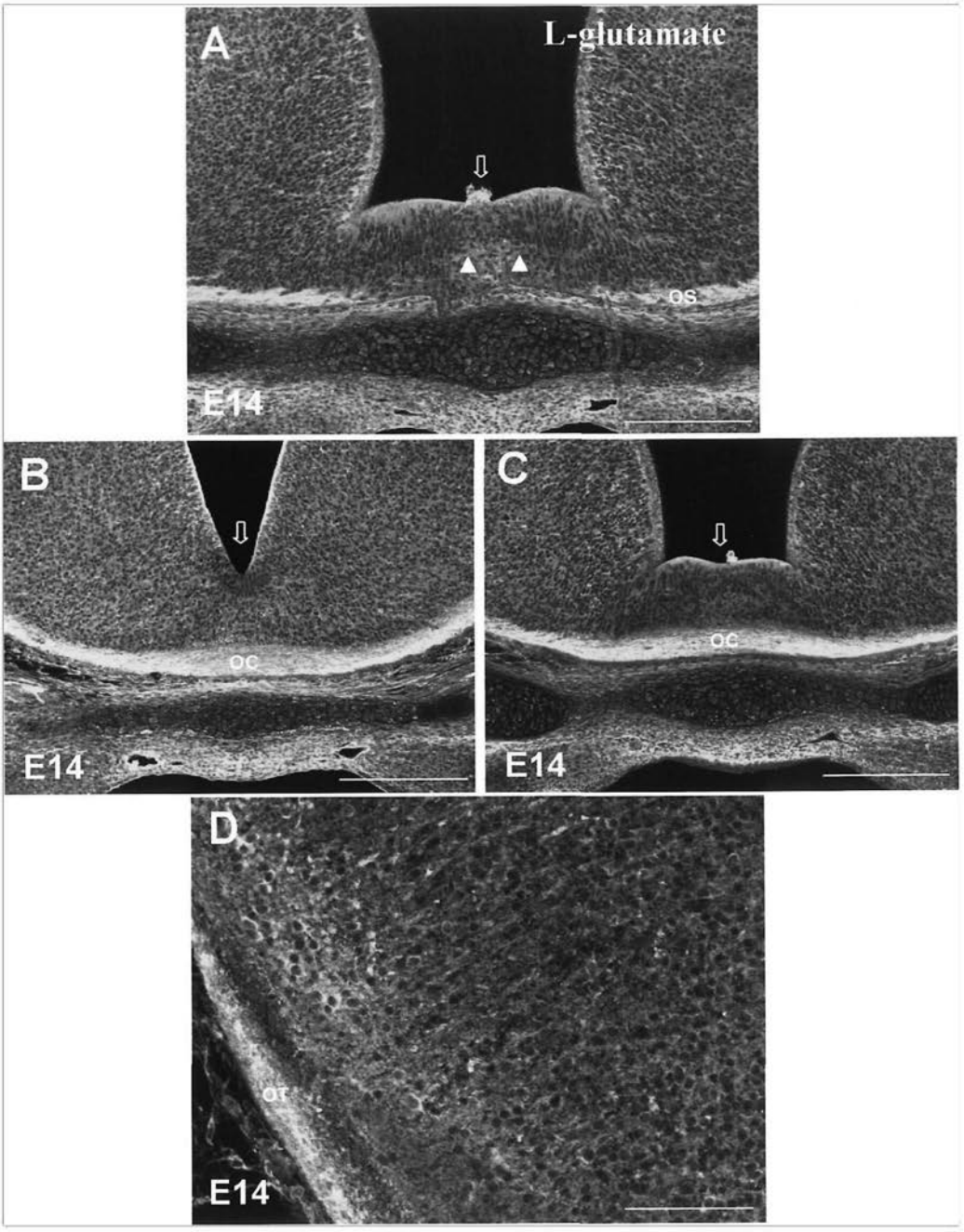
A
L-glutamate
OS
E14
B
OC
E14
C
OC
E14
D
OT
E14

Figure 5. Immunostaining of ventral diencephalic sections for (IM7) CD44 and anti-L-glutamate at E14. These were the horizontal sections; rostral was to the top and the midline was indicated by arrows. L-glutamate staining was particularly prominent on the optic stalk (OS) and the optic tract (OT); its staining was also found in the other regions of the ventral diencephalon (Fig. A). At high magnification, the L-glutamate positive cells were found near the third ventricle (Fig. B). CD44 was expressed in the chiasmatic neurons near the third ventricle (Fig. 5C). The merged image showed some of the L-glutamate positive cells could be chiasmatic neurons which were also identified by CD44 (Fig. D). At higher magnification, they showed that the L-glutamate staining could be colocalized with the CD44 staining (Fig. E-G). Scale bars = 200μm in A; 100μm in C (also applies to B-D); 50μm in E-G.

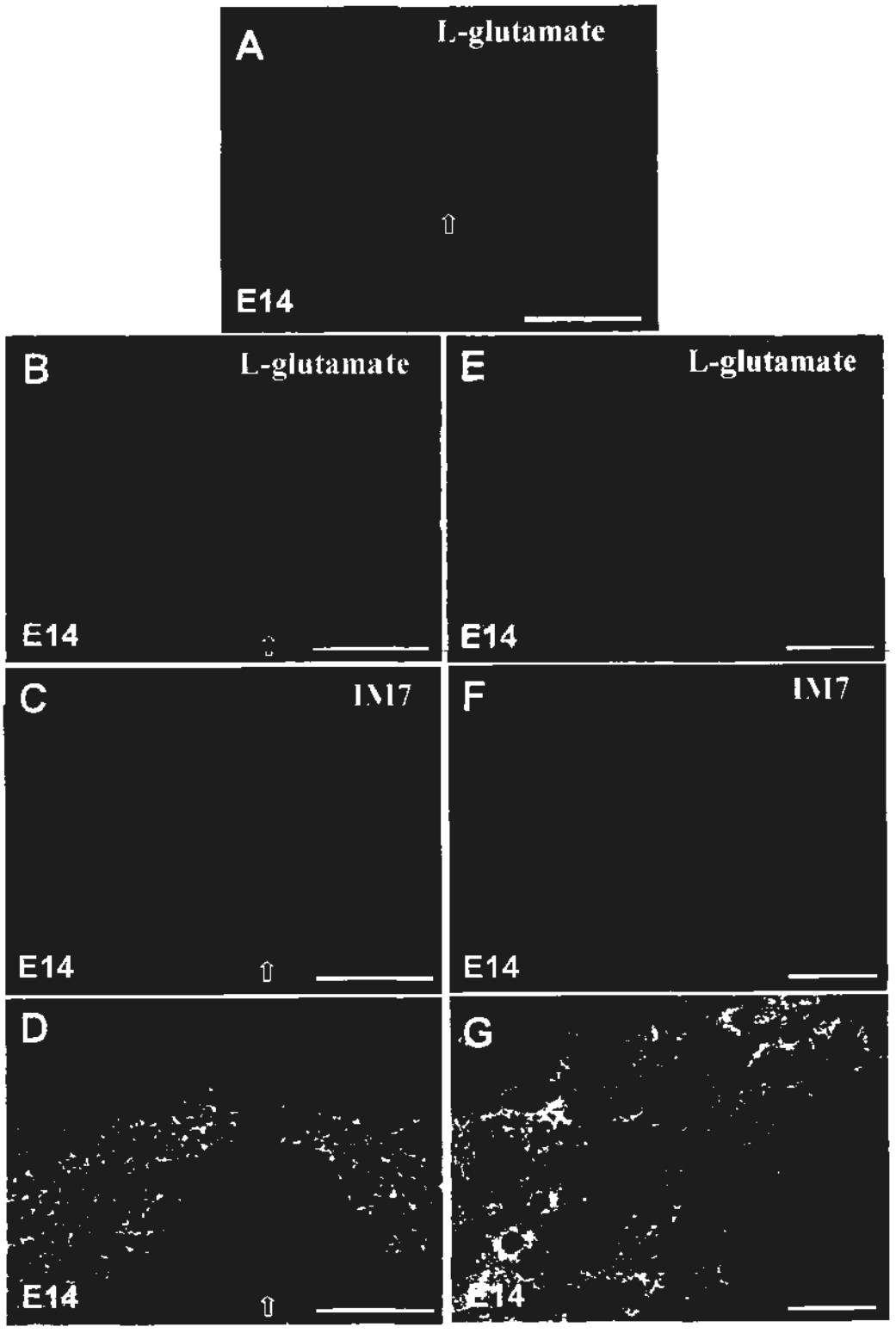
A
L-glutamate
E14
B
L-glutamate
E14
E
L-glutamate
E14
C
IM7
E14
F
IM7
E14
D
E14
G
E14

Figure 6. Effect of L-glutamate on retinal neurite outgrowth in cultured retinal explants. In control preparations to culture E14 retinal explants with the L-glutamate free and L-glutamine free medium, neurites were very sparsely distributed and grew only for a short distance (Fig. A). In the presence of the L-glutamate with different concentration (500μM, 1mM and 2mM), neurites were denser and longer when compared with those of the control ones (Fig. B-D). The plot showed that there was significant promotion to neurite outgrowth in the L-glutamate treated groups compared with the control one (Fig. E). Scale bars = 500μm (applies to A-D).

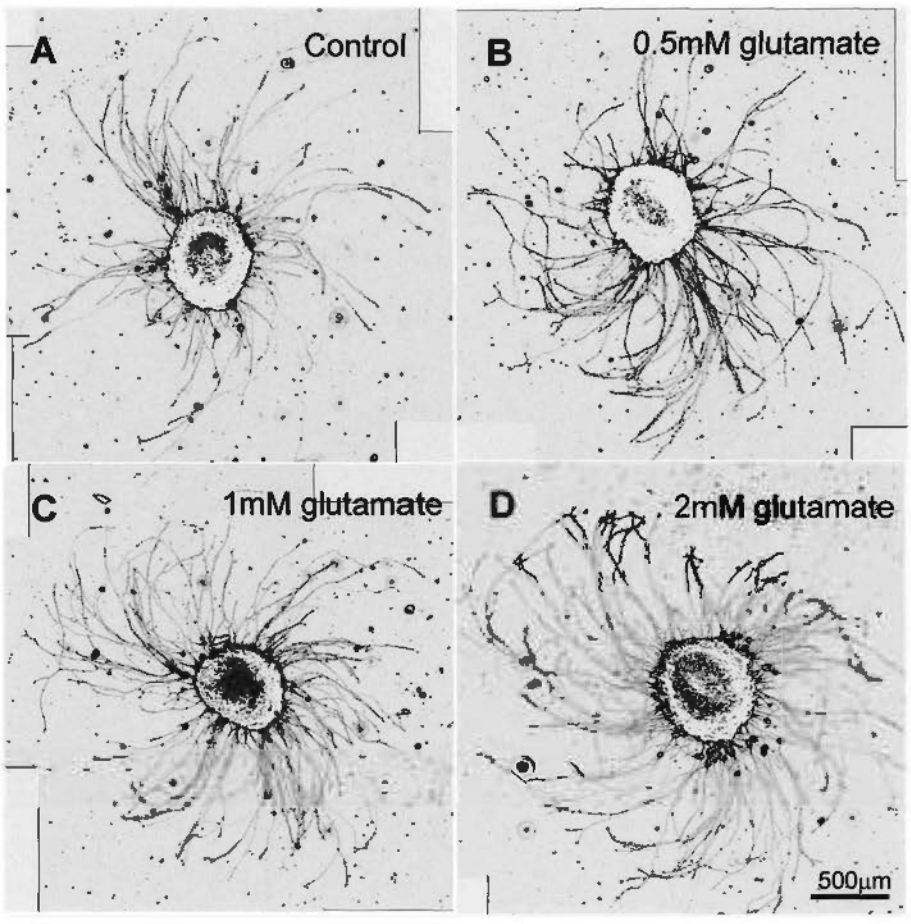
A
Control
B
0.5mM glutamate
C
1mM glutamate
D
2mM glutamate
500μm

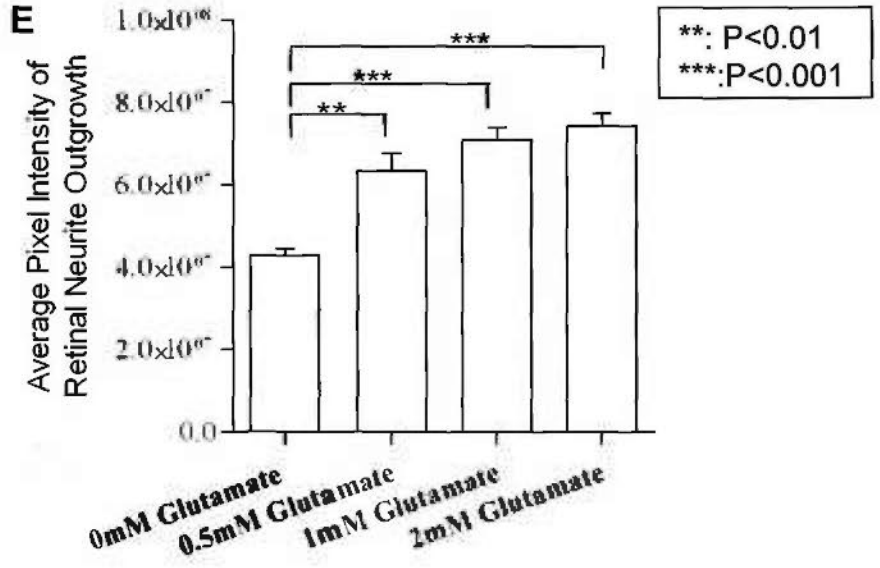
E
Average Pixel Intensity of Retinal Neurite Outgrowth
1.0x10^8
8.0x10^7
6.0x10^7
4.0x10^7
2.0x10^7
0.0
**
***
***
**: P<0.01
***:P<0.001
0mM Glutamate
0.5mM Glutamate
1mM Glutamate
2mM Glutamate

Figure 7. Different effect of L-glutamate on retinal neurite outgrowth in the dorsonasal (DN) and the ventrotemporal (VT) retinal explants. In the DN or VT retina preparations to culture E14 retinal explants in L-glutamate free and L-glutamine free medium, neurites from the DN retina were sparsely distributed and grew shorter (Fig. A). In the presence of 1mM L-glutamate, neurites from the DN retina were densely distributed and grew for a long distance (Fig. B); but neurites from the VT retina were the same as those of the VT retina cultured in L-glutamate free and L-glutamine free medium (Fig. C-D). Plot showed that The statistical there was significant difference between the DN retina groups and the 1mM L-glutamate treated DN retina ones; but there was no difference among VT retina groups and the 1mM L-glutamate treated VT retina ones (Fig. E). Scale bars = 500μm (applies to A-D).

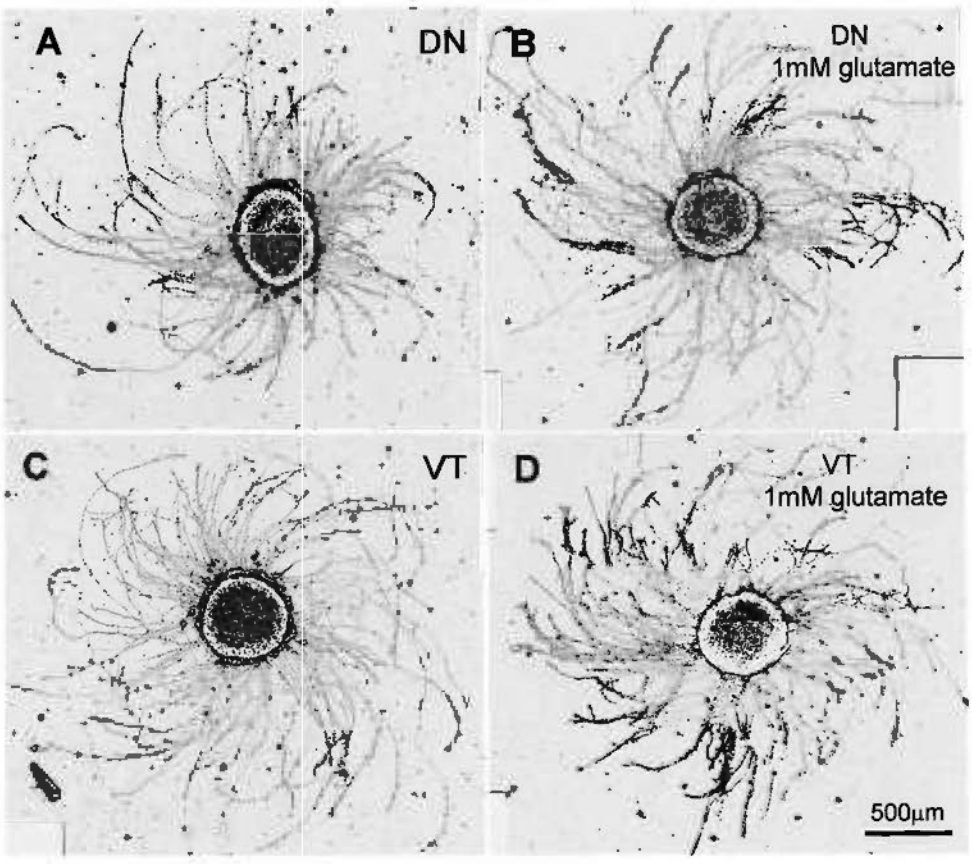
A
DN
B
DN
1mM glutamate
C
VT
D
VT
1mM glutamate
500µm

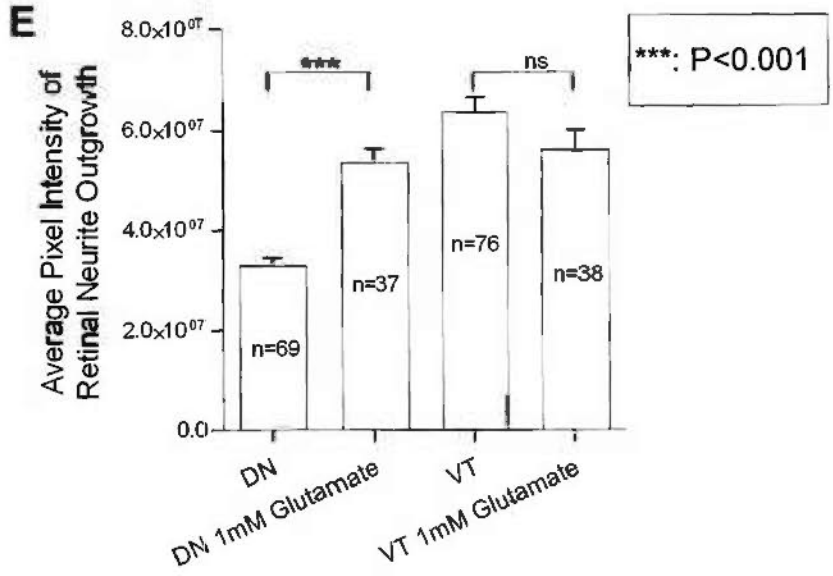
E
Average Pixel Intensity of Retinal Neurite Outgrowth
8.0x10^07
6.0x10^07
4.0x10^07
2.0x10^07
0.0
***
ns
***: P<0.001
n=69
n=37
n=76
n=38
DN
DN 1mM Glutamate
VT
VT 1mM Glutamate

CHAPTER 3

Localization and possible function of AMPA receptors in the developing mouse optic pathway

Introduction

AMPA (α-amino-3-hydroxy-5-methyl-4-isoxazole-propionic acid) is one of glutamate ionotropic receptor subtypes; AMPARs mediate most of the fast excitatory synaptic transmission. There are four isoforms of AMPAR subunits and each receptor is an oligomer composed of four of these subunits (GluR1-4, also named GluR-A-D) (Hollmann and Heinemann, 1994; Rosenmund et al., 1998). All AMPAR subunits have an intracellular C terminus, an extracellular N terminus, and four transmembrane-associated domains. There are stargazing or other transmembrane AMPAR regulatory proteins (TARPs) co-assembling with native AMPARs, which act as auxiliary subunits required for AMPAR maturation, trafficking and channel function.

Ca^{2+} entry through ionotropic glutamate receptors plays a pivotal role in synaptic plasticity, cognition (Isaac et al., 2007) and exitotoxicity (Hynd et al., 2004); it also participates in neuronal activity in the development of the CNS. AMPAR subtypes lacking GluR2 can elicit inward calcium currents, in contrast GluR2-containing

subtypes show no such permeability (Hollmann et al., 1991). Ca^{2+}-permeable AMPARs are now known to exist in a wide variety of neuronal types during development. Previous studies indicate that the impairment of GluR2 or its RNA editing at the Q/R, which will in turn increase the Ca^{2+} permeability of AMPARs, will induce neurological disorders such as epilepsy (Brusa et al., 1995), inflammatory pain (Hartmann et al., 2004) and amyotrophic lateral sclerosis (ALS) (Bogaert et al., 2010). Thus, Ca^{2+}-permeable AMPARs are also play an important role like NMDARs, which have a highly permeability to Ca^{2+}.

AMPARs are expressed in both neurons and glia throughout the CNS (Belachew and Gallo, 2004; Wisden and Seeburg, 1993b). The majority of AMPARs are GluR2-containing heteromers. The distribution of GluR1, GluR3 and GluR4 is regionally specific in the brain (Craig et al., 1993; Wenthold et al., 1996). During early postnatal development, expression of GluR2 is low compared with that of GluR1, but it increases rapidly in the first postnatal week (Monyer et al., 1991; Wisden and Seeburg, 1993b). There are also some reports that synaptic GluR2-lacking AMPARs can be detected in the neonatal pyramidal neurons during a restricted development period (Kumar et al., 2002; Pickard et al., 2000). All these may suggest that AMPARs play a prominent role in the neonatal synaptic function or early neuronal activity (Schmitz et al., 2009).

As described above, AMPARs lacking GluR2 are so important, how about GluR2 in the AMPAR family? The accumulating evidences show that GluR2 determines most of the major biophysical properties of the native receptor, such as single channel conductance, Ca^{2+} permeability, regulating other AMPAR subunits at the gene expression level, RNA editing, receptor assembly and trafficking (Feldmeyer et al., 1999; Hartmann et al., 2004; Shimshek et al., 2006a; Shimshek et al., 2006b).

Furthermore, genetic modulations of GluR2 affect phenotype of other AMPAR subunits (Higuchi et al., 2000). All these support the pivotal roles of GluR2 for the normal brain function.

As mentioned in chapter 2, glutamate is expressed extensively in the mouse developing retinofugal pathway, and in the whole ventral diencephalon. Meanwhile, the optic fibers travel along the retinofugal pathway; and glutamate as one of the neurotransmitters may act as chemoattractants for growth cone motility and synaptogenesis (Tashiro et al., 2003; Zheng et al., 1994). Therefore we want to explore localization and functionality of glutamate receptors in the retinofugal pathway. In this chapter, we chose AMPARs to study their expression pattern and further investigate their possible function in the optic fibers. For determining the function of AMPARs, we used CP465022 hydrochloride (Lazzaro et al., 2002) and GYKI52466 dihydrochloride (Paternain et al., 1995) to block the AMPARs.

Materials and Methods

Animal preparation

All the preparations followed that described in chapter 2.

Experiment reagents

Stock solutions were prepared by dissolving chemicals in water or dimethyl sulfoxide (DMSO) (1% maximal, final concentration) according to the manufacturer's recommendation. Stock solutions were either used directly at the working solution or diluted with 1xPBS, pH7.4 immediately before the experiment. The following chemicals were used: CP465022 hydrochloride (2-20μM) and GYKI 5466 dihydrochloride (25-150μM) (Tocris Co, UK).

RNA extraction and quantitation

According to Trizol Reagent instruction (Invitrogen Co, USA), RNA was extracted from the embryo retina, ventral diencephalon at different embryonic stages and in adult. In the whole process the dissected tissues were maintained in ice cold 1xPBS pretreated with diethyl pyrocarbonate (DEPC), pH 7.4.

(1).Tissues were dissected and dissolved in Trizol reagent 0.5ml per tube. (2). Added 0.1ml chloroform, shaken the tubes, and stored for 2 min at RT; then centrifuged at 12,000xg for 10 min at 4°C. (3). Transferred the aqueous phase to a new tube, added 250μl isopropyl alcohol, shaken the tubes; and stored for 10 min at RT; then centrifuged at 12,000xg for 10 min at 4°C. (4). Removed the supernatant, washed with 0.5ml 75% alcohol; then centrifuged at 7,500xg for 5 min at 4°C. Removed the supernatant again, briefly centrifuged 10 sec and then blotted the supernatant. (5). Dissolved the supernatant with appropriate DEPC water. (6). Used 1% agarose gel electrophoresis to detect the quality of the RNA. (7). Quantified the final concentration of RNA with the ultraviolet spectrophotometer, then stored in -80°C.

cDNA reverse transcription synthesis and RT-PCR analysis

According to ImProm-Ⅱ™ Reverse Transcription System kit instruction (Promega Co, USA).

(1). The whole operation was maintained in ice, mixed 2μg RNA template, 1μl Oligo(dT) and DEPC water to 5μl, then water bath 5 min in 70°C. (2). Added 4μl 5×Buffer, 4μl $MgCl_2$ (25mM), 1μl dNTP (10mM), 0.5μl RNasin, 1μl RTase and 4.5μl DEPC water to a final volume 20μl. Mixed and then water bath 5 min in 72°C, 1 hr in 37°C. (3). Finally 15 min in 70°C to inactivate enzymatic activity, stored in -20°C. (4). The polymerase chain reaction conditions were as follows: 30 cycles, each cycle consisting of denaturation at 94°C for 40 sec, anneal at different

temperature for individual gene as table 1 for 45 sec, and extension at 72°C for 45 sec. (5). Used 1.6% agarose gel electrophoresis to visual the amplified bands.

Table 1: Primers used for amplification of cDNA of AMPAR subunits and β-actin

Gene	GenBank Accession#	Sequence 5'-3'	Fragment Size (bp)
GluR1	NM_001113325		
Forward primer		GCTTCATGGACATTGACTTA	
Reverse primer		ATCTCAAGTCGGTAGGAATA	600bp
GluR2	NM_001083806		
Forward primer		AGAAAGATGGTCAACACTCG	
Reverse primer		GTCAGCTTGTACTTGAATCCA	612bp
GluR3	NM_016886		
Forward primer		AAACGATACTTGATTGACTG	
Reverse primer		GCTGATTTGTTGATCTGAGA	580bp
GluR4	NM_019691		
Forward primer		CAACTACTAGAAGAGCTTGACAGA	
Reverse primer		TTCCAATAGCCAACCTTTC	578bp
β-actin	NM_007393		
Forward primer		GCTGTATTCCCCTCCATCGTG	
Reverse primer		CACGGTTGGCCTTAGGGTTCA	362bp

Immunohistochemistry

To localize the expression of AMPAR subunits, GluR1-4, in the developing mouse retinofugal pathway, the heads of E13 to E18 embryos were fixed with 4% paraformaldehyde (PFA) in 0.1M PB at 4°C overnight. If the embryos were older than E15, usually fixed them for several hours at 4°C, changed to 1xPBS and removed the skull under the microscope as clean as possible especially that around the eyes. The following procedures were the same as described in chapter 2. The primary antibodies used were anti-GluR1 (1:100, Rabbit polyclonal IgG; Genscript,

USA), anti-GluR2/3 (1:250, Rabbit monoclonal IgG, Abcam, UK) and anti-GluR4 (1:60, Rabbit polyclonal IgG, Millipore, USA) and the corresponding secondary antibody was AF488 goat anti-rabbit IgG (1:200, Molecular Probes, USA).

Preparation of retinal explants and AMPAR subunit staining in retinal neurites and growth cones

The preparation of retinal explants was the same as described in chapter 2. The staining was processed according to the following procedures:

(1). Fixed the explants with 4% paraformaldehyde for 30 min at 4°C, and washed 5 min three times with 1xPBS. The immunostaining of GluR1-4 was carried out according to the protocol above, with the concentration of secondary antibody (AF488 conjugated goat anti- mouse IgM) at 1:500 (Molecular Probe, USA). (2). Their fluorescent signals in retinal neurites and growth cones were examined using a confocal microscope with oil lens (FV300, Olympus Co, Japan).

Western blotting

(1). Extracted protein of retina, and diencephalon of E14 embryos and from adult retina. The tissues were homogenized in RIPA buffer with a protease inhibitor cocktail (1:7; Roche Co, Switzerland). The extracted protein was quantified with DC protein assay (Bio-Rad, Hercules, and CA). (2). Prepared SDS-PAGE (7.5% or 10% separation gel and 5% stacking gel). (3). Loaded the boiled extraction protein and protein marker, 80V in the stacking gel, when running to the separation gel, then changed to 120V, stop running when bromophenol blue electrophoresis was 1cm to the bottom of gel. (4). Taken out the gel; from negative electrode to positive electrode, placed sponge-filter paper-gel-PVDF (Amersham, Sweden)-filter paper-sponge and fixed the transmembrane plate to transfer buffer, 100V, 2 hr. (5). The membrane was blocked in 5% non-fat milk in TBST (TBS with 0.1% Tween-20)

for 1 hr at RT, shaking. (6). The primary antibodies were incubated: anti-GluR1 (1:800), anti-GluR2/3 (1:5000) and anti-GluR4 (1:500) with 5% or 1% non-fat milk in TBST at 4°C overnight, shaking. (7). Washed membrane for 10 min, three times with 1xTBST, shaking. (8). Incubated HRP conjugated- Goat anti-rabbit IgG (1:3000) for 1 hr at RT, shaking. (9). Washed membrane for 10 min, three times with 1xTBST, and then changed to 1xTBS for 10 min, shaking. (10). Developed membrane with ECL Western Blotting detection kit (Amersham, Sweden). The signals were visualized on Detection Film (Fuji, UK) after being exposed in automated X-ray film developers.

Double staining with neuronal cell marker: TuJ-1 in the mouse retina

The following procedures were the same as described in chapter 2.

Double staining with Müller glial cell marker: Vimentin in the mouse retina

To identify the AMPAR subunits positive cells in the retina, Vimentin staining was performed on the retinal sections. Frontal or horizontal sections containing the retina and the optic disk were collected in 1xPBS and washed with 1xPBS for three times. The procedures were:

(1). Sections were blocked with 10% normal goat serum in 1xPBS for 1 hr at RT. (2). Incubated sections with the primary antibodies: 1) anti-GluR1, anti-GluR2/3 and anti-GluR4 and 2) Vimentin (1:100, mouse IgM, MAB1681, Chemicon, USA), a marker for Müller glia in the retina at 4°C overnight. (3). Washed sections for 10 min three times with 1xPBS; incubated sections with secondary antibodies at RT for 2 hr. The secondary antibodies for: 1) anti-GluR1, anti-GluR2/3 and anti-GluR4) and 2) Vimentin were AF488 conjugated goat anti- rabbit IgG and AF568 conjugated goat anti-mouse IgM. (4). After being washed for 10 min three times with 1xPBS, fluorescent signals on the sections were imaged using confocal microscopy (FV300,

Olympus Co, Japan). (5). Controls were prepared with the same procedures but in the absence of the primary antibody.

Double staining with the radial glial cell marker (RC2) and the stage-specific embryonic antigen (SSEA-1)

To identify the AMPAR subunits positive cells in the ventral diencephalon, RC2 or SSEA-1 double staining experiments were performed on the frontal or horizontal sections of the diencephalon. The procedures were:

(1). Sections were blocked with 10% normal goat serum in 1xPBS for 1 hr at RT. (2). Incubated with primary antibodies: GluR1, 2/3 and 4; and 1) RC2 (mouse IgM, 1:10; Developmental Studies Hybridoma Bank (DSHB), USA) in frontal sections at E14 or E15; or and 2) stage-specific antigen (SSEA-1) antibody (mouse IgM, 1:5; DSHB, USA) in horizontal sections at E13 at 4^{0}C overnight. RC2 is a marker specific for the radial glial cells in the mouse diencephalon (Mission et al., 1988; Marcus and Mason, 1995), and SSEA-1 is an antibody labeling the chiasmatic neurons in the mouse diencephalon. (3). Washed sections for 10 min three times with 1xPBS; incubated sections with secondary antibodies at RT for 2 hr. The secondary antibodies for: 1) anti-GluR1, anti-GluR2/3 and anti-GluR4 and 2) RC2 or SSEA-1 was AF488 conjugated goat anti- rabbit IgG and AF568 conjugated goat anti-mouse IgM. (4). After being washed for 10 min three times with 1xPBS, fluorescent signals on the sections were imaged using confocal microscopy (FV300, Olympus Co, Japan). (5). Controls were prepared with the same procedures but in the absence of the primary antibody.

Preparation of retinal explants and AMPAR antagonist treatments

The following procedures were the same as described in chapter 2, but the culture medium was changed to DMEM/F12 with high glucose (Invitrogen Co, USA)

supplemented with N1, 1% bovine serum albumin, and 0.4% methylcellulose (all were bought from Sigma Co, USA). For functional experiment, the AMPAR antagonists: CP465022 hydrochloride (2-20μM) or GYKI 5466 dihydrochloride (25-150μM) (Tocris Co, UK) was added to the culture medium at the beginning of the retinal explant culture. The control group was added the same volume of DMSO.

Analysis of the retinal explant outgrowth

The procedures followed that described in chapter 2.

Results

1. Expression of AMPAR subunits in different stages of the mouse retina and ventral diencephalon

1.1. AMPAR subunits expressed in distinct stages

After dissociation and reverse transcription of the total RNA of different stage retinas and ventral diencephalon, we first verified that the positive internal control (*β-actin*) could be amplified from these total RNA. Then AMPAR subunits were amplified from these total RNA (Fig. 1A). The different bands of PCR products at 600bp for *GluR1*; 612bp for *GluR2*; 580bp for *GluR3*; 578bp for *GluR4* and 362bp for *β-actin* were amplified.

All AMPAR subunits could be detected in the retina at as early as E13, with a progressive increase in receptor expression for all AMPAR subunits during the period examined. In adult retina, *GluR1* and *GluR2* remained at a high level of expression, but *GluR3* and *GluR4* were reduced to a relatively low level. In the ventral diencephalon, all these subunits except *GluR1* had no difference compared between that at E13 and E15. *GluR1* showed an obvious reduction in E15 ventral diencephalon when compared with that at E13 (Fig. 1A-B).

The different bands of protein at 106KD mol. wt for GluR1; 98KD mol. wt for GluR2/3 and 102KD mol. wt for GluR4 were detected in E14 retina and ventral diencephalon; and all of them had a low expression level in E14 retina when compared with adult retina and E14 ventral diencephalon (Fig. 1C).

1.2. Expression of AMPAR subunits on the neurites and growth cones of cultured retinal explants

As the gene and protein level was verified at as early as E13 and E14, respectively, we wanted to further confirm whether these subunits could be observed on retinal axons. Anti-GluR1, anti-GluR2/3 and anti-GluR4 were used to stain the cultured retinal explants. GluR1 and GluR4 were obviously found in the retinal neurites and growth cones; GluR2/3 could also be detected, but at a lower level than GluR1 and GluR4 (Fig. 1D).

GluR1 staining

2. Expression of GluR1 in the optic pathway during development

2.1. Expression of GluR1 in the mouse retina

2.1.1. Anti-GluR1 was stained in the retina at different stages

Anti-GluR1, a polyclonal antibody for one of the AMPA receptor subunits, was used to stain the GluR1 subunit expression in adult retina and developing retina from E13 to E18. No staining was detected in the control section at E13 (Fig. 2A). There was obvious staining in adult retina (n=2), Being strong in GCL, IPL, INL and OPL. No detectable staining was found in ONL (Fig. 2B). At E13 (n=6), the GluR1 staining was localized on the soma and processes of radial cells which span the whole thickness of the retina (Fig. 2C). In addition, strong staining of GluR1 was found in the CMZ, the lens and the blood vessels (Fig. 2C). At later stages, GluR1 displayed a

stronger neuronal localization compared with that at E13 (Fig. 2D-H). At E14 (n=6; Fig. 2D-E), there was a clearer neuronal staining pattern than that at E13; but the typically glial-like cells were disappeared. At E15 and E18 (n=5 and 2), GluR1 was intensely expressed in the inner retinal layer including the retinal axons and ganglion cells, the CMZ and the lens (Fig. 2F-H).

2.1.2. Double staining with anti-GluR1 and TuJ-1 in the retina

Double staining with anti-GluR1 and TuJ-1 was done in E14 retina. TuJ-1 positive neurons were confined to the inner layer and axon layer of the retina, which were also labeled strongly by anti-GluR1 (n=3; Fig. 3A, C-E). There was also positively double staining in the optic fibers (Fig. 3B). Furthermore, GluR1 positive staining was also found in the CMZ where TuJ-1 was nearly absent except in a few cells (Fig. 3A).

2.1.3. Double staining with anti-GluR1 and Vimentin in the retina

To identify these GluR1 positive cells, the retina was doubly stained with antibody against GluR1, and one of radial glial cell markers: Vimentin, an antibody for Müller cells in the vertebrate retina. They are critical for maintaining differentiated retinal structure and function (Bringmann et al., 2006). Recently reports have shown that Müller glia function as multipotent retinal stem cells generating retinal neurons by homeostatic and regenerative developmental mechanisms (Bernardos et al., 2007).

At E13 (n=6), most radially orientated cells stained by anti-GluR1 were Vimentin positive (Fig. 4A-D). In high magnification, the double labeled cell bodies were radially arranged in the retina and had long processes penetrated throughout the whole retina. However, there were some weak GluR1 positive cells which could not be stained by Vimentin (Fig. 4D).

2.2. Expression GluR1 in the mouse ventral diencephalon

2.2.1. GluR1 was stained in the ventral diencephalon

For the expression of GluR1, we stained the horizontal and frontal sections of the mouse ventral diencephalon from E13 to E15; GluR1 was highly detected in the OS, chiasm and the chiasmatic neurons in the E13 ventral diencephalon (n=6; Fig. 5A-B). In the OS and the OT, there were positive labels at E14 (n=8; Fig. 5C-D) However; GluR1 staining was also extensively observed in other regions of the ventral diencephalon. The same staining pattern was also shown at E15 (n=6; Fig. 5E-F). Moreover, in the frontal sections, the immunoreactive GluR1 was preferentially distributed in the OC and OT (Fig. 5G-H). In addition, it was also detected in some cells in the midline region above the axons in the OC (Fig. 5G).

2.2.2. Double staining with GluR1 and SSEA-1 in the ventral diencephalon

To examine the identity of the GluR1 positive cells in the ventral diencephalon, horizontal sections were doubly stained with antibodies against GluR1, and one of markers for the chiasmatic neurons: SSEA-1, a carbohydrate epitope (Stage Specific Embryonic Antigen-1) which is found in the chiasmatic neurons and at the midline of the chiasm (Marcus et al., 1995) that is related to the chiasmatic formation (Sretavan et al., 1995).

The double staining with anti-GluR1 and SSEA-1 showed that GluR1 was localized in SSEA-1 positive neurons in the ventral diencephalon at E13 (n=6, Fig. 6A-D). These staining suggested that part of the GluR1 positive cells dorsal to the chiasm were chiasmatic neurons. However, there were other GluR1 positive cells that were negative to anti-SSEA-1 (Fig. 6D).

2.2.3. Double staining with GluR1 and RC2 in the ventral diencephalon

To examine the identity of these GluR1 positive cells in the ventral diencephalon, frontal sections were doubly stained with antibodies against GluR1, and one of

markers for glial cell: RC2, an intermediate filament protein which is used to label the radial glial cells at the midline of the chiasm (Noctor et al., 2002). They may play a role in guiding migrating neurons or affecting their axons in the developing CNS (Rakic, 1972). The soma of a radial glial cell lies in the ventricular zone and a long radial process spans from its cell-body to the basement membrane at the pial surface.

In high magnification, the double staining with anti-GluR1 and RC2 showed that GluR1 positive cells could be colocalized with RC2 positive radial glial cell nucleus in the ventral diencephalon close to the ventricular zone at E14 (n=4; Fig. 7A-F). However, the intensity of GluR1 positive glial cells were very weak compared with that of the other regions in the chiasm (Fig. 7C, F).

GluR2/3 staining

3. Expression of GluR2/3 in the optic pathway during development

3.1. Expression of GluR2/3 in the mouse retina

3.1.1. Anti-GluR2/3 was stained in the retina at different stages

Anti-GluR2/3, a monoclonal antibody for one of the AMPA receptor subunits, was used to stain the GluR2/3 in adult retina and the developing retina from E13 to E18. In the control section at E13, no staining was detected (Fig. 8A). There was obvious staining in adult retina (n=2). The staining was localized largely in GCL, IPL, and OPL. Some cells in INL were immunopositive; there was almost no obvious in ONL (Fig. 8B). At E13 (n=8), the GluR2/3 staining was detected on the nuclei of radially arranged cells which were sparsely distributed throughout the retina and obviously in the OD, but not in the retinal axons (Fig. 8C-D). In addition, strong staining of GluR2/3 was observed in the CMZ and the blood vessels (Fig. 8C). At later stages, GluR2/3 displayed a neuronal expression pattern more obviously than that at E13,

but weakly in the retinal axons (Fig. 8E-H). At E14 (n=8), there were still some radially orientated cells in the OD and some supporting cells in optic nerve labeled by GluR2/3 antibody (Fig. 8E-F). At E15 and E18 (n=6 and 2), GluR2/3 was highly expressed in the inner regions of the retina, the CMZ and the lens, but weakly in the retinal axons (Fig. 8G-H and Fig. 15A-B).

3.1.2. GluR2/3 expressed on the TuJ-1 positive neurons in the retina

To identify the GluR2/3 positive cells, we did the double staining with anti-GluR2/3 and TuJ-1 which was labeled the developing neurons in retina. TuJ-1 positive neurons were confined to the inner layer and the axon layer of the retina, which were also strongly labeled by anti-GluR2/3 in the inner layer of the retina, weakly labeled in the axon layer at E14 (n=6; Fig. 9A-D). In addition, there are some radially arranged GluR2/3 positive glial-like cells which could no be stained by TuJ-1 (Fig. 9D).

3.1.3. GluR2/3 expressed on the Vimentin positive glia in the retina

To identify the GluR2/3 positive cells, we did the double staining with anti-GluR2/3 and Vimentin which is a glial marker, Most of the radial orientated cells stained by anti-GluR2/3 were Vimentin positive glial cells at E13 (n=4; Fig.10A-C). But the double staining was weak in the long processes of these cells (Fig. 10C). In the optic nerve, GluR2/3 positive cells could be doubly stained with Vimentin, indicating that the supporting cells in the optic nerve expressed GluR2/3 (Fig. 10D-E).

3.2. Expression GluR2/3 in the mouse ventral diencephalon

3.2.1. Anti-GluR2/3 was stained in the ventral diencephalon

For the expression of GluR2/3 in the ventral diencephalon, we stained the horizontal sections from E13 to E15. GluR2/3 was highly expressed in the cells around the midline and the third ventricle in the E13 (n=9) to E15 ventral diencephalon (Fig.

11A-H). There was intensely labeled with GluR2/3 at E14 and E15, which was found largely in the supporting cells in the optic stalk (OS). There was weakly labeled in the chiasm and the OT at E14 (n=8; Fig. 11C, E-G). Under high magnification, strong labels were observed in the supporting cells in the OS at E15 (n=4; Fig. 11F). In the upper layer of diencephalon (Fig. 11G-H), there was intensely stained in the cells around the OS, the midline near the OC and the surrounding region of the third ventricle. At E18, the staining in the OS and the OC was similar to that at earlier age, but in the diencephalon, the positive staining of GluR2/3 in the caudal regions was confined to the cell bodies and their processes (Fig. 15C-F).

In frontal sections of E15 diencephalon (n=5), GluR2/3 was strongly labeled in the cells around the third ventricle at the midline and the OC, but weak in the OS (Fig. 12A-B). Under high magnification, it showed that the staining was observed in the supporting cells, but weak in the chiasm (Fig. 12C-F).

3.2.2. GluR2/3 expressed on the SSEA-1 positive neurons in the ventral diencephalon

To identify the GluR2/3 positive cells, we did the double staining with anti-GluR2/3 and SSEA-1 which was labeled the chiasmatic neurons at E13. GluR2/3 was localized on SSEA-1 positive neurons in the ventral diencephalon (n=5; Fig. 13A-D), indicating that part of the GluR2/3 positive cells dorsal to the chiasm were chiasmatic neurons.

3.2.3. GluR2/3 stained in the RC2 positive radial glial cells in the ventral diencephalon

To identify the GluR2/3 positive cells, we did the double staining with anti-GluR2/3 and RC2 which was detected the radial glial cells in the ventral diencephalon at E14 (n=3; Fig. 14A-C). Under high magnification, there was obviously double staining

between GluR2/3 and RC2 close to the ventricular zone. However, there were still some GluR2/3 positive cells which were negative to anti-RC2 (Fig. 14C).

GluR4 staining

4. Expression of GluR4 in the optic pathway during development

4.1. Expression of GluR4 in the mouse retina

4.1.1. Anti-GluR4 was stained in the retina at different stages

Anti-GluR4, a polyclonal antibody for one of the AMPA receptor subunits, was used to stain GluR4 in adult retina and the developing retina from E13 to E18. In control section at E13, no staining was detected (Fig. 16A). There was obvious staining in adult retina (n=3). The staining was localized largely in GCL, IPL, INL, and OPL. No staining was detected in ONL (Fig. 16B). At E13 (n=7), there was obvious staining in the OD, but not in the retinal axons. In addition, strong staining of GluR4 was detected in the CMZ, lens and blood vessels (Fig. 16C, F). In high magnification, there were intensely labeled radially arranged glial-like cells in the OD and weakly in the retinal axons at E14 (n=6; Fig. 16D). There was weak staining in the retinal axons and clear in the supporting cells in the optic nerve (Fig. 16E). At later stages, GluR4 displayed a neuronal expression pattern more obviously than that at E13 (Fig. 16F-H). At E15 (n=5), GluR4 was highly expressed in the inner layer, which corresponds to the layer of ganglion cells, the CMZ and lens (Fig. 16F-H). The same pattern was detected at E18. But in all these stages, the staining in the retinal axons was relatively weak.

4.1.2. GluR4 expressed on the TuJ-1 positive neurons in the retina

To identify the GluR4 positive cells, we did the double staining with anti-GluR4 and TuJ-1 in E14 retina. TuJ-1 positive neurons were confined to the inner layer and the

axon layer of the retina, which were also strongly labeled by anti-GluR4 (n=4; Fig. 17A-C). Some TuJ-1 positive new-born neurons in the outer layer of retina were also stained (Fig. 17C). In addition, there were some GluR4 positive glial-like cells which could not be stained by TuJ-1 (arrows, Fig. 17C).

4.1.3. GluR4 expressed on the Vimentin positive glia in the retina

To identify the GluR4 positive cells, we did the double staining with anti-GluR4 and Vimentin which is a glial marker at E14 (n=6). Most of the GluR4 positive glial-like cells were Vimentin positive glial cells (Fig.18A-C). The doubly labeled cell bodies were radially arranged in the retina and had long processes extending throughout the whole thickness of the retina (Fig. 18C). However, there were also some GluR4 positive glial-like cells, which could not be stained by Vimentin (Fig.18C). These results showed that the Vimentin-positive Müller glia was also GluR4 positive; but anti-GluR4 antibody stained more than these, such as the new-born neuronal cells at this early stage.

4.2. Expression of GluR4 in the mouse ventral diencephalon

4.2.1. Anti-GluR4 was stained in the ventral diencephalon

For the expression of GluR4 in the ventral diencephalon, we stained the horizontal sections from E13 to E15 diencephalon. GluR4 was highly expressed in the chiasmatic neurons in the caudal region of the diencephalon and the cells around the OS at E13 (n=8; Fig. 19A-B). In the optic fibers, they were weakly labeled by anti-GluR4, but the obvious staining was observed in the midline region at E14 (n=5; Fig. 19C-D). In high magnification, GluR4 staining was clearly detected in the midline region at the OC (Fig. 19D). The same staining pattern was also shown at E15 (n=4; Fig. 19E-F). In the frontal sections, GluR4 was weakly labeled in the OC

and OT; it was also obviously shown in the glial-like cells along the ventricular zone and some cells in the midline region above the axons in the OC (Fig. 19G-H).

4.2.2. GluR4 expressed on the SSEA-1 positive neurons in the ventral diencephalon

To identify the GluR4 positive cells, we did the double staining with anti-GluR4 and anti-SSEA-1 which labeled the chiasmatic neurons at E13 (n=4; Fig. 20A-D). GluR4 was localized on SSEA-1 positive neurons in the ventral diencephalon, indicating that some of the GluR4 positive cells at the midline were chiasmatic neurons.

4.2.3. GluR4 stained in the RC2 positive radial glial cells in the ventral diencephalon

To identify the GluR4 positive cells; we did the double staining with anti-GluR4 and RC2 which labels the radial glial cells at the chiasm at E14 (n=6; Fig. 21A-F). Under high magnification, RC2 positive radial glia extended processes that ramified in the axon layer at the midline of the OC (Fig. 21A-B). There was also strong GluR4 staining at the midline of the OC, which was colocalized with RC2 staining (Fig. 21C, F); and these midline regions at the frontal sections were corresponding with the midline regions of the OC at the horizontal sections (Fig. 19 D, F).

5. AMPAR antagonists inhibited the retinal neurite outgrowth

To determine the function of AMPARs on the retinal axons, we cultured the E14 retinal explants as controls in vitro, neurites from the control retinal explants were densely distributed and grew a long distance. With the addition of different concentration of CP465022 hydrochloride (2-20μM, a noncompetitive AMPAR antagonist) or GYKI52466 dihydrochloride (25-150μM, a noncompetitive AMPAR antagonist), neurites were inhibited at the minimal concentrations: 5μM CP465022

hydrochloride and 50μM GYKI52466 dihydrochloride, respectively ($P<0.001$, $P<0.01$) (Fig. 22A-E and Fig. 23A-F).

Statistical data showed that there was significant reduction in neurite outgrowth in the presence of CP465022 hydrochloride or GYKI52466 dihydrochloride when compared with that of the corresponding control (Fig. 22F and Fig. 23G), confirming that activation of AMPARs could promote retinal axon outgrowth during the early prenatal periods of retinal pathway development.

As AMPARs are glutamate ionotropic receptors, blocking their activities in the explants cultures might induce the depolarization of cells through changing the ion concentration in the cytoplasm. Therefore, we tested the effects of depolarization with different concentrations of KCl. There was no difference between the different concentrations of KCl treated groups and control one (Fig. 24A-D), showing that inhibition of AMPAR antagonists was not induced by cellular ionic changes.

Discussion

AMPARs have been reported to mediate most of the fast excitatory synaptic transmission in the CNS, which can induce neurological disorders such as epilepsy (Brusa et al., 1995), inflammatory pain (Hartmann et al., 2004) and amyotrophic lateral sclerosis (ALS) (Bogaert et al., 2010). Previous studies report that high concentration of glutamate inhibits the axonal growth in culture hippocampal neurons (Mattson et al., 1988; McKinney et al., 1999); on the contrary, new-born neurites of cultured embryonic *Xenopus* spinal neurons can turn toward a local gradient of glutamate in a concentration dependent manner (Zheng et al., 1996). The recent study shows that glutamate can control dopaminergic axons grow and branch (Schmitz et al., 2009). Therefore, both endogenous and exogenous factors may

determine if glutamate can result in an effect on axonal growth. Here, we characterize the localization of GluR1-4 with three different antibodies that identify all of the subunits in the embryonic mouse retinofugal pathway, and explore preliminarily their function in the retinal axons.

1. Expression levels of AMPAR subunits are different in distinct stages

The distinct AMPA receptor subunits are detected at both mRNA and protein level in the mouse retina, ventral diencephalon and adult retina. All AMPA receptor subunit mRNAs are detected at as early as E13; and especially in retina, their mRNAs expression level gradually increases as the embryos grow. But in adult retina, GluR1 and GluR2 will be similar to that at P1; GluR3 and GluR4 will decrease to a relatively low level. At P1, their mRNAs expression level will become close to the maximal levels. This expression pattern agrees with the previous publications reporting that the functional glutamate receptors are corresponding to their optimal levels at E18 and postnatal days (Haberech et al., 1997; Monica L et al., 2007); and at these stages, the bipolar and amacrine cells will emerge from the ganglion cell layer in the retina.

GluR1, GluR2/3 and GluR4 subunit proteins are detected in adult retina, embryonic retina and ventral diencephalon at E14, which will be earlier than the previously reported embryonic stage (Watanabe et al., 1994; Zhang et al., 1996), and at adult. Especially, the expression level of these subunits is low in E14 retina compared with adult retina and ventral diencephalon. AMPAR subunits also express in the retinal neurites and growth cones at E14 with weak staining of GluR2/3 compared with the relatively strong GluR1 and GluR4 signals. However, the function of these subunits in the embryonic retina at this early stage of development remains unknown.

2. AMPAR subunits express in the mouse retinofugal pathway

2.1. AMPR subunits express in the retina

According to immunocytochemical and in situ hybridization studies of receptor subunits, all the pharmacologically defined ionotropic glutamate receptors are found in the adult as well as the developing mouse retina (Hartveit et al., 1994; Zhang et al., 1996; Wenzel et al., 1997; Sucher et al., 2003). There are only a few reports about AMPA receptor subunits expression in the E13 to E15 retina. To determine their localization, we used GluR1, GluR2/3 and GluR4 antibodies to stain the developing retina.

At E13 and E14, all these antibodies could stain the neurons in retinal inner layer and some Vimentin expressing glial (Müller) cells. Müller cell is the only glial cell type in the developing retina, its processes span from the inner layer to the outer limiting membrane. It might be the analogous to the radial glial cell in the central nerves system (CNS). The glial cell scaffold can play a guidance role for the neuron migration (Leber et al., 1990; Hattern, 1999). Müller cell in the retina might also play a similar role to stabilize cell columns during the retinal development (Willbold et al., 1995). Some other studies indicate that as Müller cells develop, they could change to neurons via the neurogenic retinal progenitor cells (Fischer and Reh, 2003). Compared with L-glutamate staining in the glial-like cells in the retina, the AMPA receptor subunits are more commonly found on Müller cells, staining the cell body and its processes. Especially around the optic disk, all these antibodies can stain the supporting glial cells; but only GluR1 antibody strongly stains the axons in the optic disk. The distribution of the ligand (glutamate which has been described in the chapter 2) and its receptor subunits might give us some cues to predict possible function of L-glutamate which is related to the formation of retinofugal pathway in

the prenatal periods.

At E14 and E15, through the double staining with TuJ-1 antibody, which is a neuronal marker, all these receptor subunits can be colocalized with TuJ-1 antibody in the retinal inner layer (RGC layer). GluR1 can also be found in the retinal axon layer. Our experiments provided for the first time evidence for AMPA receptor subunits (GluR1 and GluR4) clustering along the cell plasma membrane in sections, and on the explant neurites and the growth cones in vitro. However, in retina, only GluR1 can be strongly stained in the axon layer; GluR4 was weakly in the axon layer. For GluR2/3, it can be stained weakly in the axon and the growth cones in vitro. In retina, the GluR2/3 staining clusters in the nucleus of the neuron and the glial cell; there is almost no staining in the axon layer. This staining pattern exists in the immature retina; there are also some reports in the immature brain consistent with our study that AMPAR subunits stain the axonal and dendritic growth cones (Martin et al., 1998; Vaughn, 1989). Previous studies show that AMPA receptors cluster along the plasma membrane and at presynaptic and postsynaptic neuritic components of emerging synapses (Martin et al., 1993; Petralia and Wenthold, 1992). In morphologically mature synapses, GluR1 is solely found in the postsynaptic terminals and extensively stains in the somatodendritic compartment. In hippocampal neuronal cultures, GluR1 is located in both dendritic and axonal growth cones, but the localization of GluR1 becomes restricted to the somatodendritic compartment as neurons establish their polarity (Craig et al., 1993). GluR1 can be found presynaptically at developing synapses in immature brain but not presynaptically in mature brain (Martin et al., 1993).

The staining of GluR2/3 is localized in the nucleus in the developing retina. As the retina grows, the staining will extend to the whole cell then restricted to the

somatodendritic compartment, but not on the axonal growth cones. This staining pattern may suggest that Ca^{2+}-permeable AMPARs lacking GluR2 may participate in neuronal activity during the retinal development (Kumar et al., 2002). From the staining pattern, AMPA receptor is thought to participate in regulating dendritic and axonal outgrowth and later synapogenesis of retinal cells (Mattson et al., 1988; Pearce et al., 1987), thus they might function in regulating early activity dependent maturation of neurites and formation of synapse.

2.2. AMPR subunits express in the ventral diencephalon

Through this study, we find that GluR1 evidently expresses in the optic stalk, optic chiasm and optic tract. There are also some unknown neurons labeled by this antibody near the ventricular zone. At E14, the GluR1 positive cells can be colocalized with RC2 positive glial cells at the midline in the frontal sections, where the GluR1 staining is found on the glial cell nucleus different with that in other cells; but the staining in the diencephalic glial cells is weak. It also stains chiasmatic neurons, which is identified by SSEA-1 antibody. SSEA-1 is a specific neuronal marker for the chiasmatic neurons which are generated earlier than the retinofugal pathway.

For GluR2/3, it stains the supporting cells in the optic nerve and optic chiasm; it can not stain the axons in the retinofugal pathway. The GluR2/3 staining is observed in the nucleus but not on the cell membrane as the staining in the retina; but as the diencephalon develops, the staining will change to the somatodendritic compartment (shown in Fig. 15). This variable staining pattern is obvious; but their function remains to be clarified. One hypothesis is that receptors with GluR2 subunit are not calcium permeable, if these AMPA receptors play a role in axon growth through the calcium-dependent pathway, it is reasonable that GluR2 free receptors dominating in

the axons. For GluR4, it stains some supporting cells in the optic nerve, weakly in the optic fibers; but strong intensity is found at the midline in the ventral diencephalon. With the double staining, both GluR2/3 and GluR4 can be labeled in the RC2 positive and SSEA-1 positive cells. Especially for GluR2/3 staining, it will strongly label glial cell nucleus near the ventricular zone; this pattern is different between GluR1 and GluR4 staining. GluR4 staining is also different with other subunits; in the frontal sections, there is obvious staining identified by RC2 and the colocalization is not only found on the glial cells but also on the processes. These GluR4 positive glial cells are prominent near the midline; and they have some short processes, but not extend to the optic chiasm axon layer. However, their function in the glial cells of ventral diencephalon needs us further investigation.

3. AMPAR antagonists inhibit the retinal neurite outgrowth

Glutamate can promote the retinal axon growth in the retinal explant culture experiment at E14. We want to investigate whether AMPARs are involved in this axon growth activity. Our data demonstrate that both CP465022 hydrochloride and GYKI52466 dihydrochloride can inhibit retinal axon outgrowth. This result may correspond with the staining results, which show the GluR2/3 staining is localized in the nucleus in the embryonic stages, not on the cell bodies and axons; and GluR1 and GluR4 are expressed in retinal neurites and growth cones. This pattern suggests that Ca^{2+}-permeable AMPA receptors may play a critical role in the retinal axon growth.

As a summary, the staining pattern of these specific subunits might be different; but they are all found in the Vimentin and RC2 positive glial cells, TuJ1 and SSEA-1 positive ganglion cells and chiasmatic neurons respectively. These positive cells took parts in the retinofugal pathway formation. For individual subunit, the immunoreactive GluR1 is preferentially distributed in the optic fibers along the

pathway; the immunostaining of GluR2/3 and GluR4 are largely found in the supporting cells around the pathway, although weak staining of GluR4 could be detected in the optic fibers and typically in the midline. All these subunits with different composition might affect the retinal axon growth.

Figures

Figure 1. The expression of AMPAR subunits in the retinas and ventral diencephalons at different stages. *GluR1-4* and *β-actin* were respectively detected in adult retina, E13 retina (E13R), E15 retina (E15R), E16 retina (E16R), P1 retina (P1R), E13 ventral diencephalon (E13VD) and E15 ventral diencephalon (E15VD) (Fig. A). The plot showed that a progressive increased in receptor enrichment expression for all AMPAR subunits during the period examined. But in the adult retina, *GluR1* and *GluR2* remained at a high level of expression; but *GluR3* and *GluR4* were reduced to a relatively low level. In the ventral diencephalon, all these subunits except *GluR1* had no obvious difference compared between that at E13 and E15; *GluR1* showed an obvious reduction in E15 ventral diencephalon when compared with that at E13 (Fig. A-B). Western blotting showed that different bands with 106KD, 98KD and 102KD were identified for GluR1, GluR2/3 and GluR4 subunits at E14 (Fig. C). Immunostaining of retinal explant culture of GluR1-4 subunits indicated that retinal neurites and growth cones (arrows) were expressed with AMPAR subunits; the intensity of GluR2/3 was weaker compared with that of the others (Fig. D). Scale bars = 50μm in GluR1 (also applies to GluR4); 20μm in GluR2/3.

A

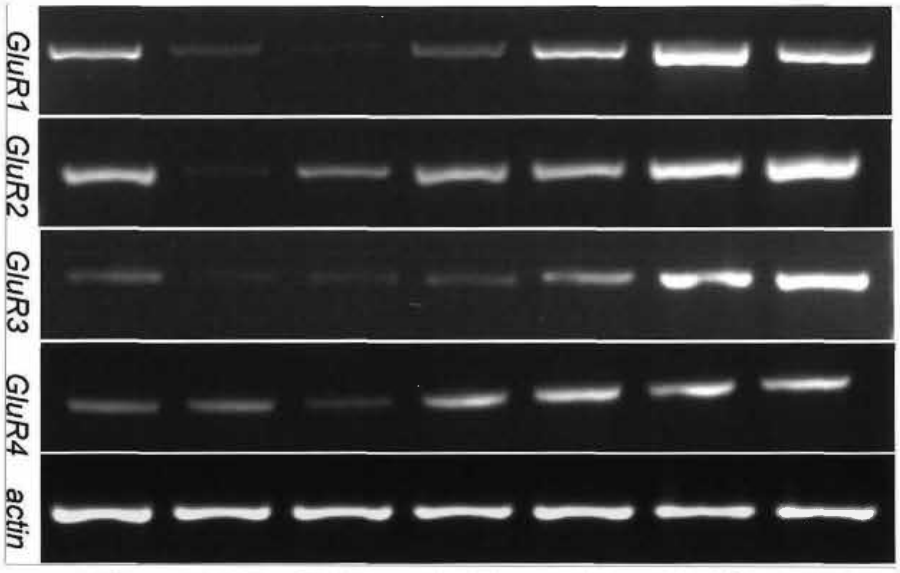
GluR1
GluR2
GluR3
GluR4
actin
AR
E13R
E15R
E16R
P1R
E13VD
E15VD

B

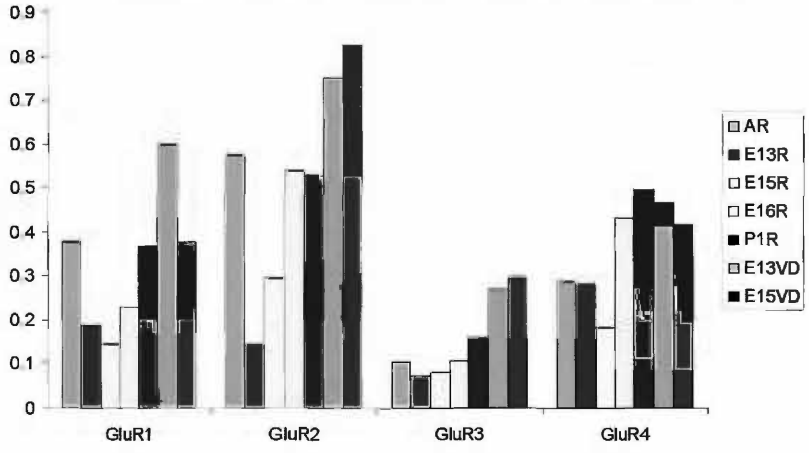
0.9
0.8
0.7
0.6
0.5
0.4
0.3
0.2
0.1
0
GluR1
GluR2
GluR3
GluR4
AR
E13R
E15R
E16R
P1R
E13VD
E15VD

C

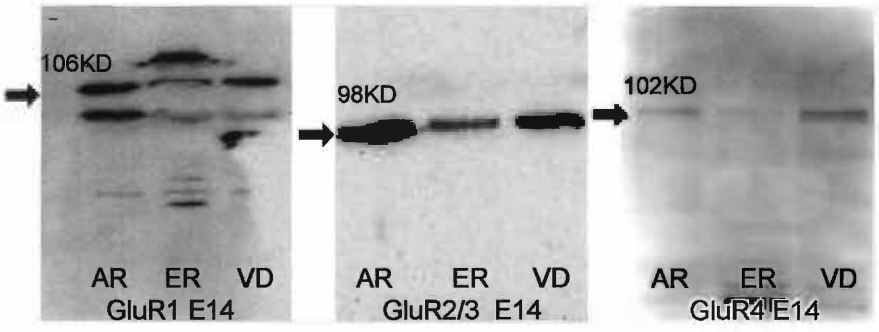
106KD
98KD
102KD
AR ER VD
GluR1 E14
AR ER VD
GluR2/3 E14
AR ER VD
GluR4 E14

D

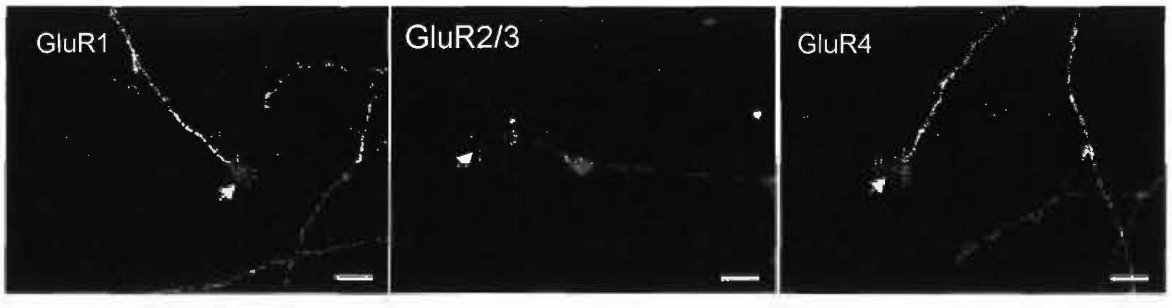
GluR1
GluR2/3
GluR4

GluR1 staining

Figure 2. Immunostaining of retinal sections for anti-GluR1 at different stages. In control section at E13, no staining was detected. L was for lens, R for retina (Fig. A). There was obvious staining in adult retina (n=2), being strong in GCL, IPL, INL, and OPL. No detectable staining was observed in ONL (Fig. B). At E13 (n=6), the staining was localized in the cell body and the processes of radially arranged cells (arrow) (Fig. C). In addition, strong staining of GluR1 was abundantly detected in the ciliary marginal zone (CMZ) (asterisks), the lens and the blood vessels (arrows) (Fig. C). At E14 (n=6; Fig. D-E), there was a clearer neuronal staining pattern than that at E13; but the typically glial-like cells were disappeared. At E15 (n=5; Fig. F-G), there were strongly labeled in the axon layer and the inner layer of the retina. The GluR1 staining was also detected in the OD and the surrounding glial-like cells (arrows) (Fig. F). There was a same staining pattern at E18 as those at E14 and E15 (n=2; Fig. H). Scale bars = 200μm in A (also applies to C-D); 50μm in B (also applies to H); 100μm in E (also applies to F-G).

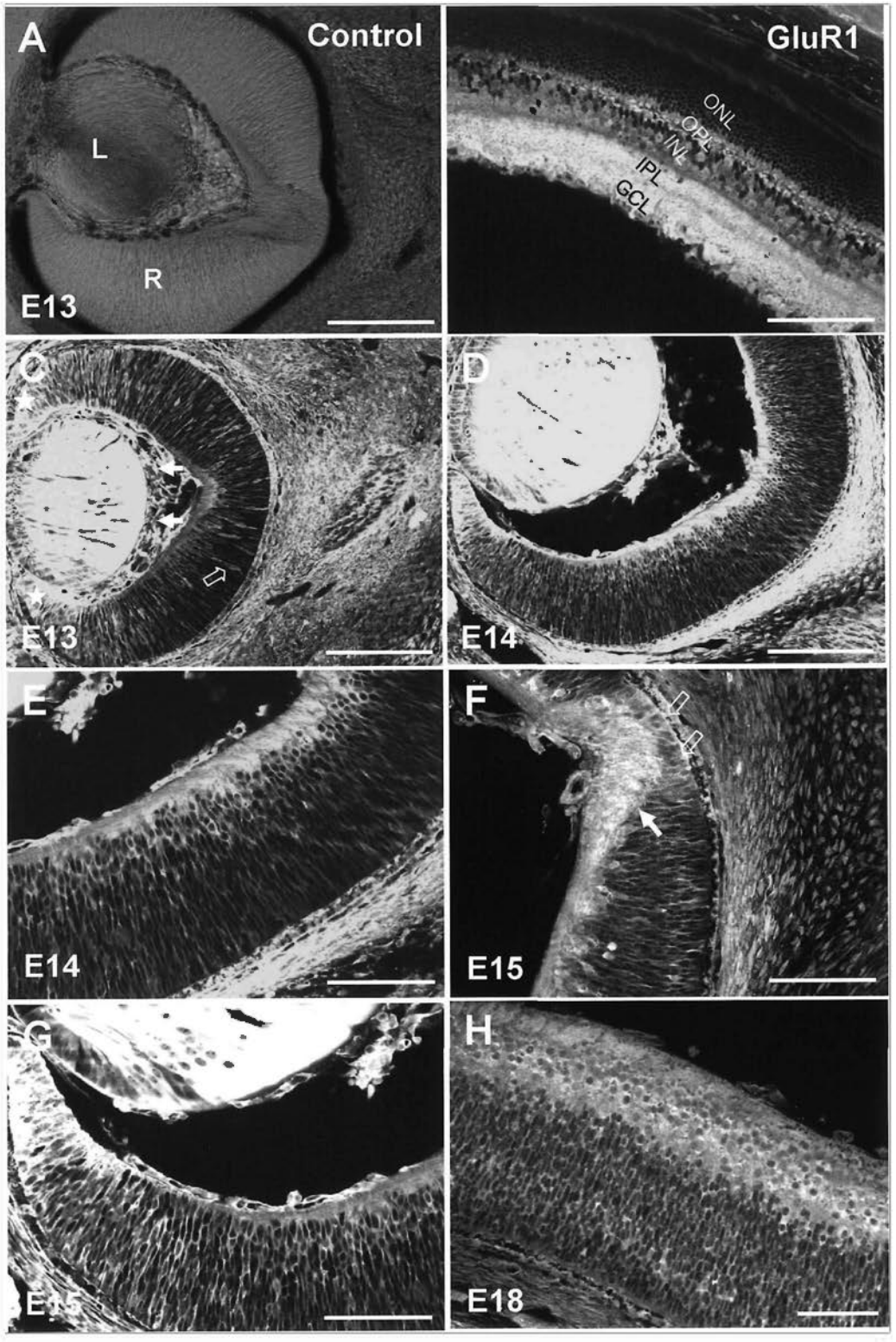
A
Control
L
R
E13
GluR1
ONL
OPL
INL
IPL
GCL
C
E13
D
E14
E
E14
F
E15
G
E15
H
E18

Figure 3. Immunostaining of retinal sections for TuJ-1 and anti-GluR1 at E14. In low magnification, GluR1 positive staining was colocalized with TuJ-1 positive neurons except in the ciliary marginal zone (CMZ) (arrow) at E14 (n=3; Fig. A); and could also be merged together in the optic nerve (arrow) (Fig. B). In high magnification, prominent TuJ-1 staining was shown in the inner layer and the axon layer of retina (Fig. C). At the same section, the strong GluR1 staining was detected in the axon layer, the cell body of the inner layer and radially arranged cells in the outer layers (Fig. D). In the merged image, it revealed that most GluR1 staining was localized in TuJ-1 positive neurons, including the retinal axons (arrows and arrowheads) (Fig. E). Scale bars = 200μm in A (also applies to B); 100μm in C (also applies to D-E).

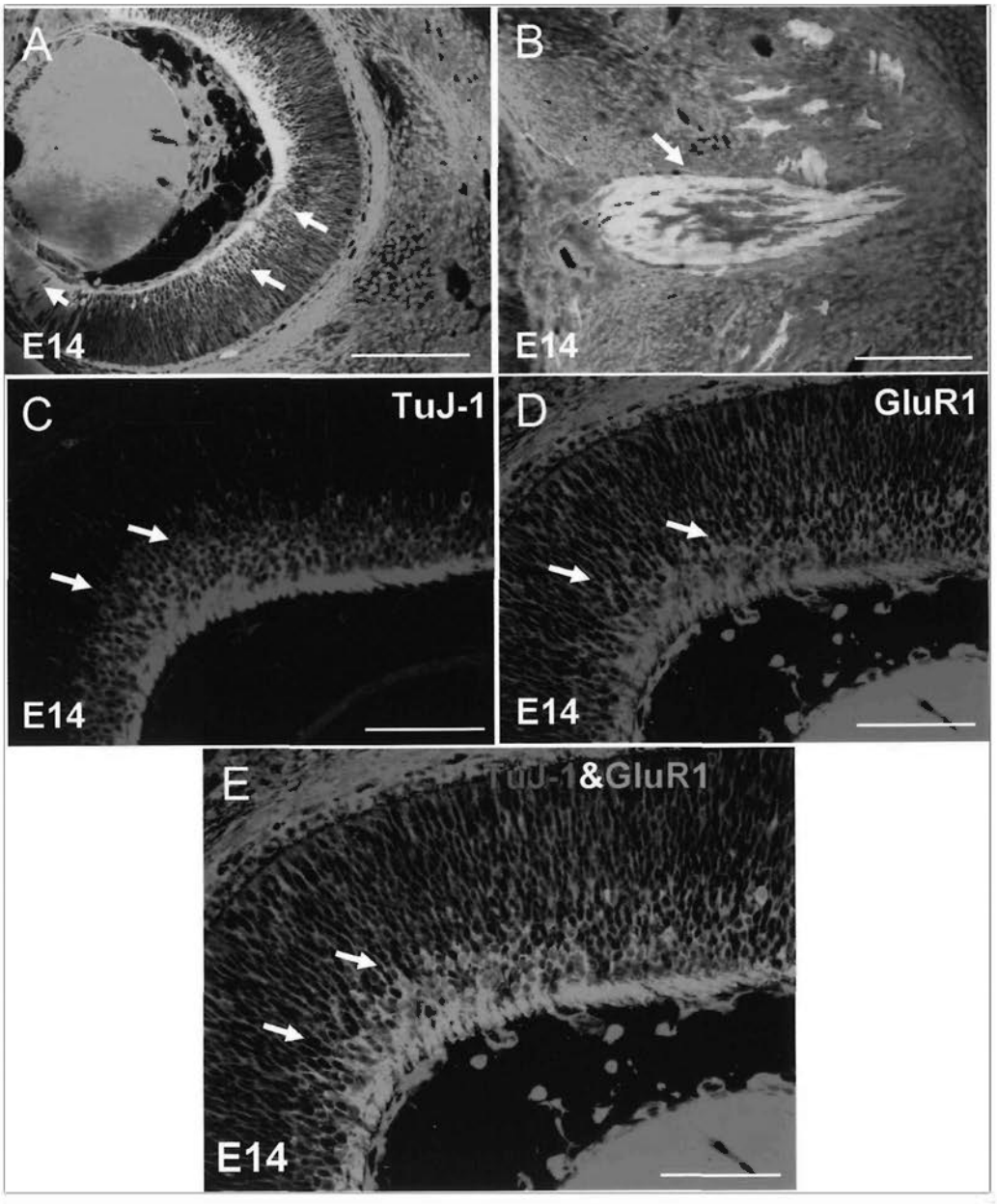
A
E14
B
E14
C
TuJ-1
E14
D
GluR1
E14
E
TuJ-1 &GluR1
E14

Figure 4. Immunostaining of retinal sections for Vimentin and anti-GluR1 at E13. In high magnification, the cell body and the processes of Müller glia in the retina was obviously labeled by Vimentin antibody in the outer layers (arrows) (n=6; Fig. A). At the same section, GluR1 was expressed in the radial cells and the processes of these cells (arrows) (Fig. B). The merged image indicated that GluR1 could be stained in the Vimentin positive Müller glia (arrows) (Fig. C). The higher magnification images showed the merged staining of these two antibodies (arrows) (Fig. D). Scale bars = 100μm in A (also applies to B-C); 20μm in D.

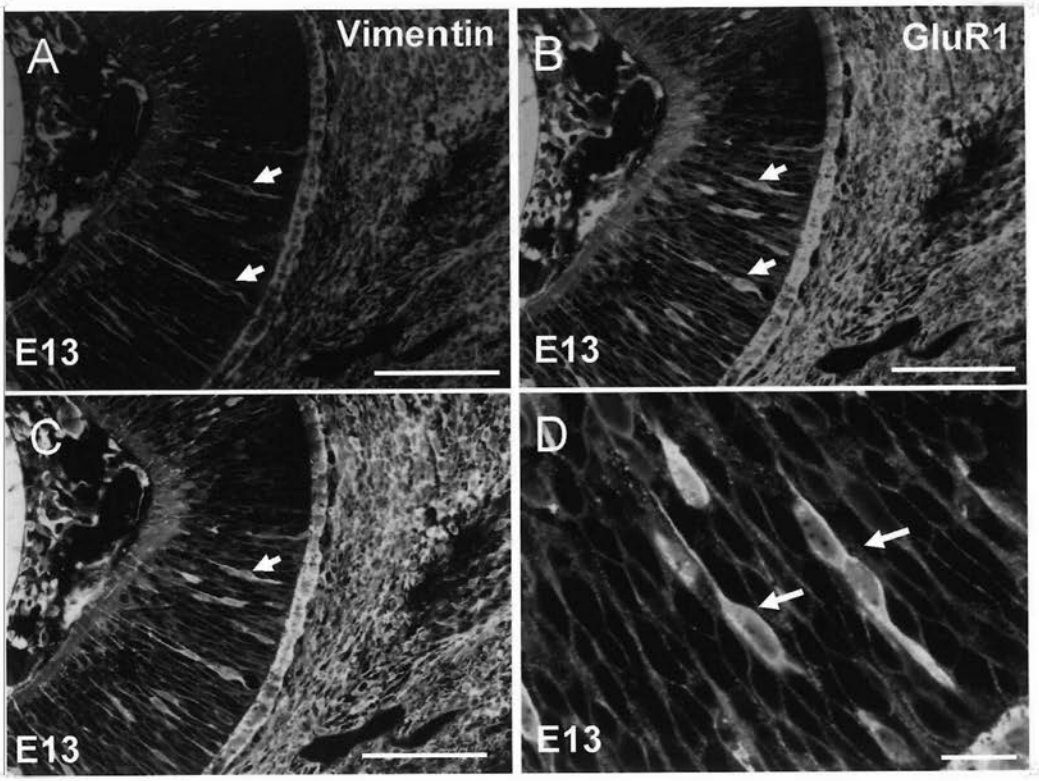
A
Vimentin
E13
B
GluR1
E13
C
E13
D
E13

Figure 5. Immunostaining of ventral diencephalic sections for anti-GluR1 at different stages. In the horizontal sections, rostral was to the top and the midline was indicated by the arrows. In the frontal sections, dorsal was to the top and the midline was indicated by the arrows. GluR1 was highly expressed in the cells beside the third ventricle in the E13 ventral diencephalon (n=6; Fig. A). Further image showed that the GluR1 positive cells shaped an upside down 'v' in the ventral diencephalon (Fig. B). GluR1 was stained in the OS, the optic tract (OT) and the cells around the third ventricle at E14 (n=8, Fig. C). The GluR1 staining was showed in high magnification at E14 (Fig. D). There was the positive label same as the E14 staining at E15 (n=6; Fig. E). In high magnification, there was strong staining in OS which was entering the optic chiasm (arrowheads); and in the cells around the midline (arrows) (Fig. F). In the frontal sections, there was strong staining in the optic chiasm (OC) and OT; and some cells (arrowheads) were dorsal to the OC (Fig. G-H). Scale bars = 200μm in A (also applies to C, E, H); 200μm in B (also applies to D); 100μm in F (also applies to G).

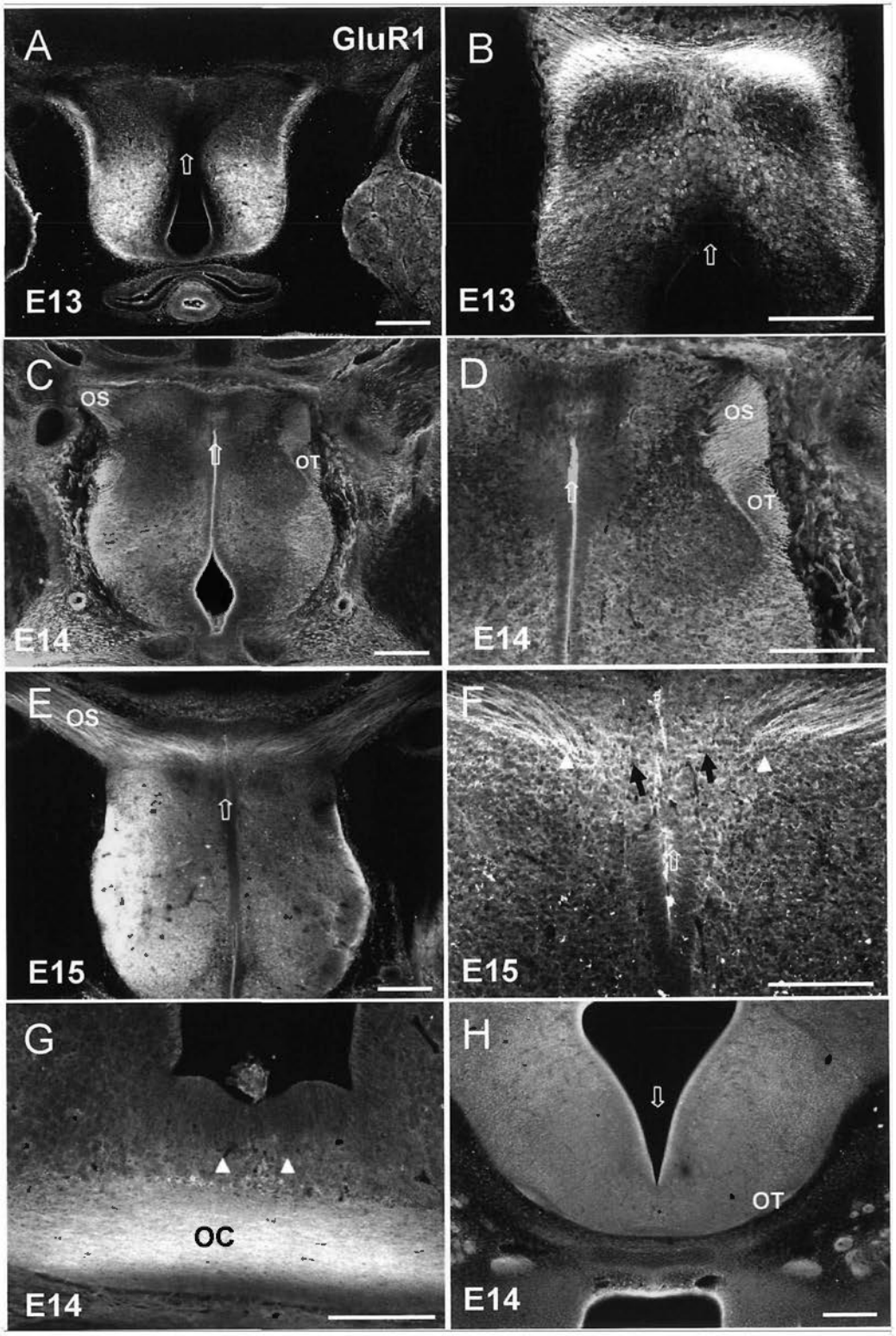
A
GluR1
E13
B
E13
C
OS
OT
E14
D
OS
OT
E14
E
OS
E15
F
E15
G
OC
E14
H
OT
E14

Figure 6. Immunostaining of ventral diencephalic sections for SSEA-1 and anti-GluR1. These were the horizontal section; rostral was to the top and the midline was indicated by the arrow. The merged staining with GluR1 and SSEA-1 was colocalized beside the third ventricle in low magnification at E13 (n=6; Fig. A). In the high magnification, the GluR1 and SSEA-1 staining was also obviously detected beside the third ventricle of diencephalon (Fig. B-C). The merged image showed that some of the GluR1 positive cells dorsal to the chiasm were the SSEA-1 positve chiasmatic neurons (Fig. D). Scale bars = 200μm in A; 100μm in B (also applies to C-D).

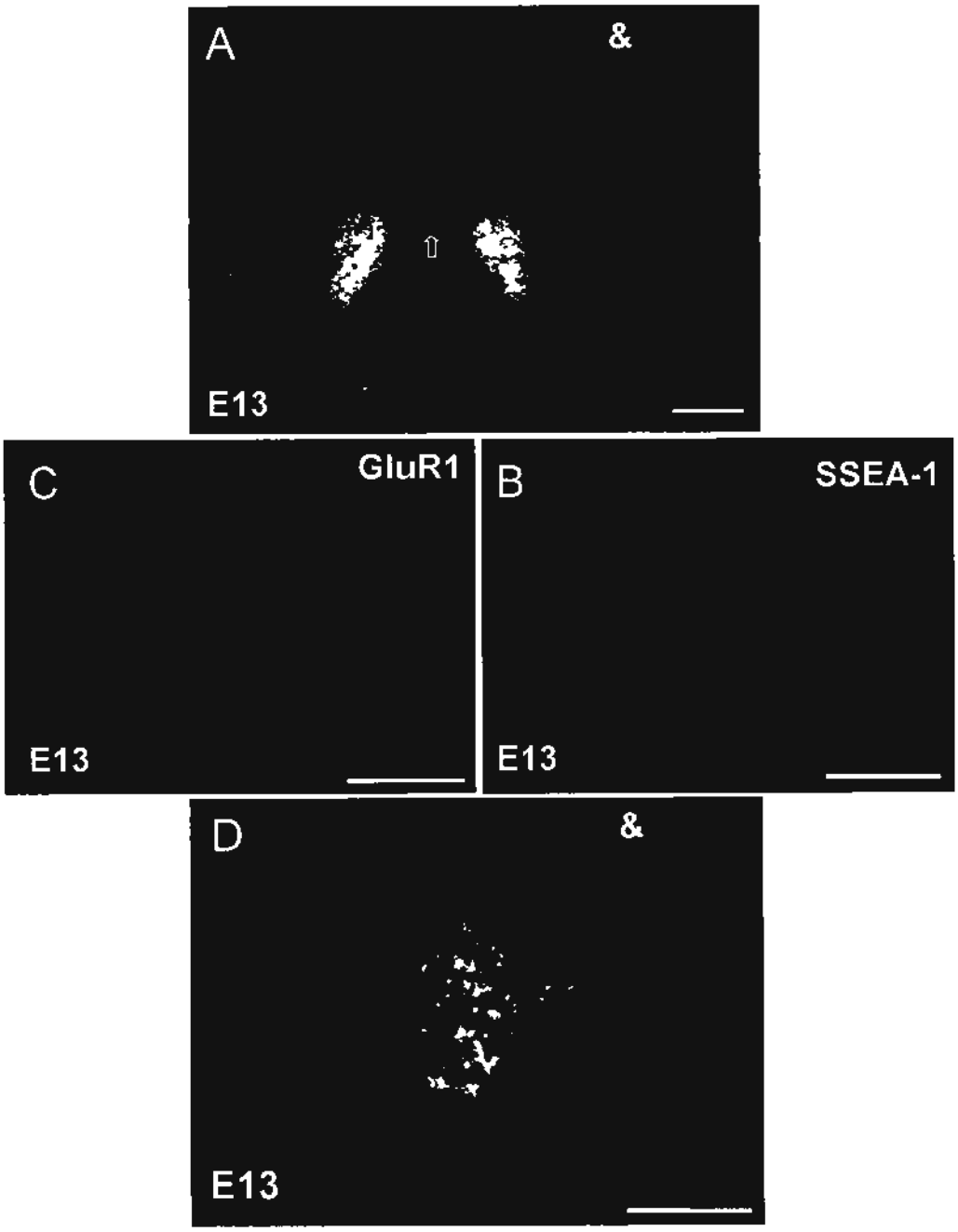
A
&
E13
C
GluR1
E13
B
SSEA-1
E13
D
&
E13

Figure 7. Immunostaining of ventral diencephalic sections for RC2 and anti-GluR1. The RC2 staining was found in the whole cell and its process (n=4; Fig. A, D). The GluR1 staining was obviously detected in the OC (Fig. B, E). The double staining with anti-GluR1 and RC2 antibody showed that GluR1 positive cells could be colocalized with RC2 positive radial glial cell nucleus in the ventral diencephalon close to the ventricular zone at E14 (n=4; Fig. C, F). However, the intensity of GluR1 positive glial cells was very weak compared with the other regions in the chiasm; the obvious staining was not RC2 positive cells, but some cells in the midline region above the axons in the OC (Fig. B, E). Scale bars = 50μm in A (also applies to B-G).

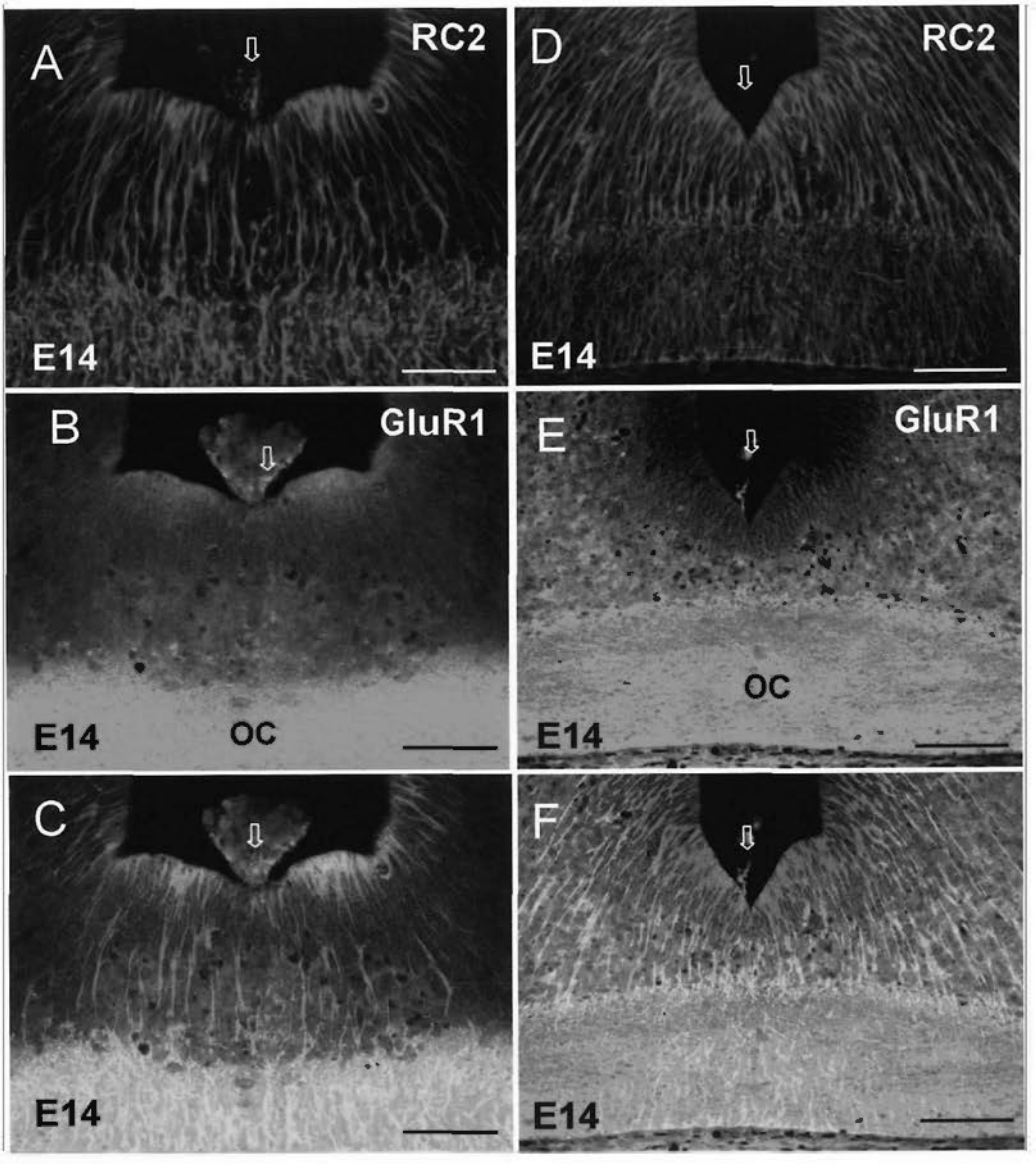
A
RC2
E14
D
RC2
E14
B
GluR1
E14
OC
E
GluR1
OC
E14
C
E14
F
E14

GluR2/3 staining

Figure 8. Immunostaining retina sections for anti-GluR2/3 at different stages. In control section at E13, no staining was detected. L was for lens, R for retina (Fig. 8A). There was obvious staining in adult retina (n=2). The staining was localized largely in GCL, IPL, and OPL. Some cells were observed in INL; there was almost no obvious in ONL (Fig. B). At E13 (n=8), the staining was localized on the nuclei and almost no staining in the processes of radial arranged cells (Fig. C). In addition, strong staining of GluR2/3 was abundantly detected in the ciliary marginal zone (CMZ) (asterisks), the surrounding cells of the optic disk (OD) and the blood vessels (arrows); but weakly stained in the axon layer of retina (Fig. C). In high magnification, there was obviously labeled the form of the radially arranged nuclei and very weakly labeled in the retinal axons. Furthermore, there were strongly labeled glial-like cells around the OD (Fig. D). At E14 (n=8), there still were some radially orientated GluR2/3 positive cells in the outer layers, but the strong staining was focused on the inner layer; and in the surrounding cells in OD (arrows) and the optic stalk, almost no labeling in the axon layer (Fig. E-F). At E15 (n=6), GluR2/3 was highly expressed in the retinal inner cellular layer (arrows); and the radially orientated cells in the outer layers (arrows) (Fig. G-H). Scale bars = 200μm in A (also applies to C, E, G); 100μm in B (also applies to D, F, H).

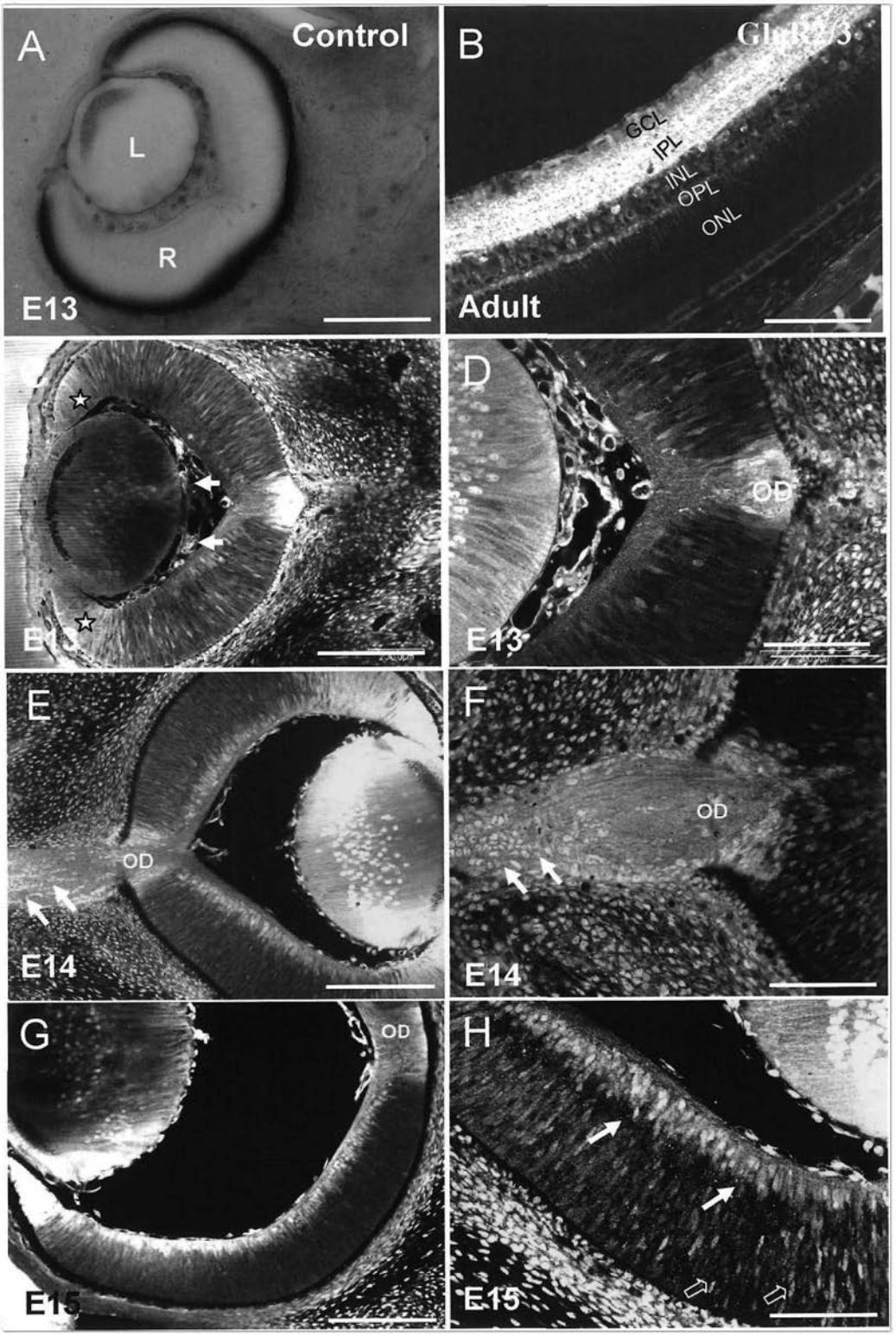
A
Control
L
R
E13
B
GCL
IPL
INL
OPL
ONL
Adult
D
OD
E13
E
OD
E14
F
OD
E14
G
OD
E15
H
E15

Figure 9. Immunostaining of retinal sections for TuJ-1 and anti-GluR2/3. In low magnification, L was for lens, R for retina; GluR2/3 positive staining was colocalized with TuJ-1 positive neurons except in the ciliary marginal zone (CMZ) (arrow) (n=6; Fig. A). In high magnification, prominent TuJ-1 staining was shown in the axon layer and inner layer of retina, sparsely labeled developing neurons in the outer layers at E14 (Fig. B). At the same section, strong GluR2/3 staining was revealed in the nuclei of the inner layer and radially shaped cell nucleus in the outer layers; but very weakly labeled in the axon layer (Fig. C). In the merged image, it showed that most GluR2/3 staining was localized in TuJ-1 positive neurons (arrows), but weakly labeled in the axons. There still were other GluR2/3 positive cells which could not be stained by TuJ-1 in the outer layers (arrows) (Fig. D). Scale bars = 200μm in A; 100μm in B (also applies to C-D).

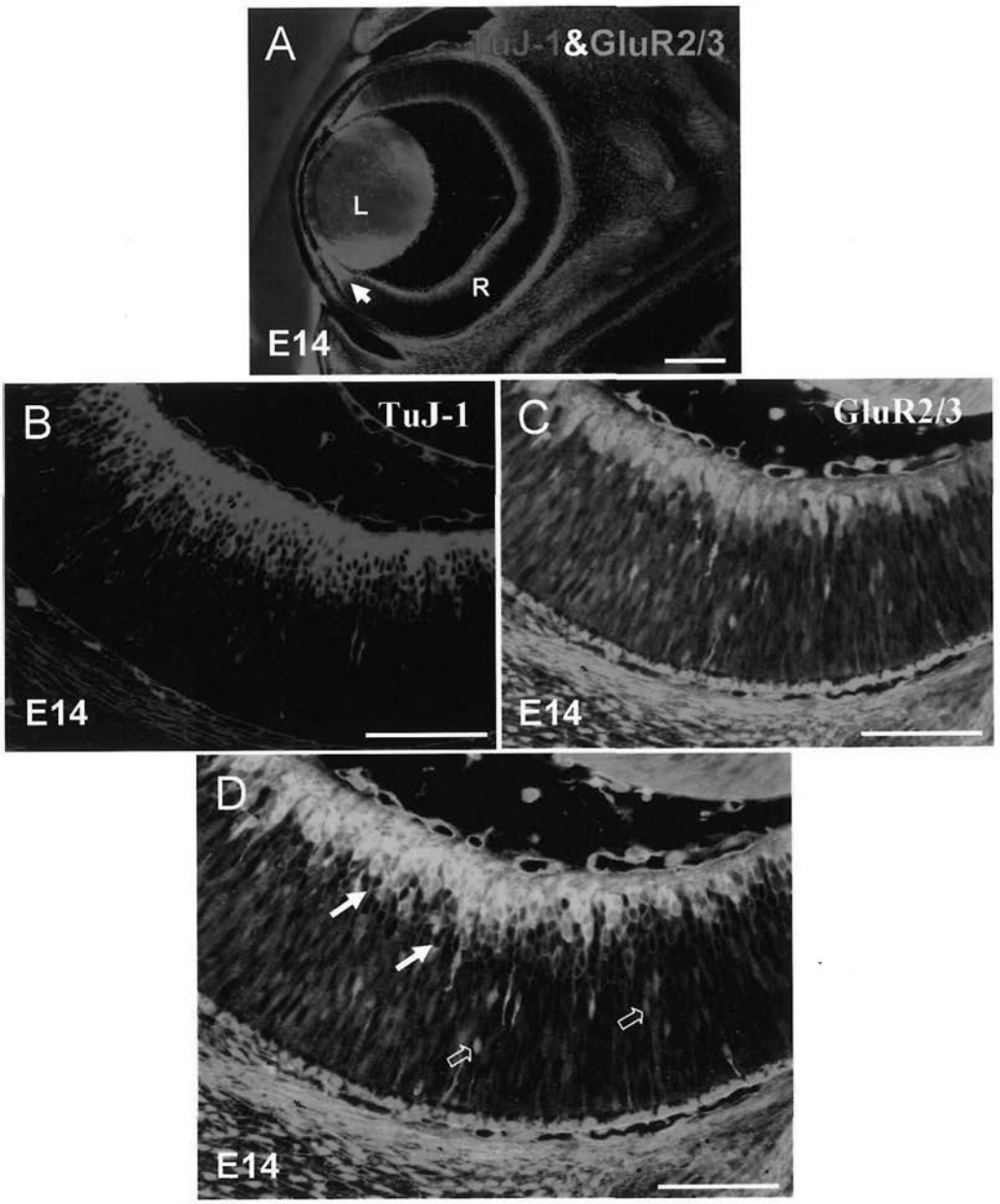
A
TuJ-1&GluR2/3
L
R
E14
B
TuJ-1
E14
C
GluR2/3
E14
D
E14

Figure 10. Immunostaining of retinal sections for Vimentin and anti-GluR2/3. In high magnification, the cell bodies and the processes of Müller glia in the retina was obviously labeled by Vimentin antibody in the outer layers (n=4; Fig. A). At the same section, GluR2/3 was expressed in the nuclei of glial-like cells, and almost no staining in the processes of these cells (Fig. B). The merged image indicated that GluR2/3 could be stained in the Vimentin positive Müller glia (arrows); but the staining was confined to the nuclei (Fig. C). The GluR2/3 antibody was labeled in the supporting cells in the optic stalk (Fig. D). The merged image showed that GluR2/3 positive cells could be doubled with Vimentin in the optic stalk (arrows) (Fig. E). Scale bars = 20μm in A (also applies to B-E).

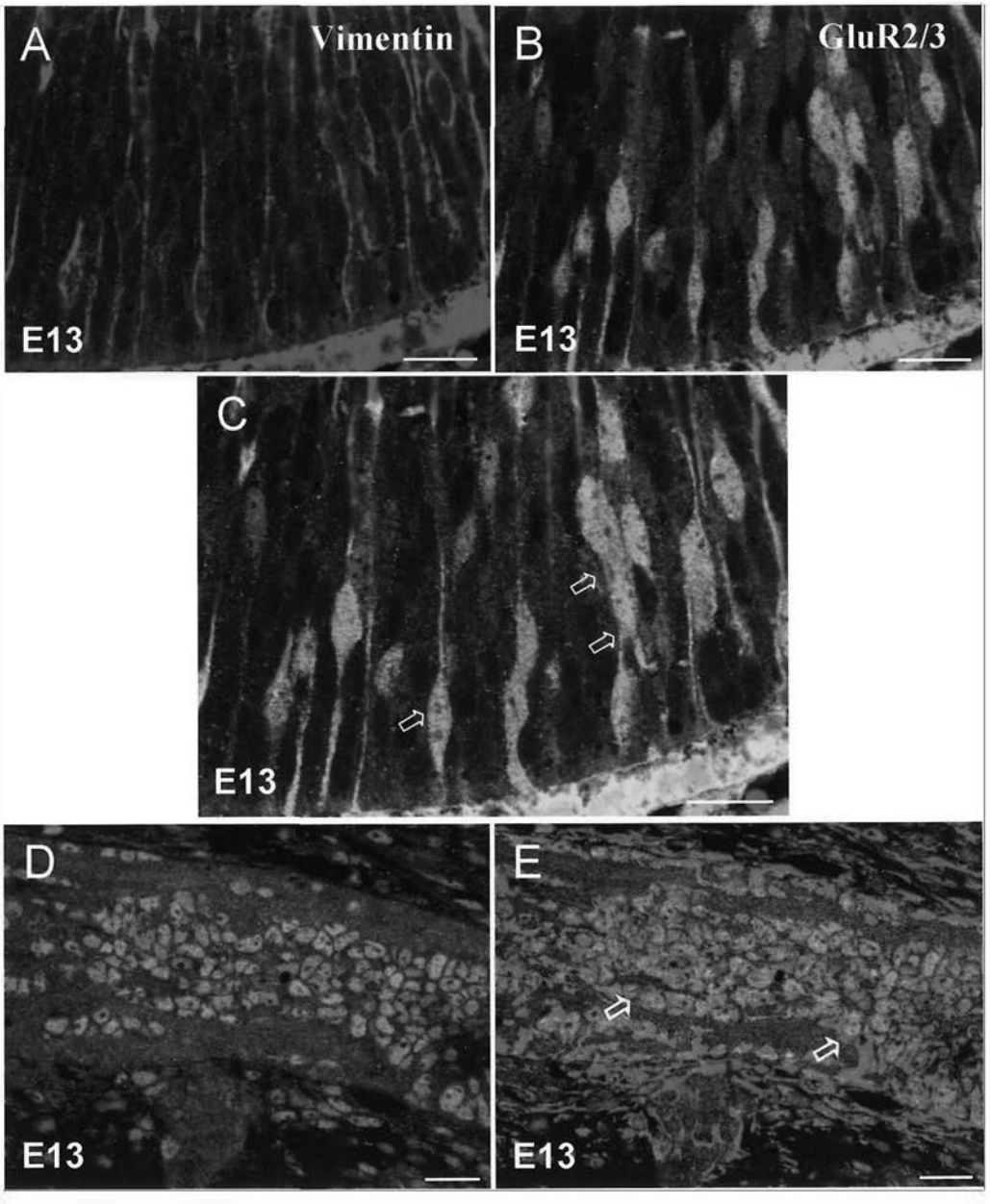
A
Vimentin
E13
B
GluR2/3
E13
C
E13
D
E13
E
E13

Figure 11. Immunostaining of ventral diencephalic sections for anti-GluR2/3 at different stages. Rostral is to the top and the midline is indicated by the white arrows. GluR2/3 was highly expressed in the cells around the midline and the third ventricle in the E13 ventral diencephalon (n=9; Fig. A). Further images showed the positive cells were distributed around midline and the third ventricle (arrowheads) (Fig. B). The same staining pattern which was confined to the midline was shown at E14 (arrowheads) (n=5, Fig. C-D), but the positive staining was also shown in supporting cells in the optic stalk (OS) (Fig. C). In the lower section under the optic chiasm (OC), there were strongly labeled cells surrounding the midline (arrowheads) (Fig. E). Under high magnification, there was no staining in the optic fibers; but clear staining in the supporting cells in OS at E15 (n=4; Fig. F). In the higher section of the OC, the immunoreactive GluR2/3 staining was obviously expressed in the supporting cells in the OS and surrounding the midline (Fig. G-H). Scale bars = 20μm in A (also applies to B-E). Scale bars = 200μm in A (also applies to C); 200μm in B (also applies to D-H).

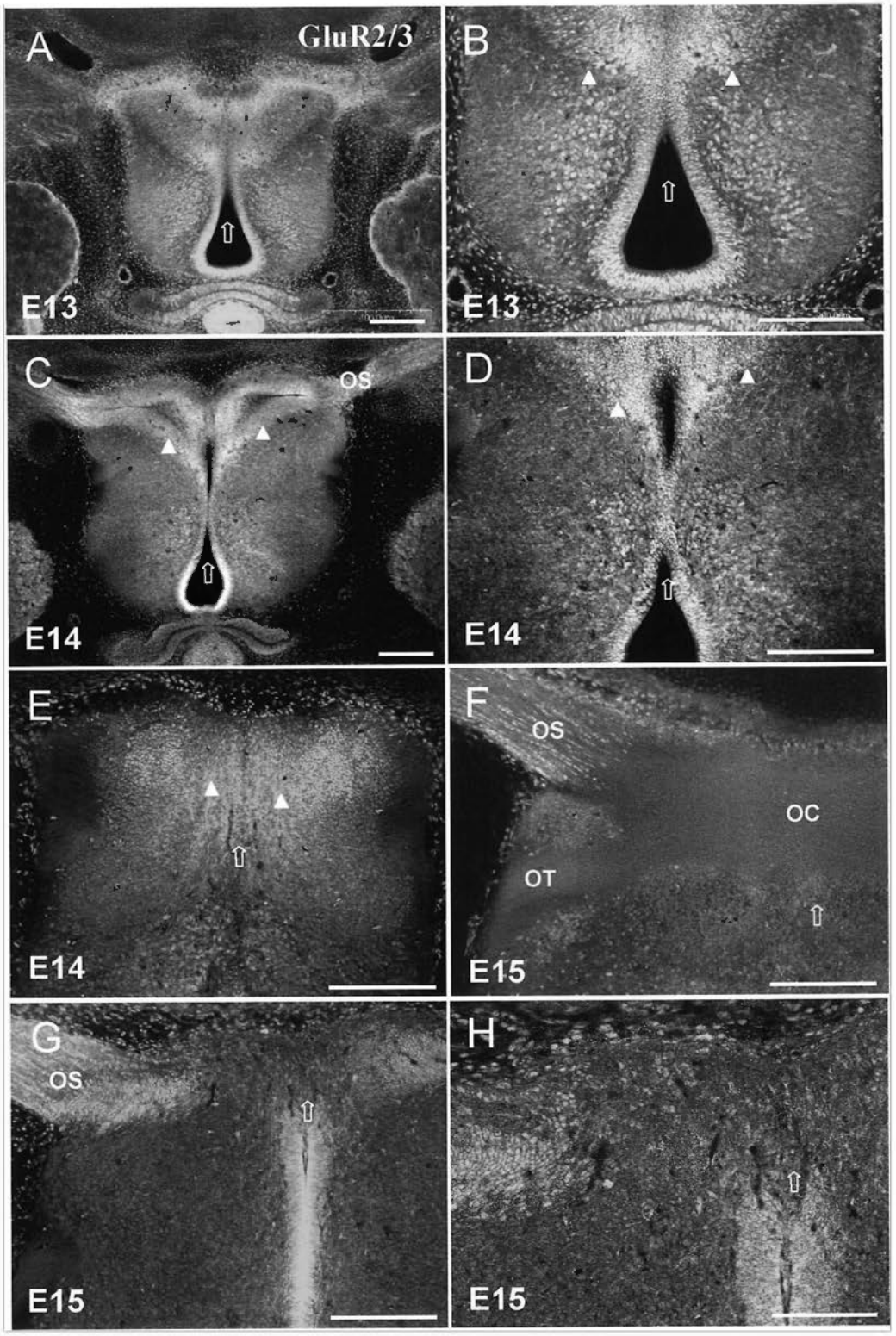
A
GluR2/3
E13
B
E13
C
OS
E14
D
E14
E
E14
F
OS
OC
OT
E15
G
OS
E15
H
E15

Figure 12. Immunostaining of ventral diencephalic frontal sections for anti-GluR2/3. Dorsal is to the top and the midline is indicated by the white arrows. GluR2/3 was strongly labeled in the cells around the third ventricle and at the midline of the chiasm (arrowheads) (n=5; Fig. A-D, F). Almost no staining was found in the optic fibers in the chiasm (Fig. A-F). Scale bars = 200μm in A (also applies to B, E-F); 100μm in C (also applies to D).

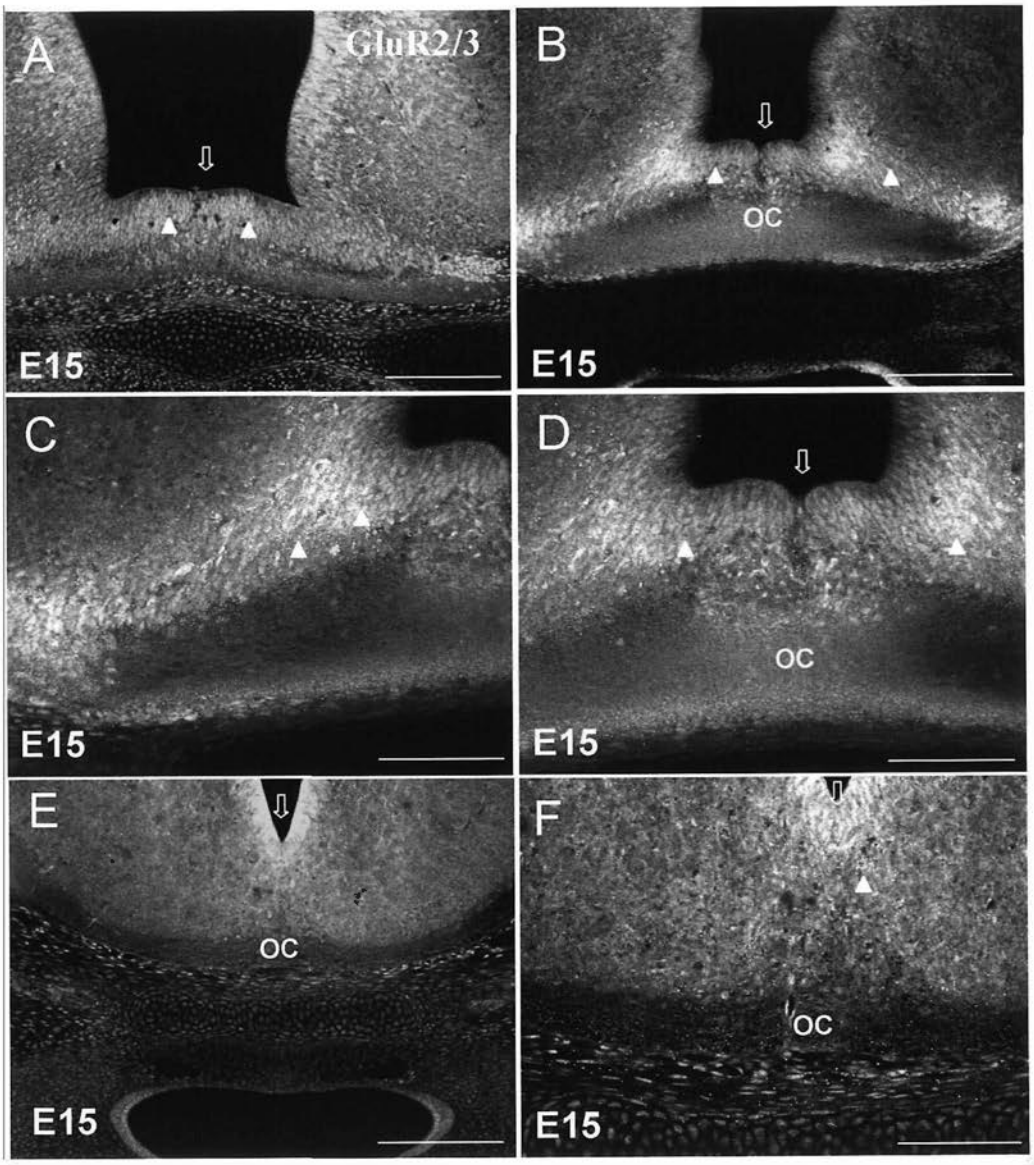
A
GluR2/3
E15
B
OC
E15
C
E15
D
OC
E15
E
OC
E15
F
OC
E15

Figure 13. Immunostaining of ventral diencephalic sections for SSEA-1 and anti-GluR2/3. These were the horizontal sections; rostral was to the top and the midline was indicated by the arrow. In low magnification, GluR2/3 was localized in SSEA-1 positive neurons (n=5; Fig. A). The GluR2/3 staining was around the third ventricle at E13 (Fig. B). The SSEA-1 staining was strongly expressed in the cell body of the chiasmatic neurons near the third ventricle (Fig. C). The merged image showed that the GluR2/3 staining could be colocalized with the SSEA-1 staining (arrows) (Fig. D). Scale bars = 200μm in A; 50μm in B (also applies to C-D).

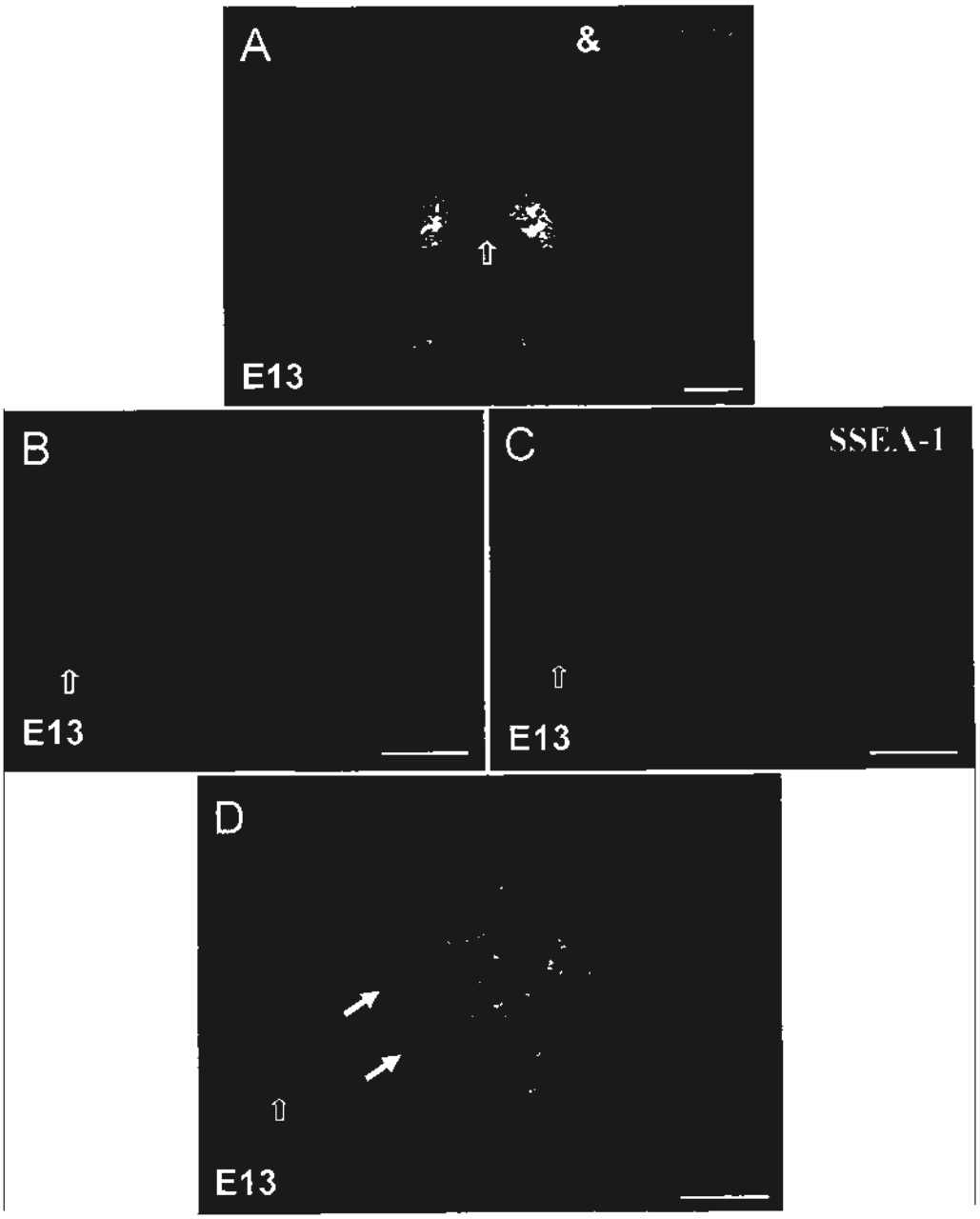
A
&
E13
B
E13
C
SSEA-1
E13
D
E13

Figure 14. Immunostaining of ventral diencephalic sections for RC2 and anti-GluR2/3. All these images were frontal sections, dorsal was to the top and the midline was indicated by the arrow. In low magnification, GluR2/3 was localized in RC2 positive neurons (n=3; Fig. A). The GluR2/3 staining was clearly observed in the nuclei which were radial arranged between the third ventricle and the pial at E14 (n=3; Fig. B). The RC2 staining was in the soma and the processes of the radial glial cells, their processes stretched the whole area from the third ventricle to the optic chiasm (Fig. C). The merged staining of GluR2/3 and RC2 showed that GluR2/3 was expressed in the radial glial cell nuclei (arrows); but there were also some GluR2/3 positive cell nucleus just between the optic chiasm (OC) and the ventricular zone which was negative to RC2 (Fig. D). Scale bars =200μm in A; 50μm in A (also applies to B-D).

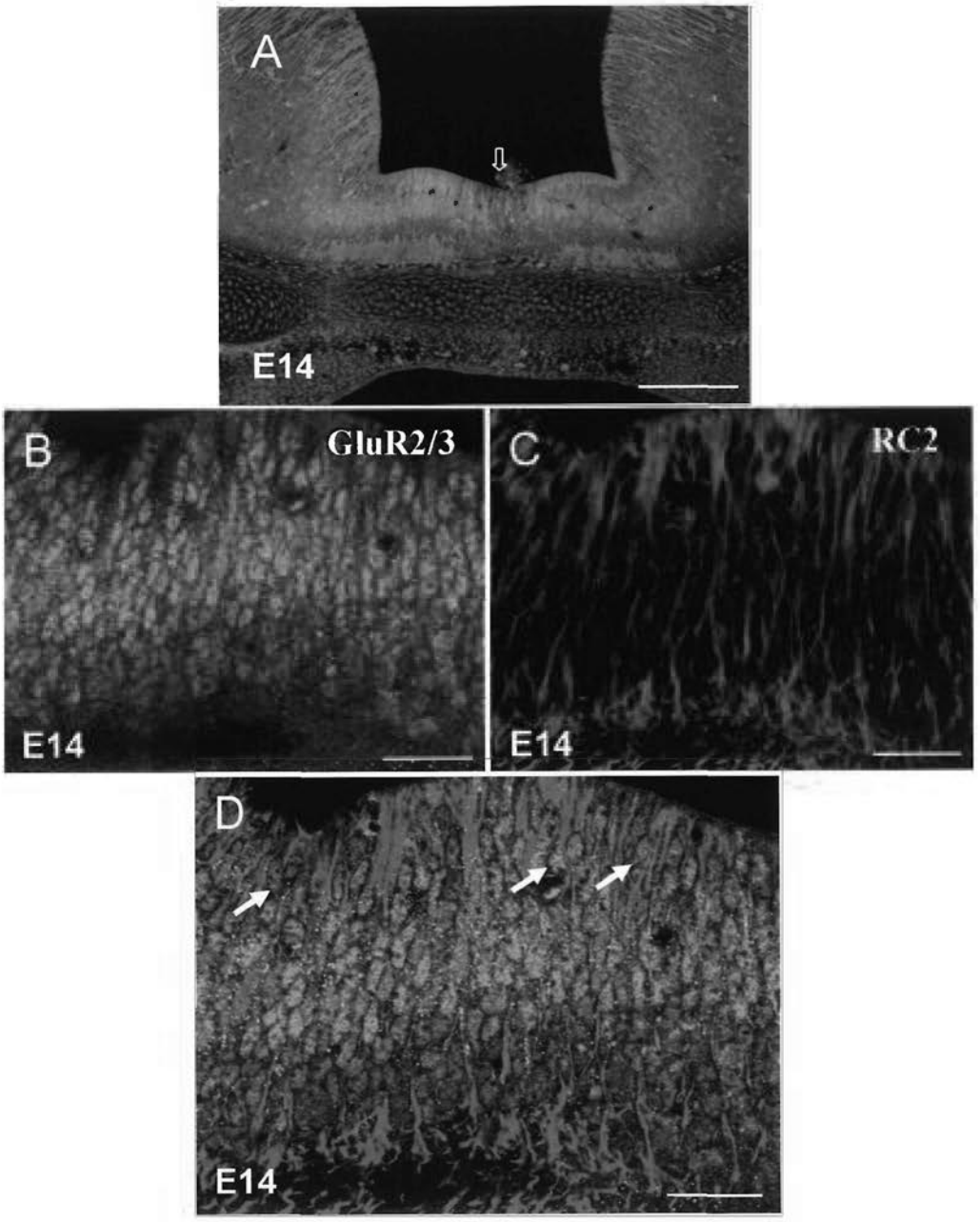
A
E14
B
GluR2/3
E14
C
RC2
E14
D
E14

Figure 15. Immunostaining of ventral diencephalic and retinal sections for anti-GluR2/3. These were the horizontal sections; rostral to the top and the midline was indicated by the arrow. In the retina, the staining of GluR2/3 was observed in the inner layer, lens and the ciliary marginal zone (CMZ) which became very small (n=2; Fig. A). In high magnification, the GluR2/3 staining was highly expressed in the retinal ganglion layer; but no staining in the axon layer. In the outer layers, there still were radially arranged GluR2/3 positive cell nuclei (Fig. B). The obvious staining of GluR2/3 was detected in the optic stalk (OS), optic chiasm (OC) (box area) and the diencephalon (dashed box area) at E18 (Fig. C). The high magnification images showed that the positive staining in the OS and OC was observed in the supporting cell nucleus (Fig. C-E); but the staining in the diencephalon was confined to the cell bodies and their processes (Fig. F). Scale bars = 200μm in A (also applies to C); 50μm in B (also applies to F); 100μm in D (also applies to E).

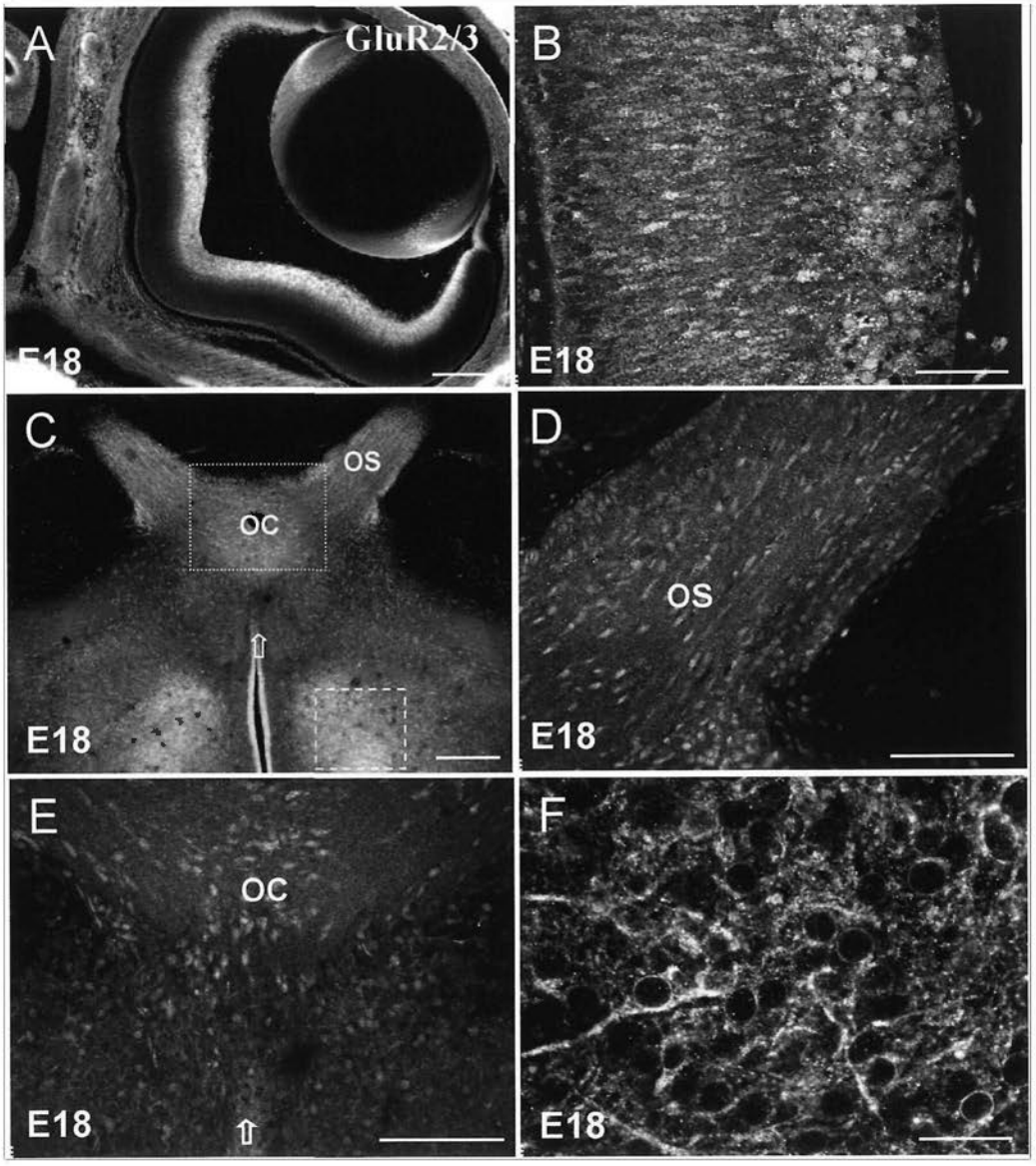
A
GluR2/3
E18
B
E18
C
OS
OC
E18
D
OS
E18
E
OC
E18
F
E18

GluR4 staining

Figure 16. Immunostaining of retinal sections for anti-GluR4 at different stages. In control section at E13, no staining was detected. L was for lens, R for retina (Fig. A). There was obvious staining in adult retina (n=2). The staining was localized largely in GCL, IPL, INL, and OPL. No staining was detected in ONL (Fig. B). At E13 (n=7), there was obvious staining in the optic disk (OD) (arrows), but not in the axon layer. Strong staining of GluR4 was abundantly detected in the ciliary marginal zone (CMZ) (asterisks), the lens and the blood vessels (arrows) at E13 (Fig. C). In high magnification, there was a strong label in the glial-like cells in the OD and in the inner layer of the retina (arrow), and weak in the retinal axons at E14 (n=6; Fig. D). There was weak staining in the retinal axons and clearly in the supporting cells in the optic stalk (arrows) (Fig. E). At E15 (n=5), GluR4 was highly expressed in the inner cell layer, the CMZ and the lens (Fig. F-G). The same pattern was observed at E18 (n=2, Fig. H). But in all these stages, the staining in the retinal axon layer was relatively weak. Scale bars = 200μm in A (also applies to C, F); 100μm in B (also applies to D-E, G-H).

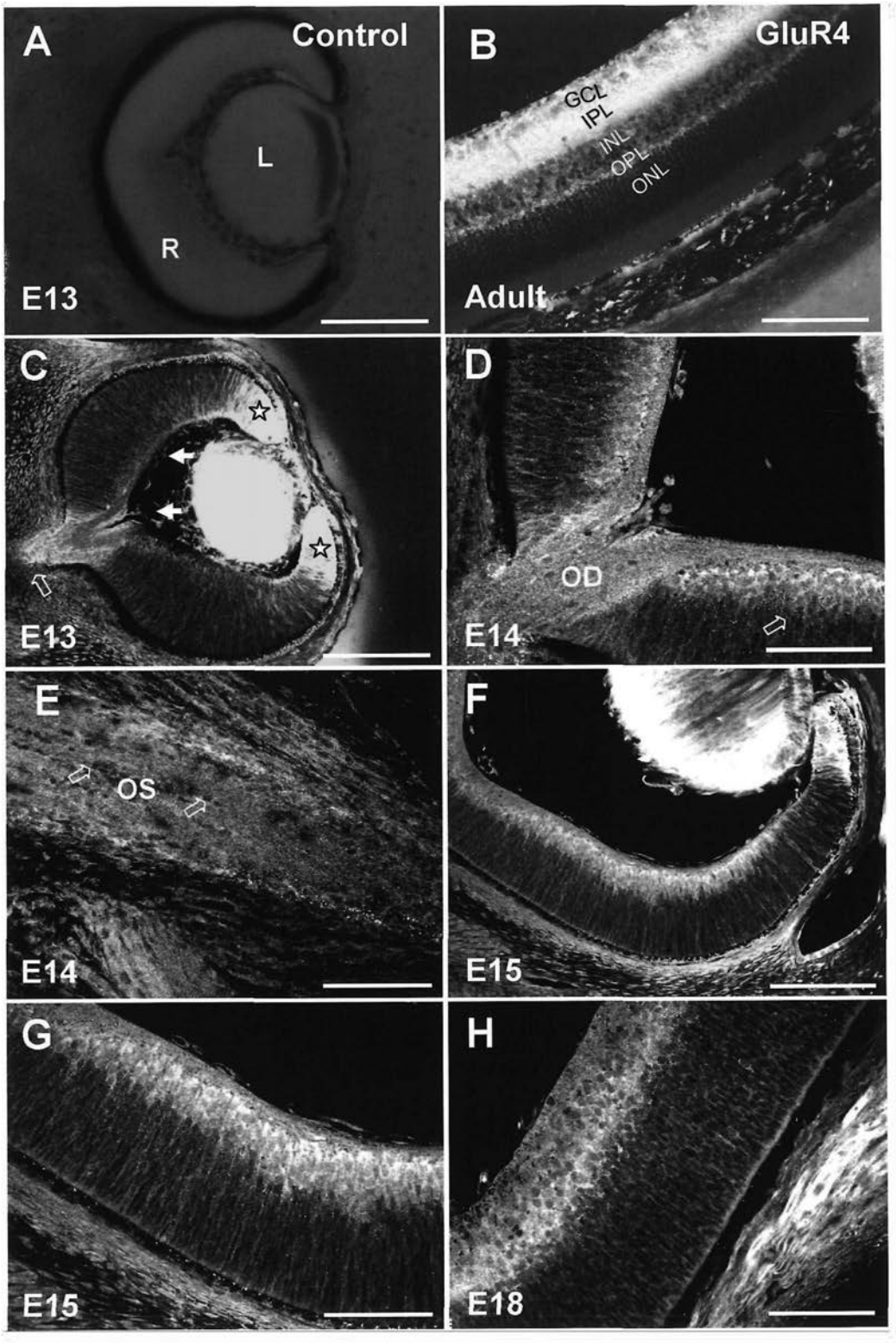
A
Control
L
R
E13
B
GluR4
GCL
IPL
INL
OPL
ONL
Adult
C
E13
D
OD
E14
E
OS
E14
F
E15
G
E15
H
E18

Figure 17. Immunostaining of retinal sections for TuJ-1 and anti-GluR4. In high magnification, the prominent TuJ-1 staining was shown in the inner layer and axon layer of the retina at E14 (arrows) (n=4; Fig. A). At the same section, the immunoreactive GluR4 staining was revealed in the inner layer and radially shaped cells in the outer layers; but weakly labeled in the axon layer (arrows) (Fig. B). In the merged image, it showed that most of the GluR2/3 staining was colocalized with TuJ-1 positive neurons (arrows), weakly in the retinal axons. There still were other GluR2/3 positive cells that could not be stained by TuJ-1 (Fig. C). Scale bars = 100μm in A (also applies to B-C).

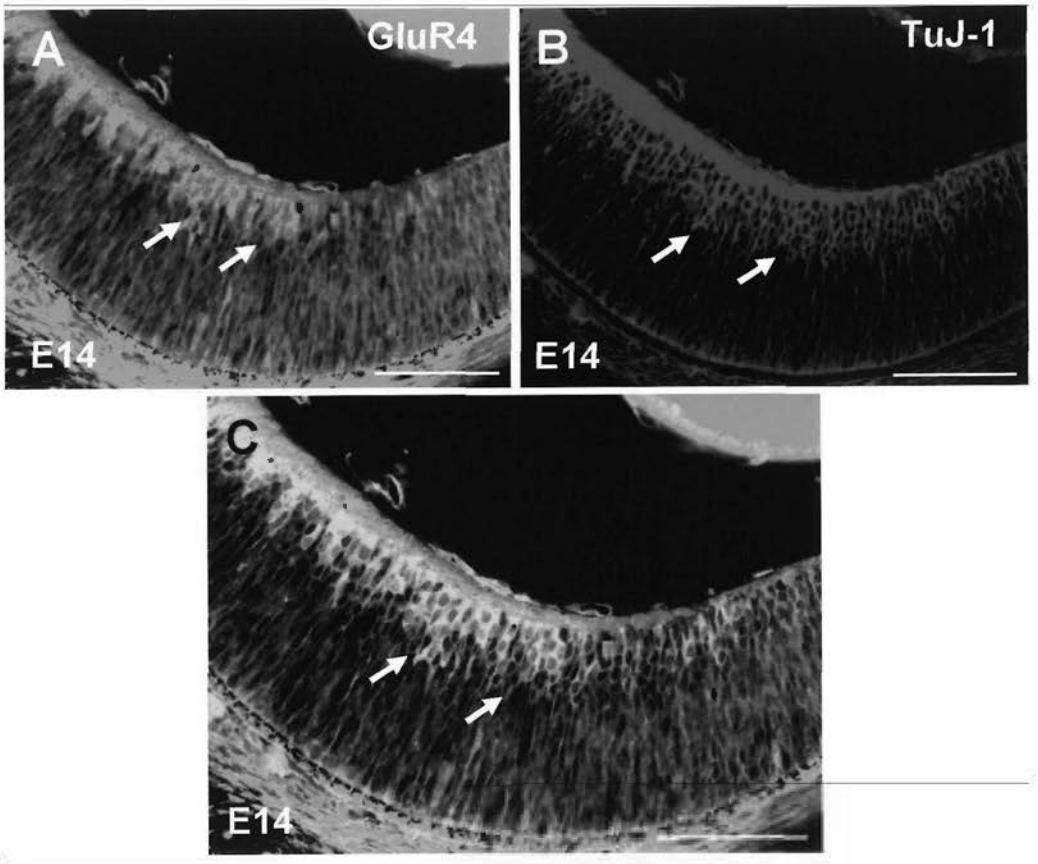
A
GluR4
E14
B
TuJ-1
E14
C
E14

Figure 18. Immunostaining of retinal sections for Vimentin and anti-GluR4. In high magnification, the cell bodies and the processes of Müller glia were obviously labeled by Vimentin in the outer layers (arrows) (n=6; Fig. A). At the same section, GluR4 was expressed in the radially arranged whole cells and the long processes extending throughout the whole thickness of the retina (arrows) (Fig. B). The merged image indicated that GluR4 positive cells could be doubled with the Vimentin positive Müller glia (arrows) (Fig. C). Scale bars = 100μm in A (also applies to B-C).

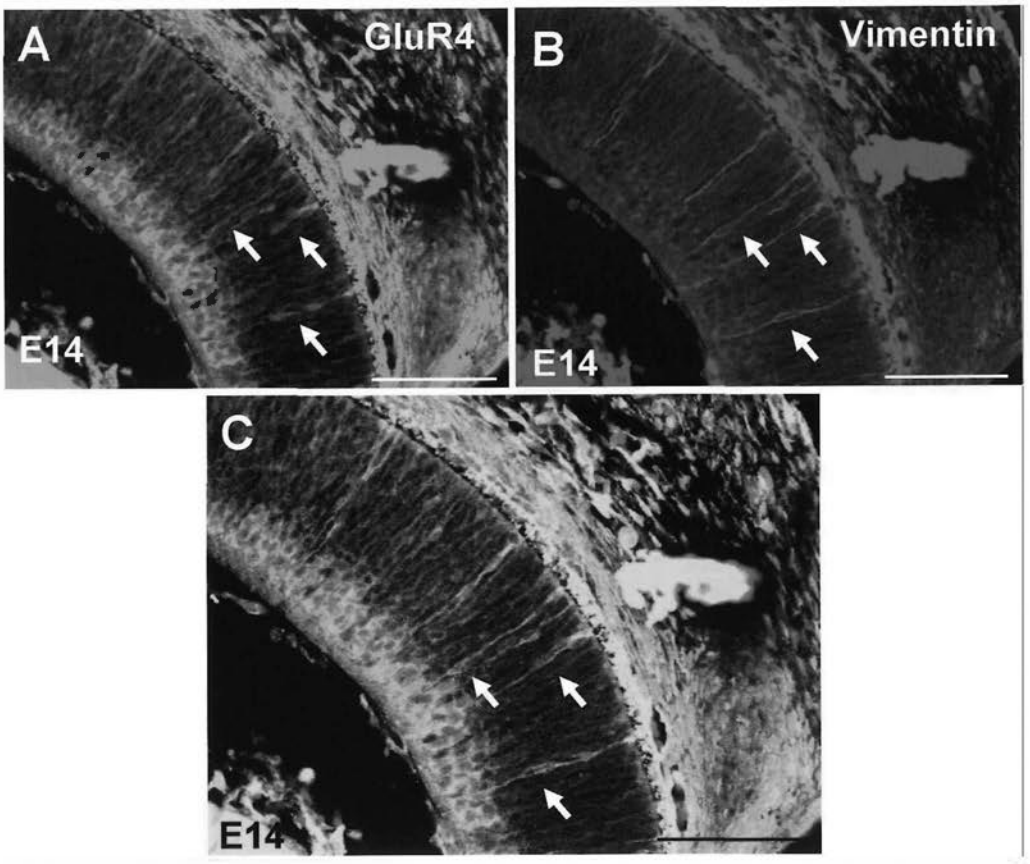
A
GluR4
E14
B
Vimentin
E14
C
E14

Figure 19. Immunostaining of ventral diencephalic sections for anti-GluR4 at different stages. For the horizontal sections, rostral is to the top; for the frontal sections, Dorsal is to the top. And the midline is indicated by the white arrows. GluR4 was preferentially detected with some cells in the caudal region of the diencephalon and the cells around the optic stalk (OS) at E13 (n=8; Fig. A-B). In the optic fibers, they were weakly labeled by anti-GluR4, but obvious stain was observed in the midline region (arrows) at E14 (n=5; Fig. C-D). In high magnification, GluR4 staining was clearly shown in the midline region at the chiasm (arrows) (Fig. D). The same staining pattern was also shown at E15 (n=4; Fig. E-F). In the frontal sections, GluR4 was weakly labeled in the optic chiasm (OC) and optic tract (OT), but obvious stained in the glial-like cells (arrows) and some cells in the midline region above the axons in the OC (Fig. G-H). Scale bars = 200μm in A (also applies to C, E); 200μm in B (also applies to D, F); 100μm in G (also applies to H).

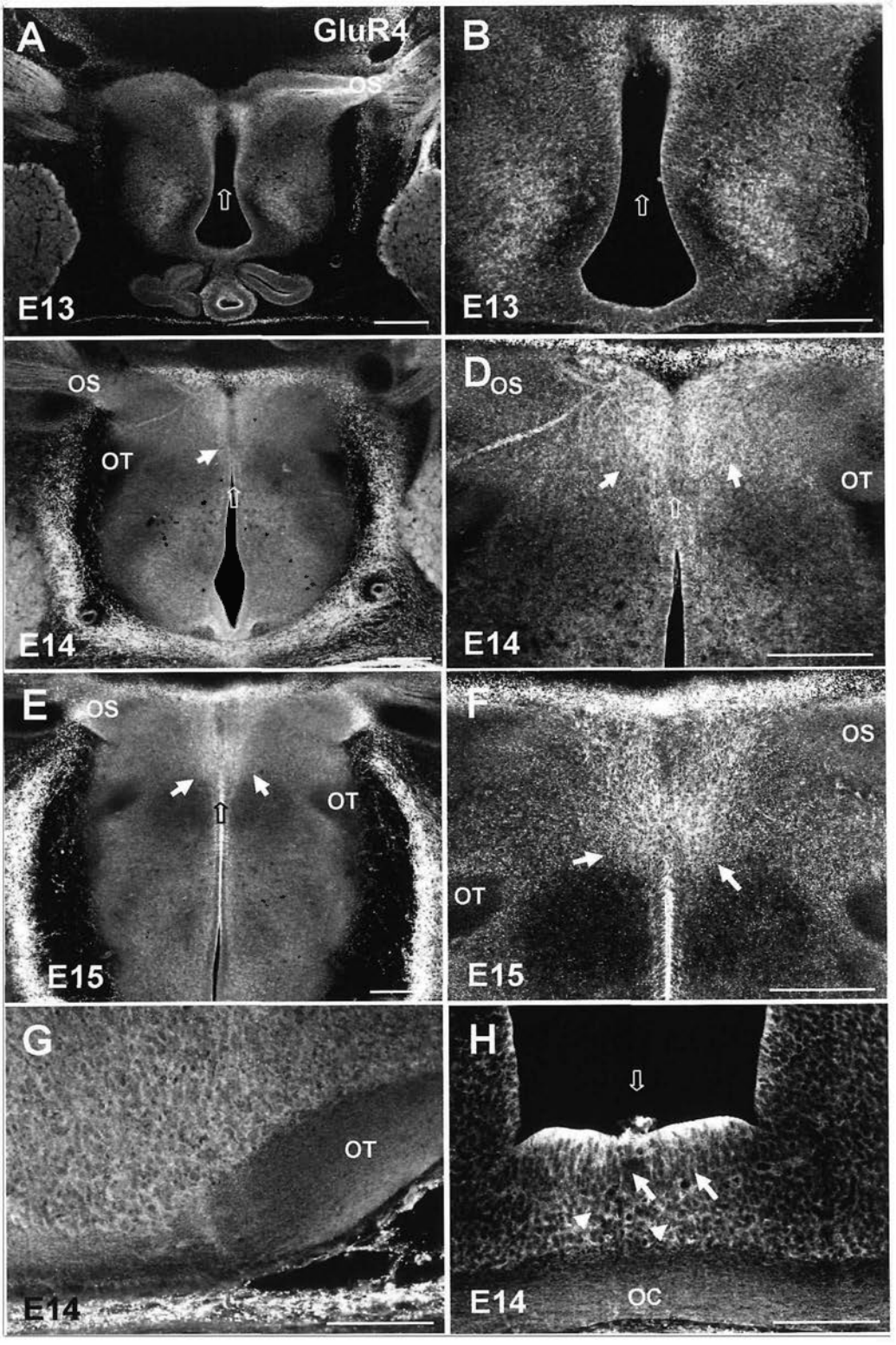
A
GluR4
OS
E13
B
E13
OS
OT
E14
D
OS
OT
E14
E
OS
OT
E15
F
OS
OT
E15
G
OT
E14
H
E14
OC

Figure 20. Immunostaining of ventral diencephalic sections for SSEA-1 and anti-GluR4. These were the horizontal section; rostral was to the top and the midline was indicated by the arrow. In low magnification, it showed that GluR4 expressed in SSEA-1 positive neurons, and in other regions in diencephalon (n=4; Fig. A). The SSEA-1 staining was labeled the cell bodies of the chismatic neurons near the third ventricle at E13 (Fig. B). In the same section, the GluR4 staining was also detected near the third ventricle (Fig. C). The merged image showed that the GluR4 staining could be colocalized with the SSEA-1 staining (arrows); but the GluR4 positive cells were observed in other regions of diencephalon which could not be stained by SSEA-1 (Fig. D). Scale bars = 200μm in A; 100μm in B (also applies to C-D).

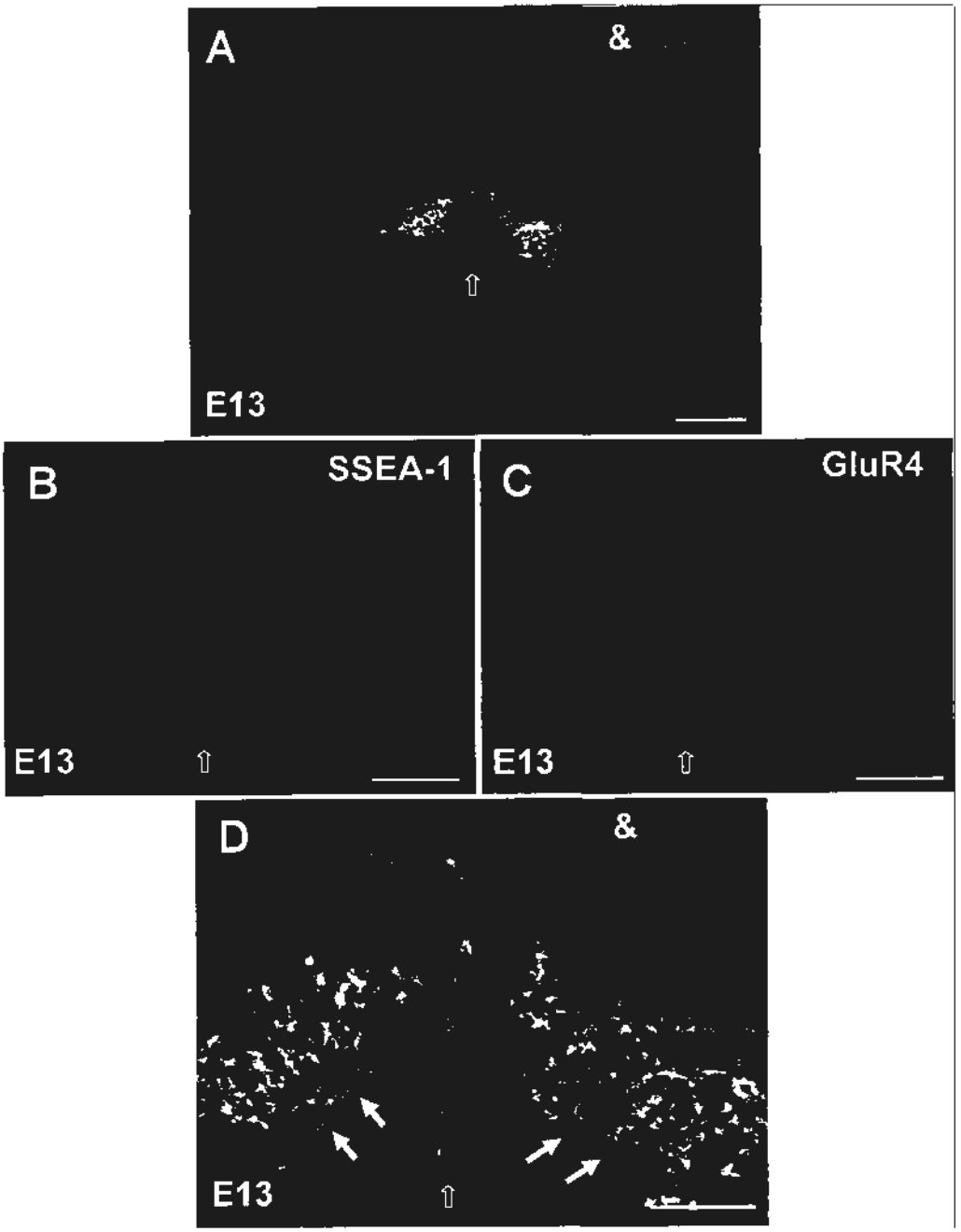
A
&
E13
B
SSEA-1
E13
C
GluR4
E13
D
&
E13

Figure 21. Immunostaining of ventral diencephalic sections for RC2 and anti-GluR4. All these images were frontal sections, dorsal was to the top and the arrow indicated the midline. The RC2 staining was detected in the cell bodies and the processes of the radial glia, their processes ramified in the axon layer at the midline of the chiasm (n=6; Fig. A-B). The GluR4 staining was distinctly observed in the cells near the ventricular zone (Fig. C-D). The merged staining indicated that GluR4 positive cells were colocalized with RC2 positive radial glia (arrows), but there still were some GluR4 positive cells in the midline region above the axons in the OC which were absent to RC2 (Fig. E-F). Scale bars = 100μm in A (also applies to B-F).

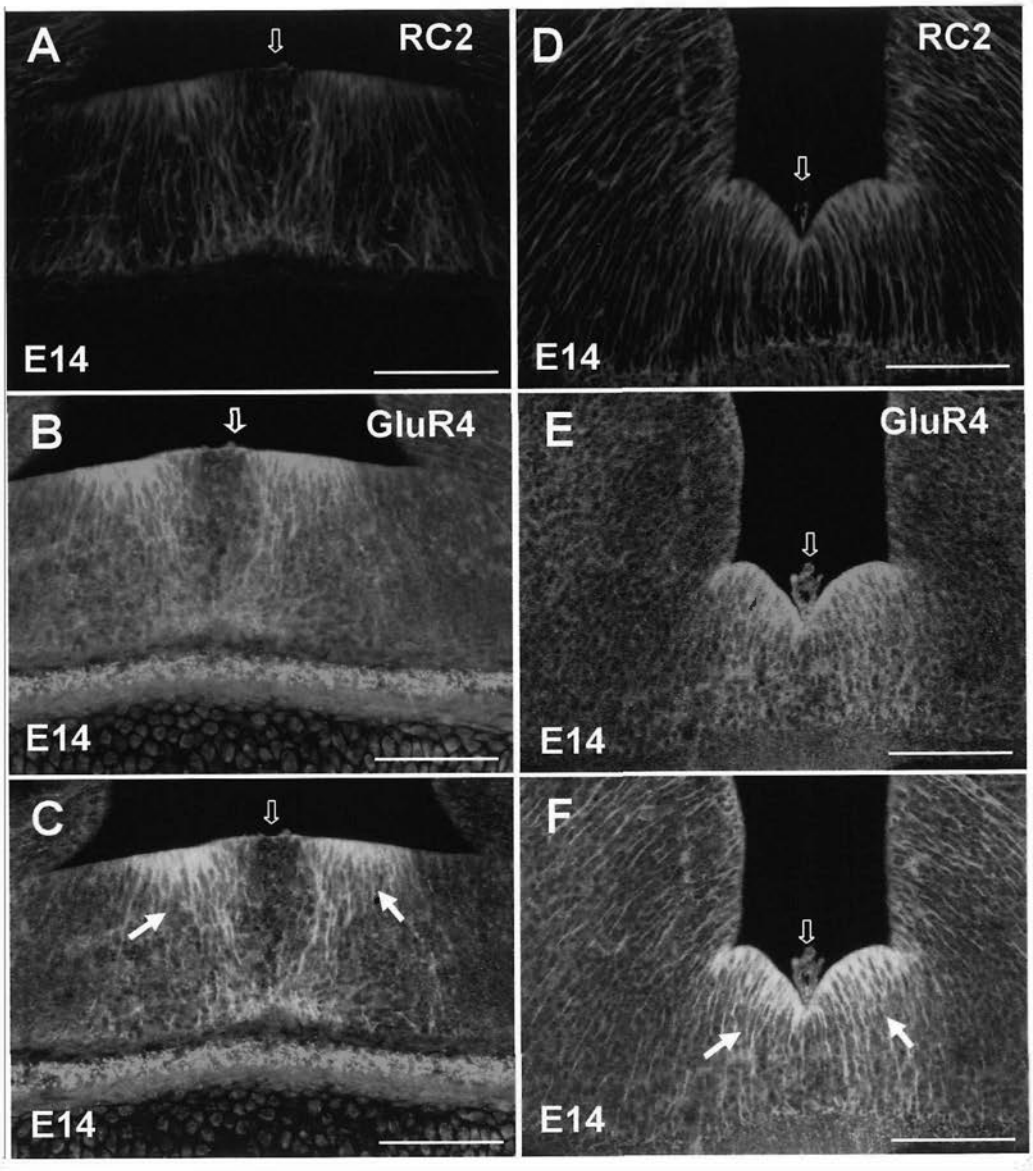
A
RC2
E14
D
RC2
E14
B
GluR4
E14
E
GluR4
E14
C
E14
F
E14

Figure 22. Effect of CP465022 hydrochloride on retinal neurite outgrowth in cultured retinal explants. In control preparations at E14, neurites from the retinal explants grew normally (Fig. A). In the presence of the CP465022 hydrochloride with different concentration (2μM, 5μM, 10μM and 20μM; a noncompetitive AMPAR antagonist), neurites outgrowth from the retinal explants became inhibited (Fig. B-E). Plot showed that there was significant difference to neurite outgrowth in the CP465022 hydrochloride treated groups compared with that of the control one (Fig. F). Scale bars = 500μm.

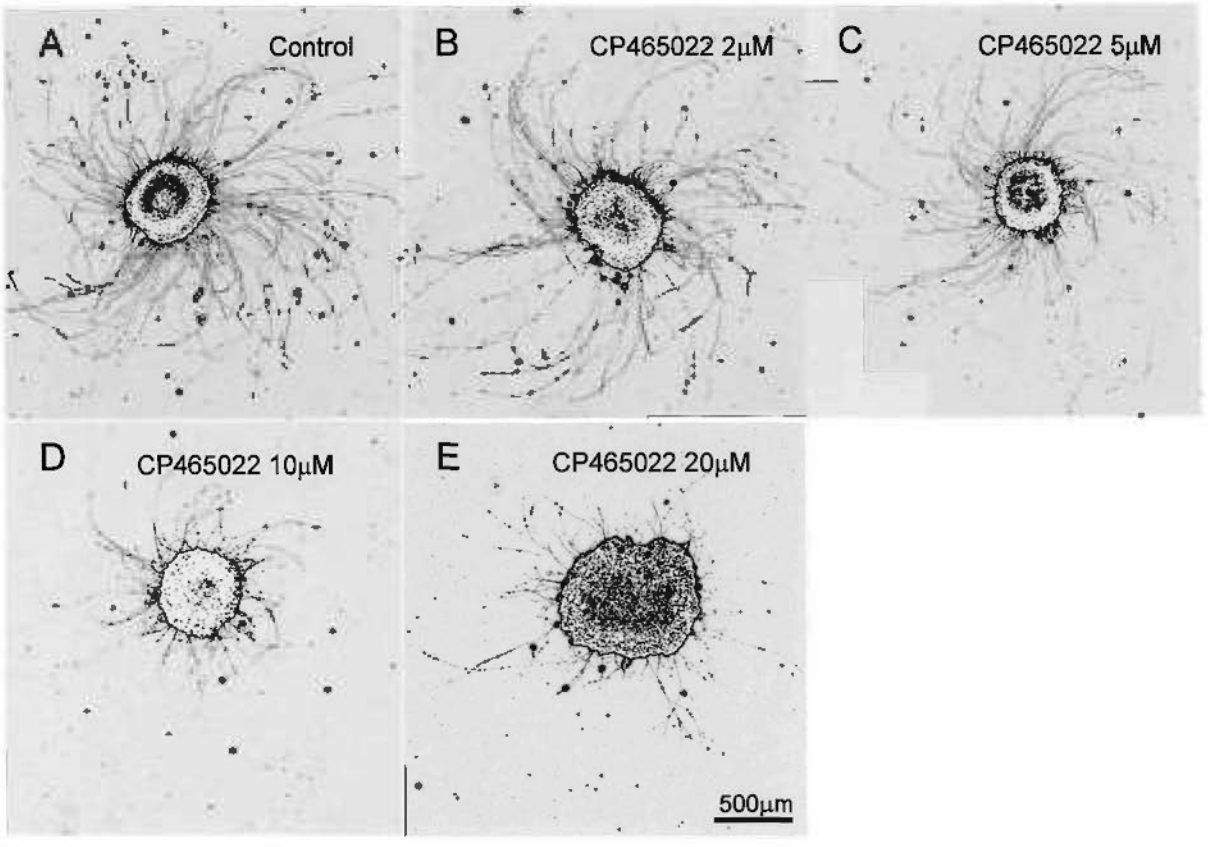
A
Control
B
CP465022 2μM
C
CP465022 5μM
D
CP465022 10μM
E
CP465022 20μM
500μm

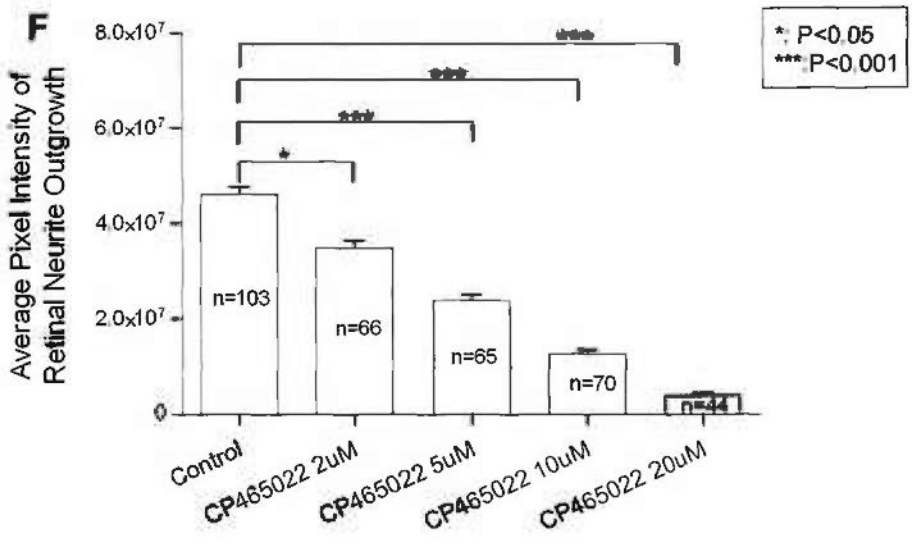
F
Average Pixel Intensity of Retinal Neurite Outgrowth
8.0x10^7
6.0x10^7
4.0x10^7
2.0x10^7
0
*: P<0.05
***: P<0.001
n=103
n=66
n=65
n=70
n=44
Control
CP465022 2uM
CP465022 5uM
CP465022 10uM
CP465022 20uM

Figure 23. Effect of GYKI52466 dihydrochloride on retinal neurite outgrowth in cultured retinal explants. In control preparations at E14, neurites from the retinal explants grew normally (Fig. A). In the presence of the GYKI52466 dihydrochloride with different concentration (50μM, 75μM, 100μM and 150μM; a noncompetitive AMPAR antagonist), neurites outgrowth from the retinal explants became inhibited (Fig. B-F). Plot showed that there was significant difference to neurite outgrowth in the GYKI52466 dihydrochloride treated groups compared with that of the control one (Fig. G). Scale bars = 500μm.

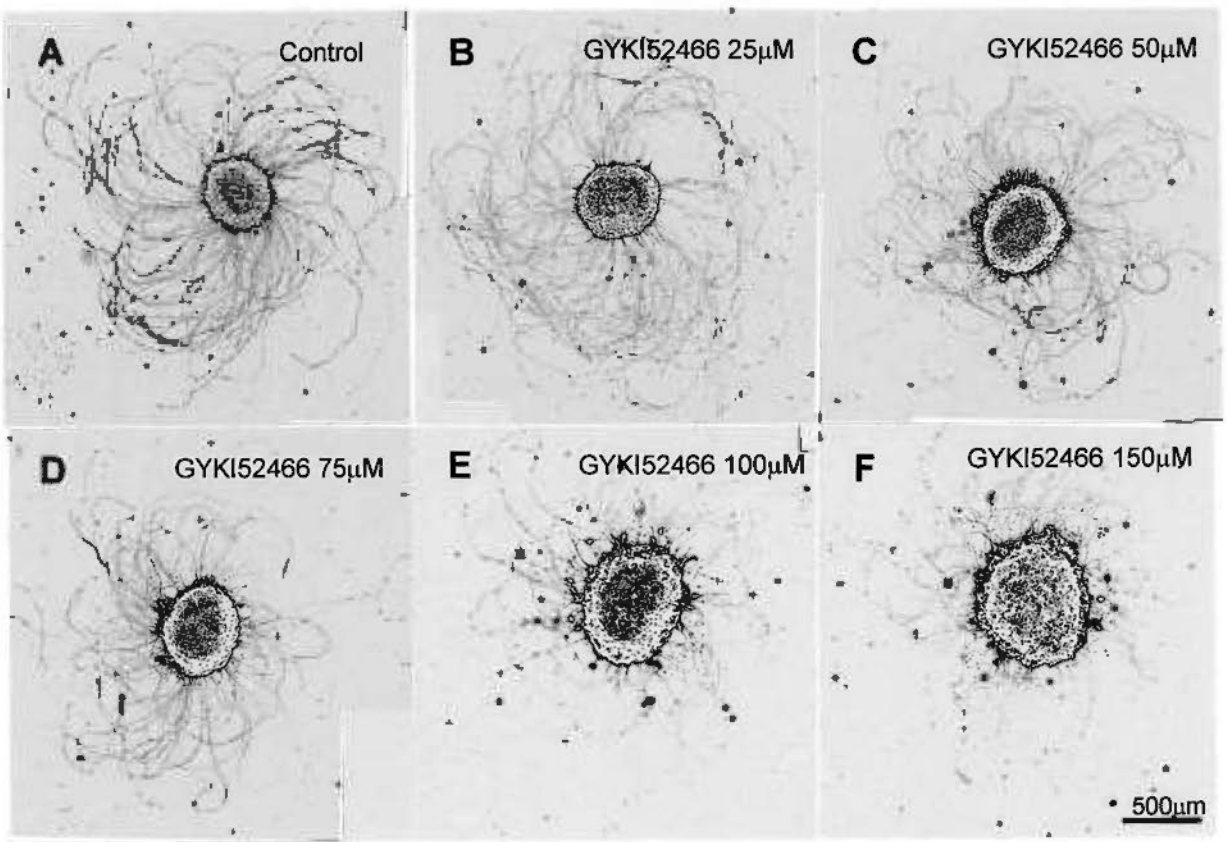
A
Control
B
GYKI52466 25μM
C
GYKI52466 50μM
D
GYKI52466 75μM
E
GYKI52466 100μM
F
GYKI52466 150μM
500μm

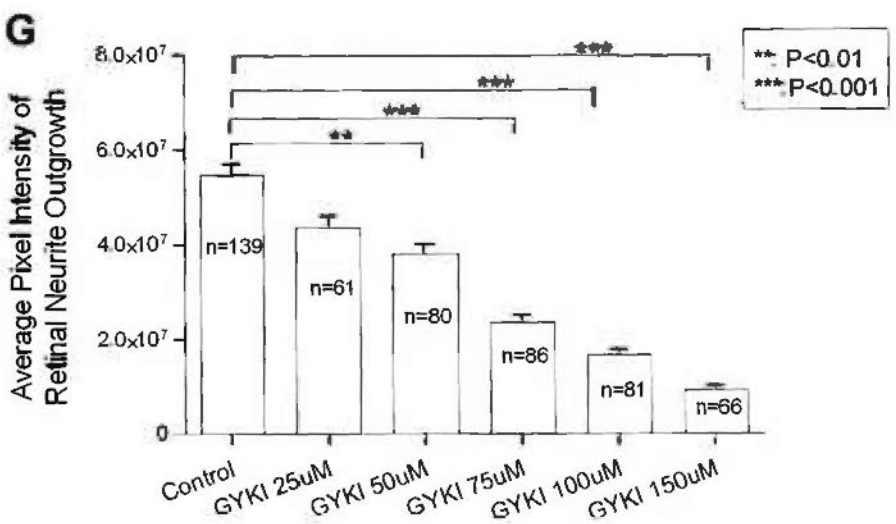
G
Average Pixel Intensity of Retinal Neurite Outgrowth
8.0x10^7
6.0x10^7
4.0x10^7
2.0x10^7
0
** P<0.01
*** P<0.001
n=139
n=61
n=80
n=86
n=81
n=66
Control
GYKI 25uM
GYKI 50uM
GYKI 75uM
GYKI 100uM
GYKI 150uM

Figure 24. Effect of KCl on retinal neurite outgrowth in cultured retinal explants. In control preparations at E14, neurites from the retinal explants grew normally (Fig. A). In the presence of the KCl with different concentration (10mM and 15mM), neurites from the retinal explants also grew normally (Fig. B-C). Plot showed that there was no statistical significance to neurite outgrowth in the KCl treated groups compared with the control one (Fig. D). Scale bars = 500μm.

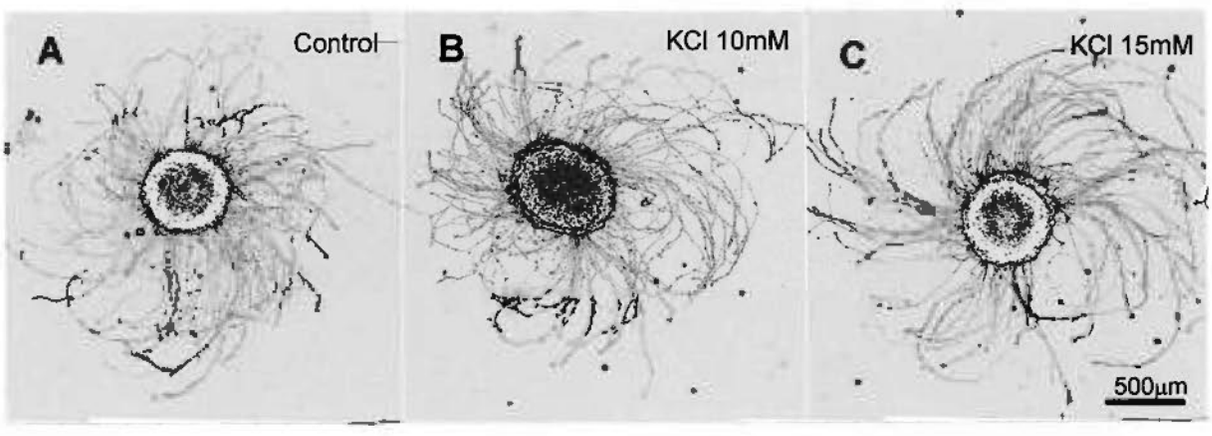
A
Control
B
KCl 10mM
C
KCl 15mM
500µm

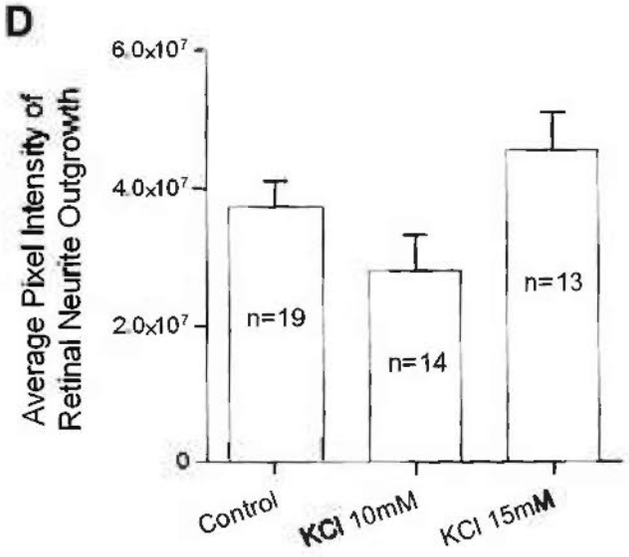
D
Average Pixel Intensity of Retinal Neurite Outgrowth
6.0x10⁷
4.0x10⁷
2.0x10⁷
0
n=19
n=14
n=13
Control
KCl 10mM
KCl 15mM

CHAPTER 4

Localization and possible function of Kainate receptors in the developing mouse optic pathway

Introduction

L-glutamate as a neurotransmitter is the major fast excitatory amino acid in the CNS; it acts its role through ionotropic or metabotropic receptors. NMDA receptors (NMDARs), AMPA receptors (AMPARs) and kainite receptors are belonging to the ionotropic receptors (Hollmann and Heinemann, 1994; Watkins and Evans, 1981), which function as ligand-gated ion channels. However, metabotropic receptors function through signaling cascades. There are extensively studies focusing on the NMDARs and AMPARs, while relatively few reports the role of the kainate receptors, particularly in the development of the CNS. Kainate receptors are obviously expressed in the CNS (Bahn et al., 1994; Wisden and Seeburg, 1993). They have been implicated in various functions in the CNS, such as excitatory and inhibitory neurotransmission and induction and expression of long-term potentiation (Bortolotto et al., 1999; Frerking and Nicoll, 2000), and in diseases for example epilepsy (Bloss and Hunter, 2010; Lerma et al., 2001; Vincent and Mulle, 2009) and schizophrenia (Woo et al., 2007).

Molecular cloning has identified 5 subunits belonging to the kainate receptors: GluK1-5 which can co-assemble in various combinations to form functional receptors (Dingledine et al., 1999). The kainate receptors can also be subdivided into two classes based upon structural homology and functional characteristics. GluR5-7 receptor subunits share a high degree of homology and are able to form functional channels when expressed in heterologous systems. The KA1 -2 receptor subunits are unable to form functional channels on their own, but when co-expressed with GluR5-7 receptor subunits, they form channels with high affinity for kainate (Ren et al., 2003a; Ren et al., 2003b; Wisden and Seeburg, 1993). Like AMPA receptors, the functional unit of endogenous kainate receptors might be a tetramer, which can be either homomeric or heteromeric. At present, the kainate receptor subunits that were previously named as GluR5-7 are now as GluK1-3; and those formerly named as KA1 and KA2 are now as GluK4 and GluK5. Their corresponding genes are: *Grik1-5* (Collingridge et al., 2009); and every individual gene may have at least one transcript, such as *Grik2* has ten transcripts, eight of them can translate to proteins. All these increase the pharmacological heterogeneity in the kainate receptor family; on the other hand, it also has its merit to allow kainate receptor subunit trafficking to be specifically regulated. Another problem is that kainate receptor agonists including kainate itself act on both AMPARs and kainate receptors. Although there are some antagonists used to block the kainate receptors, there are lacks of selective kainate receptor antagonists.

As above-mentioned, most of the reported functional information regarding the specific kainate receptor subunits in neuronal types or neurons based on kainate receptor subunit-deficient mice or/and combined with pharmacology. In our following experiments: 1) although anti-GluR5/6/7 is not a high-quality

subunit-selective antibody, it can simultaneously detect the GluR5, 6, and 7 subunits (Huntley. G W. 1993); it can give us one outline of exact intracellular location of kainate receptors. 2) For the antagonists we used, CNQX is a competitive antagonist towards AMPARs and kainate receptors; UBP 310 is a potent antagonist to kainate receptors displaying about 30-fold selectivity over AMPARs, but it will has a much lower affinity for GluK4 and GluK5 (Jane et al., 2009).

The exact physiological roles of kainate receptor subunits are unclear, but they may take part in the synaptic integration, synaptic plasticity and controlling neuronal excitability (Kidd and Isaac, 1999; Lerma et al., 2001; Park et al., 2006; Woo et al., 2007). Kainate receptor subunits have a remarkable diversity and specificity not only between neuronal types but also within individual neurons, which function through a powerful and specific regulatory mechanism. Such as, within hippocampal CA3 pyramidal neurons, kainate receptors are targeted to the axons and presynaptic terminals at which they regulate neurotransmitter release to CA1 pyramidal neurons and CA1 GABAergic interneurons (Isaac et al., 2004). Moreover, activation of AMPA/ kainate receptors affects axonal filopodial motility in culture (Chang and De Camilli, 2001; Schenk et al., 2003) and in hippocampal slices (Tashiro et al., 2003); and glutamate and acetylcholine act as chemoattractants for growth cones emitted by *Xenopus laevis* motoneurons (Zheng et al., 1994; Zheng et al., 1996). Therefore, it is supposed that glutamate may release locally, one way may be through an autocrine, and the other may be through local glutamatergic communication (Metin et al., 2000), to affect growth cone motility and synaptogenesis at the development (Tashiro et al., 2003).

As mentioned in chapter 2, glutamate was extensively expressed in the mouse developing retinofugal pathway, and in the whole ventral diencephalon. Meanwhile,

retinal axons travel along the retinofugal pathway: the optic nerve, chiasm (axons from nasal retina cross at this location to the contralateral side, axons from ventral temporal retina turn to the ipsilateral side), optic tract, and finally to the visual cortex (Chan et al., 1998; Colello and Guillery, 1990). And glutamate as one of the neurotransmitters may act as chemoattractants for growth cone motility and synaptogenesis (Tashiro et al., 2003; Zheng et al., 1994). Therefore we want to explore glutamate receptors localization and function in the retinofugal pathway. In this chapter, we chose kainate receptors to study their expression in the mouse optic pathway and further investigate their possible function in the retinal axons.

Materials and Methods

Animal preparation

All the procedures followed that described in chapter 2.

Experiment reagents

Stock solutions were prepared by dissolving drugs in water or dimethyl sulfoxide (DMSO) (1% maximal, final concentration) according to the manufacturer's recommendation. Stock solutions were either used directly as working solution or diluted with the 1xPBS, pH7.4 immediately before the experiment. The following drugs were used: CNQX (50-500μM) and UBP 301 (5-25μM) (Tocris Co, UK).

RNA extraction and quantitation

The procedures followed those described in chapter 3.

cDNA reverse transcription synthesis and RT-PCR analysis

The procedures were the same as those described in chapter 3.

Table 2: Primers used for amplification of cDNA of KA receptor subunits and β-actin was the same as that described in Chapter 3.

Gene	GenBank Accession#	Sequence 5'-3'	Fragment Size (bp)
GluR5 (*Grik1*)	NM_146072		
Forward primer		TTTGGCGTTGGAGCTCTCATG	
Reverse primer		GTTGGCAGTGTAGGATGAGATGA	123bp
GluR6 (*Grik2*)	NM_010349		
Forward primer		GGTTTCTGGTTTGGAGTTGGAG	
Reverse primer		CAAATGCCTCCCACTATGCTG	89bp
GluR7 (*Grik3*)	NM_001081097		
Forward primer		TCTGGTTTGGAATGGGCTC	
Reverse primer		GGTGAAGAACCACCAGATGC	98bp
KA1 (*Grik4*)	NM_17548		
Forward primer		GTACTACCGGCAGCGAAACTG	
Reverse primer		GAGAATGGCCAGGTCGAACTC	121bp
KA2 (*Grik5*)	NM_008168		
Forward primer		CAGGCGCCTCAATTGCAAC	
Reverse primer		TGCAGGATGGCCAGTGTGA	117bp

Immunohistochemistry

Expression of GluR5/6/7 was investigated in the developing mouse retinofugal pathway. The heads of E13 to E18 mouse embryos were fixed with 4% paraformaldehyde (PFA) in 0.1M PB at 4°C overnight. Primary antibody used was anti-GluR567 (1:1000, mouse monoclonal IgM; Millipore, USA), which was used to detect the Kainate receptors (KAs): GluR5/6/7; the corresponding secondary antibody was AF488 or AF568 conjugated goat anti-mouse IgM (1:200 Molecular Probes, USA).

Preparation of retinal explants and KAR subunits staining on neurites and growth cones

The procedures were the same as those described in chapter 2 and 3. Immunostaining of GluR5/6/7 was carried out according to the protocol above with the concentration of secondary antibody (AF488 conjugated goat anti-mouse IgM) at 1:500 (Molecular Probe, USA).

Western blotting

The procedures were the same as those described in chapter 3. But the primary antibody (anti-GluR567) was diluted (1:1000) with 5% or 1% non-fat milk in TBST at 4°C overnight, shaking; and the corresponding secondary antibody was diluted: HRP conjugated- Goat anti-mouse IgM (1:5000).

Double staining with neuronal cell marker: TuJ-1 in the mouse retina

The procedures were the same with chapter 2 description.

Double staining with chiasmatic neuronal marker: CD44 in the mouse ventral diencephalon

The following procedures were the same as those described in chapter 2.

Preparation of retinal explants and kainate receptor antagonist treatments

The procedures were the same as those described in chapter 2, but the culture medium was changed to DMEM/F12 with high glucose (Invitrogen Co, USA) supplemented with N1, 1% bovine serum albumin, and 0.4% methylcellulose (all were bought from Sigma Co, USA). For the functional experiment, kainate receptor antagonist: UBP 301 (5μM to 20μM) or CNQX (50μM to 500μM) (Tocris Co, UK) was added to the culture medium at the beginning of the retinal explant culture. The control culture group was added the same volume of Dimethyl Sulphoxide (DMSO).

Analysis of the retinal explant outgrowth

The procedures followed that described in chapter 2.

Results

1. Expression of kainate receptor subunits in the retina and ventral diencephalon

1.1. Differential expression of kainate receptor subunit mRNA

After dissociation and reverse transcription of the total RNA from retinas and ventral diencephalon at different stages, we first verified that the internal control (*β-actin*) could be amplified from these total RNA. Then kainate receptor subunits were amplified from these total RNA. The different bands of PCR products at 123bp for *GluR5*; 89bp for *GluR6*; 98bp for *GluR7*; 121bp for *KA1*; 117bp for *KA2* and 362 for *β-actin* were amplified (Fig. 1A).

All these subunits could be detected in the retina at earliest stage examined (E13), with a progressive increase in receptor expression in *GluR6* and *KA1* during the prenatal periods. In the adult retina, *GluR6* and *KA1* are reduced to a relatively low level. For the *GluR5*, it increased to its maximum at the adult retina; and remained at a relatively low level in the prenatal periods. *GluR7* remained at a same low level in the retina throughout the prenatal development. *KA2* showed a progression reduction in its expression during the embryonic stages, although it was expressed distinctly at E13 and in adult retina (Fig. 1A-B). All these subunits showed little difference compared in the ventral diencephalon at E13 and E15.

Anti-GluR567 is a mouse monoclonal antibody from Millipore that recognizes kainate receptor subunits-GluR5/6/7 (Huntley et al., 1993). Through Western-blotting, different bands of protein were detected in crude extracts of the retina and ventral diencephalon at E15, and that of in adult retina. There were

different isoforms for various subunits: 1) GluR5 has three transcripts, the protein weights are: 94, 98 and 101KD mol. Wt. 2) GluR6 has ten transcripts in this gene, two transcripts don't translate protein, their protein weights are: two 102; two 98; two 38; 100 and 62KD mol. Wt. 3) GluR7 has one transcript, the protein weight is 104KD mol. wt. Most of these subunits were detected in the retina and ventral diencephalon at E14 (Fig. 1C).

1.2. Kainate receptor subunit (GluR5/6/7) expressed in the growth cones of the retinal neurites

As the gene and protein level was verified at E13 and E14, respectively. We wanted to further confirm whether these subunits could be stained on the retinal axons. Anti-GluR567 was used to stain the retinal explants in vitro. Anti-GluR567 could obviously stain the growth cones and neurites of the explants isolated from the E14 retina (Fig. 1D). These results suggested that kainate receptor subunits proteins might express on the neurites and growth cones during the embryonic periods.

2. Expression of GluR5/6/7 in the optic pathway during embryonic development

2.1. Expression of GluR5/6/7 in the mouse retina

2.1.1. Anti-GluR567 was stained in the retina at different embryonic stages

Anti-GluR567 is a mouse monoclonal antibody used to stain GluR5/6/7 in the adult and the developing retina at E13 to E15. No staining was detected in control section at E13 (Fig. 2A). There was obvious staining in the adult retina (n=2): strongly localized in the nerve fiber layer (NFL), GCL, and IPL; sparsely in the INL, OPL, and ONL (Fig. 2B). At E13 (n=5), the staining was localized in the soma and processes of radially orientated cells which spanned the whole thickness of the retina; little staining was found in the retinal axons (Fig. 2C-D). In addition, strong staining of GluR5/6/7 was detected in the CMZ, lens and blood vessels (Fig. 2C). In high

magnification, it showed that there was intensely stained in the axon layer and the optic disk (OD) and some glial-like cells near the OD (Fig. 2E). At later stages, GluR5/6/7 displayed a neuronal expression pattern more obviously than that at E13. At E14 (n=9), GluR5/6/7 was expressed in the retinal axons extending to the OD and the cells in the inner layer of retina under high magnification (Fig. 2F). At E15 (n=7), GluR5/6/7 was highly expressed in the inner cellular layer and the axon layer of retina (Fig. 2G). GluR5/6/7 was also expressed weakly on the cells in the outer layers. Similar staining pattern could be seen in the retina at E18 (n=2, Fig. 2H).

2.1.2. GluR5/6/7 expressed on the TuJ-1 positive neurons in the retina

To identify the GluR5/6/7 positive cells in retina, we did the double staining with anti-GluR1 and TuJ-1 which labeled developing neurons including the retinal ganglion cells. TuJ-1 positive neurons were confined to the inner layer and axon layer of retina, which also strongly labeled by anti-GluR567 at E15 (n=3; Fig. 3A-D). In addition, some TuJ-1 positive new-born neurons in the outer layer of retina were also detected, but there still were some GluR5/6/7 positive radial cells which could not be identified by TuJ-1 (Fig. 3C). Furthermore, GluR5/6/7 positive staining was also found in the CMZ where TuJ-1 was nearly absent except in a few cells (Fig. 3A).

2.2. Expression of GluR5/6/7 in the mouse ventral diencephalon

2.2.1. Anti-GluR567 was stained in the ventral diencephalon

For the expression of GluR5/6/7, we stained the horizontal sections of the mouse ventral diencephalon from E13 to E15. GluR5/6/7 was highly expressed in the OS and the chiasmatic neurons that are arranged in an inverted V-shape domain in the E13 ventral diencephalon (n=8; Fig. 4A-B). At E14, there were strong labels of GluR5/6/7 in the OS and the OT (n=8; Fig. 4C-D). However, GluR5/6/7 staining was

also observed in the other regions of the ventral diencephalon. The same staining pattern was shown at E15 (n=6; Fig. 4E-F). Furthermore, in the E14 frontal sections, GluR5/6/7 was strongly labeled in the OC and OT (Fig. 5A-F). In addition, GluR5/6/7 positive cell bodies were arranged along the ventricular surface; it also detected some cells in the midline region above the axons in the OC (arrow, Fig. 5C).

2.2.2. GluR5/6/7 expressed on the CD44 positive neurons in the ventral diencephalon

To identify the GluR5/6/7 positive cells, we did the double staining with anti-GluR567 and CD44 which detected the chiasmatic neurons related to the formation of the optic pathway in the ventral diencephalon. At E14 (n=2; Fig. 6A-G), GluR5/6/7 was localized in CD44 positive neurons in the ventral diencephalon, indicating that part of anti-GluR567 positive cells were chiasmatic neurons. However, there were other anti-GluR5/6/7 positive cells that are negative to anti-CD44.

3. Kainate receptor antagonists had no effect on the retinal neurite outgrowth

To determine possible function of kainate receptors on the retinal axons, we cultured the E14 retinal explants in vitro. The control culture was treated with the same volume of DMSO. Different concentration of UBP301 (5μM to 20μM; a potent KAR antagonist) and CNQX (50μM to 500μM; a competitive AMPAR and kainate receptor antagonist) was added to the culture dish. The results showed that neurites from the retinal explants treated with UBP301/CNQX was not effected significantly when compared with control groups (Fig. 7A-D and Fig. 8A-D).

Statistical data showed that there was no statistical difference between the UBP301 or CNQX treated groups and the corresponding controls (Fig. 7E and Fig. 8E), confirming that suppression of kainate receptors cannot promote retinal axon outgrowth. On the other hand, the previous study reports that activation of kainate

receptors may induce a fast and reversible growth cone stalling (Ibarretxe et al., 2007). Furthermore, our study from the statistical plots shows that low concentration of kainate receptors antagonists might have the tendency of slightly promoting the axon outgrowth.

Discussion

Kainate receptors have been extensively studied in synaptic plasticity, epileptic activity and certain psychiatric conditions such as schizophrenia and major depression (Bloss and Hunter, 2010; Bortolotto et al., 1999; Woo et al., 2007). The specific physiological implications for generating and modulating network activity are just starting to recognize. Functional kainate receptors are expressed at presynaptic and postsynaptic sites, and their activation has a varied effect dependent on their localization and distinct subunits composition (Isaac et al., 2004). The previous study shows that transient activation of kainate receptors induces a fast and reversible growth cone stalling, accompanied by an increase in shape irregularity; and this function needs GluR6 subunit participation (Ibarretxe et al., 2007). Here, we characterize the localization of GluR5/6/7 with an antibody that identifies all of these subunits in the embryonic mouse retinofugal pathway, and explore preliminarily their function in the retinal axons.

1. Expression levels of kainate receptor subunits differ in distinct stages

The expression of kainate receptor subunits varies at different embryonic stages of retinal development. *GluR5* preferentially expresses in the adult retina, but low in the embryonic retinas. *KA2* expresses distinctly in the adult and E13 retinas, and reduces at later embryonic stages. *GluR6* and *KA2* may have a gradual increase during the embryonic stages, and then maintain at a low level in the adult retina. *GluR7* is

consistent throughout the development of the retinas. And they also express with little difference in the ventral diencephalon at E13 and E15.

The previous studies through in situ hybridization and immunostaining or immunoblotting together with RT-PCR show that glutamate receptors have been detected in many, but not all cells in the ganglion cell layer (Grunder et al., 2000; Jakobs et al., 2007; Muller et al., 1992; Vitanova, 2007). The knock-out mice deficient in GluR5 (*Grik1*) and GluR6 (*Grik2*) expressions show that these two kainate receptors play distinct roles in kainate-induced gamma oscillations and epileptiform burst activity. Ablation of GluR5 leads to higher susceptibility of the network to KA-induced gamma oscillation, but lack of GluR6 prevents this action (Fisahn et al., 2004). This study indicates that kainate receptors fulfill different roles in the neuronal network depending on their distinct subunit distribution. From our study, kainate receptor subunits express in the retina and ventral diencephalon, and on the retinal neurites and growth cones. However, the function of these subunits on embryonic retina is still unknown.

2. Kainate receptor subunit (GluR5/6/7) expresses in the mouse retinofugal pathway

In the embryonic retina, there are two types of cells: one is new-born RGCs (Colello and Guillery, 1990); the other is the Müller cells at early stage retina (Bhattacharjee and Sanyal, 1975). At E13, GluR5/6/7 expresses in the glial-like cells. Few RGCs are stained at this early stage; but in the optic disk, there are obvious staining with the radially arranged glial-like cells and retinal axons. The previous studies have reported that some molecules such as Slit2, may take part in the retinal axon path-finding in the optic disk (Thompson et al., 2006). Kainate receptors might also take part in the formation of the optic disk and guide the retinal axons; but their role

in the optic disk needs future study. At later stages, the GluR5/6/7 staining is localized on the axon layer and the inner cellular layer of retina. To identify the inner layer cell, we do double staining with GluR5/6/7 and TuJ-1. All the TuJ-1 positive neurons can be labeled by GluR5/6/7. The other cells might be glial-like cell.

In the ventral diencephalon, anti-GluR567 can distinctly stain the optic nerve, optic stalk, optic chiasm and optic tract. Although it stains the whole diencephalon, it can clearly stain the glial-like cells at the ventricular zone and some cells in the midline region above the chiasm in the optic chiasm in the frontal sections. Double staining with anti-GluR567 and CD44 which is a specific marker for the chiasmatic neurons in the mouse embryos (Sretavan et al., 1994), indicating that all the CD44 positive neurons can be labeled by anti-GluR567. Different previous reports show that ablating the CD44 positive neurons will induce the retinal axons being unable to grow into the chiasm; specific antibodies to CD44 will induce severe defects in routing of the retinal axons across the midline which arrive early in the chiasm (Lin and Chan, 2003; Sretavan et al., 1995). Through these, we infer that kainate receptors may participate in the regulation of the early optic pathway formation. Whereas, there are still some other GluR5/6/7 positive cells which cannot be stained by CD44.

As kainate receptor subunits express in the retinal axons, the optic nerve, chiasm and the optic tract, and they may also be labeled in the chiasmatic neurons, some glial-like cells in the ventricular zone, we propose that they might play a role in the neuronal activity of retinal fibers in the developing period.

3. Kainate receptor antagonists have no effect in the retinal neurite outgrowth

As chapter 2 and 3 mentioned, glutamate can promote the retinal axon growth in the E14 retinal explants culture experiment, and activation of AMPARs may participate in this promotion. We want to investigate whether kainate receptors are involved in

this axon growth activity. Our data demonstrate that both UBP301 (a potent kainate receptor antagonist) and CNQX (a competitive AMPAR and kainate receptor antagonist) cannot block retinal axon growth. On the contrary, there is a tendency from the plot that both at a lower concentration may slightly promote retinal axon growth, although there is no statistical significance. These data alone demonstrate that retinal axons respond to kainate receptors activation with growth inhibition or little effect on axon growth, which is different from the results that AMPAR activation can promote axon growth in similar experimental conditions. Further investigation of the ionotroptic receptor function will be described in the following chapter.

Recent study shows that activation of GluR6-containing kainate receptors by bath application of kainate stalls reversibly growth cones of hippocampal neurons; and this growth cone motility can be blocked by CNQX, not by GYKI53655 (a noncompetitive AMPAR antagonist) (Ibarretxe et al., 2007). Our results support the notion that kainate receptors cannot participate in the promotion of retinal axon outgrowth, instead they may play the role of halting the growth cones during development so as to let them expose other guidance cues. However, low concentration of kainate does not affect rapid growth cone motility, but can decrease the rate of axonal outgrowth by a mechanism involving metabotropic signaling cascades (Ibarretxe et al., 2007; Lerma, 2003; Pinheiro and Mulle, 2006). This phenomenon needs to be investigated whether retinal axons also have such a mechanism, and low concentration of kainate receptor antagonists could promote retinal axon outgrowth.

Figures

Figure 1. Expression of kainate receptor subunits in the retinas and ventral diencephalons at different stages. *Grik1-5* and *actin* as positive internal control were respectively detected in adult retina, E13 retina (E13R), E15 retina (E15R), E16 retina (E16R), P1 retina (P1R), E13 ventral diencephalon (E13VD) and E15 ventral diencephalon (E15VD) (Fig. A). The plot showed that *GluR5* increased to its maximum at the adult retina, and remained at a relatively low level in the prenatal periods. *GluR6 and KA1* showed a progressive increase during the prenatal periods, but they reduced to a relatively low level in adult retina. *GluR7* remained same low level in the retina throughout the prenatal development and adult retina; *KA2* showed a progressive reduction in its expression during the embryonic stages, although it was expressed distinctly at E13 and in adult retina. All these subunits showed little difference compared in the ventral diencephalon at E13 and E15 (Fig. A-B). Western-blotting showed that different bands with 62KD; 98KD; 102KD and 104KD were identified for GluR5/6/7 subunits at E15, respectively (Fig. C). Immunostaining of retinal explant cultures of GluR5/6/7 indicated that retinal neurites and growth cones (arrows) were labeled by anti-GluR567 antibody (Fig. D).

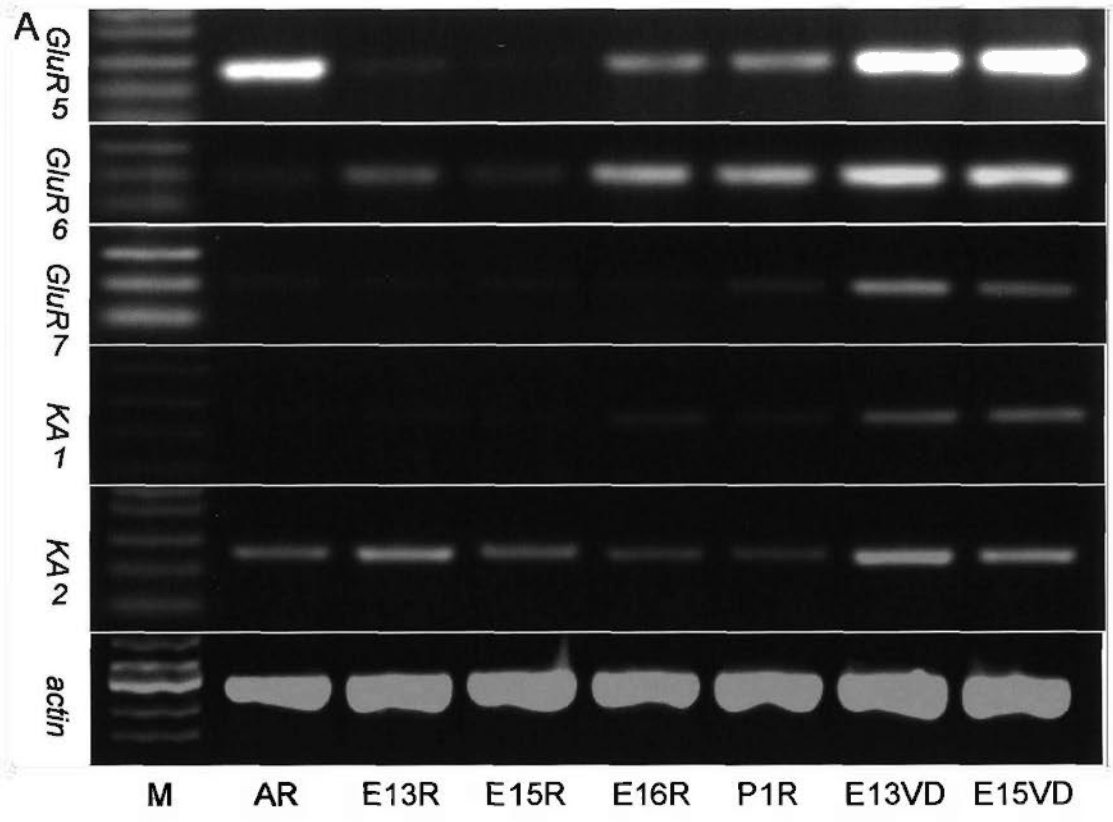
A
GluR5
GluR6
GluR7
KA1
KA2
actin
M
AR
E13R
E15R
E16R
P1R
E13VD
E15VD

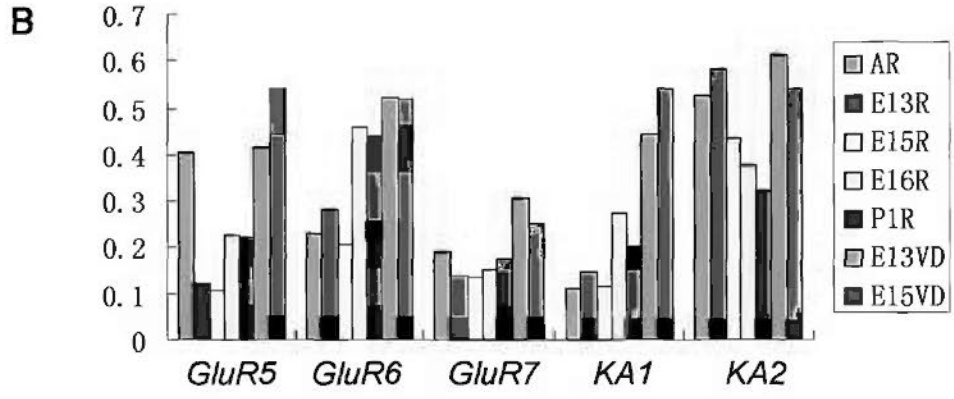
B
0.7
0.6
0.5
0.4
0.3
0.2
0.1
0
GluR5
GluR6
GluR7
KA1
KA2
AR
E13R
E15R
E16R
P1R
E13VD
E15VD

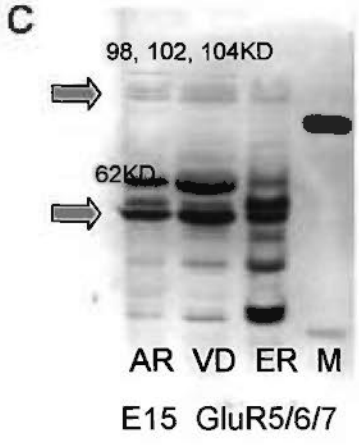
C
98, 102, 104KD
62KD
AR VD ER M
E15 GluR5/6/7

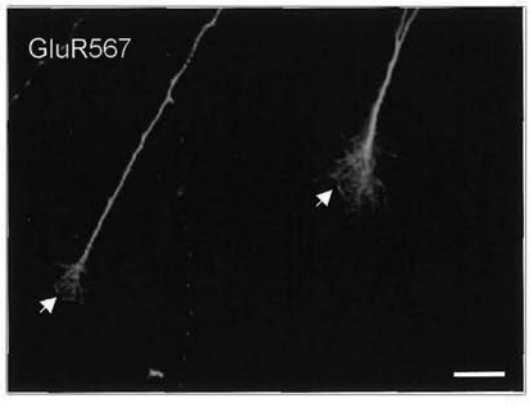
D
GluR567

Figure 2. Immunostaining of retinal sections for GluR5/6/7 at different stages. No staining was detected in control section at E13. L was for lens, R for retina (Fig. A). There was obvious staining in adult retina (n=2). The immunostaining strongly localized in NFL, GCL, and IPL; sparsely in INL, OPL, and ONL (Fig. B). At E13 (n=5), the immunoractive GluR5/6/7 is preferentially stained in the radial glial-like cells and some optic fibers especially in the optic disk (OD) (Fig. C). In addition, strong staining of GluR5/6/7 was detected in the ciliary marginal zone (CMZ) (asterisks), lens and blood vessels (arrows) (Fig. C). In high magnification, most of the GluR5/6/7 staining was detected in the soma and the processes of radially oriented cells which spanned the whole retina (arrows) (Fig. D). At E13 and E14 (n=9; Fig. E-F), GluR5/6/7 was expressed in the optic fibers extending to the OD and some glial-like cells around the OD (arrows) under high magnification (Fig. E-F). At E15 (n=7), GluR5/6/7 was highly expressed in the retinal axon layer and inner cellular layer (Fig. G). At E18 (n=2), the pattern of immunopositive GluR5/6/7 was the same as E15 (Fig. H). Scale bars = 200μm in A (also applies to C); 100μm in B (also applies to C-H).

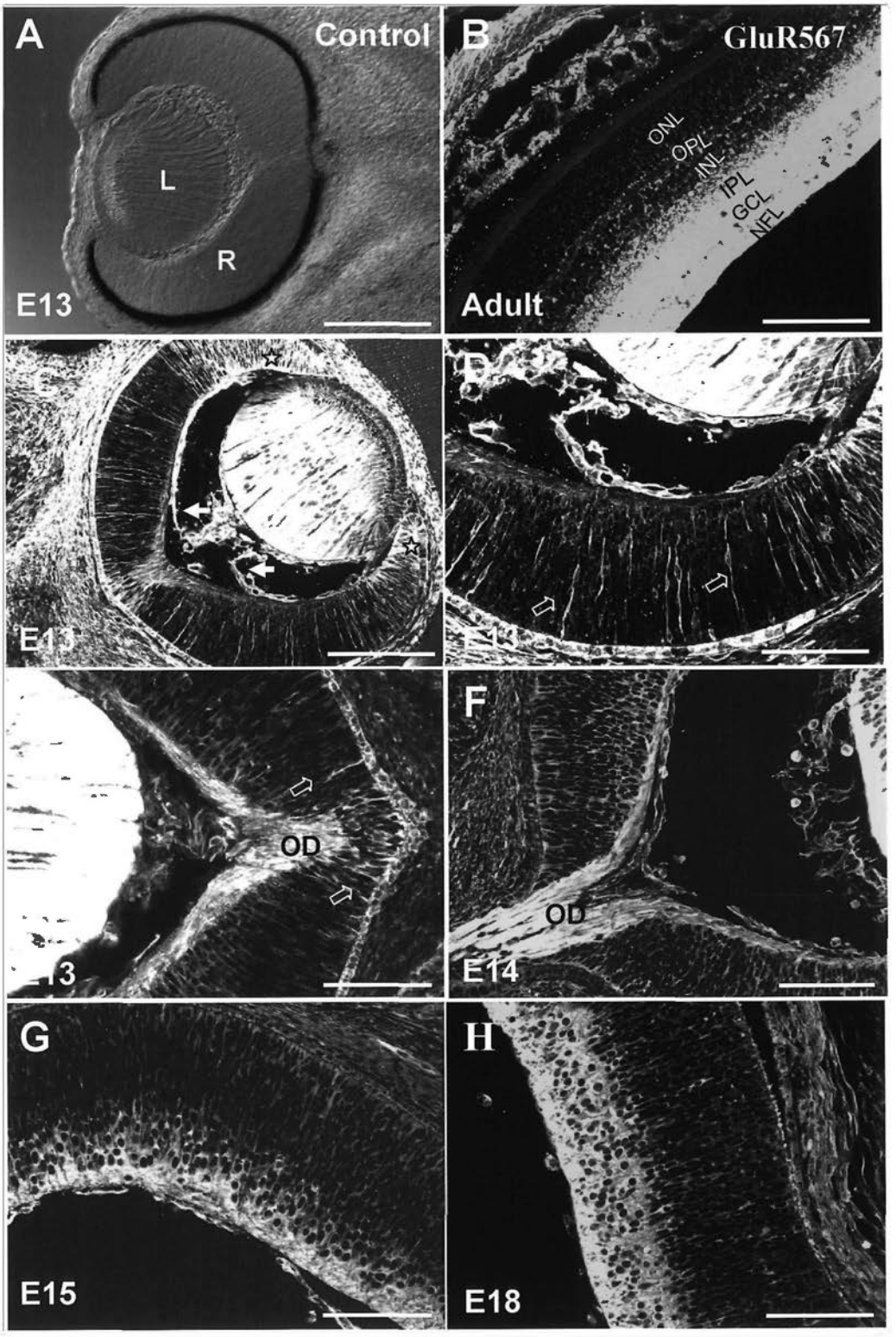
A
Control
L
R
E13
B
GluR567
ONL
OPL
INL
IPL
GCL
NFL
Adult
E13
D
OD
OD
F
OD
E14
G
E15
H
E18

Figure 3. Immunostaining of retinal sections for TuJ-1 and anti-GluR567 at E15. In the low magnification, GluR5/6/7 positive staining was colocalized with TuJ-1 positive neurons except in the ciliary marginal zone (CMZ) where could not be stained by TuJ-1 antibody at E15 (arrow) (n=3; Fig. A). The intensities of immunopositive TuJ-1 and anti-GluR567 were confined to the inner layer of retina which included the ganglion cell layer and the optic fiber layer (Fig. B-C). In the merged image, it showed the colocalization of these two antibodies (Fig. D). Scale bars = 200μm in A; 100μm in B (also applies to C-D).

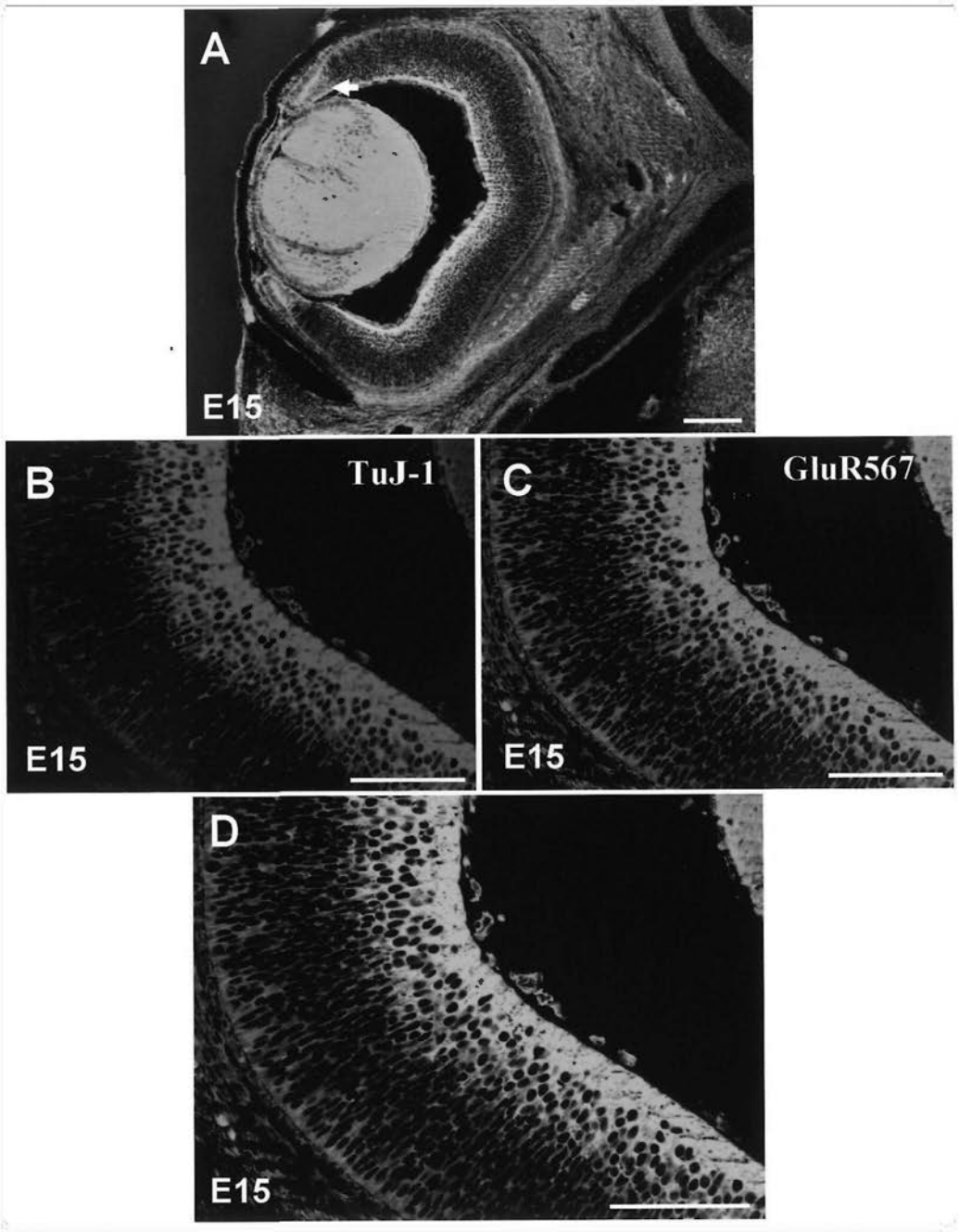
A
E15
B
TuJ-1
E15
C
GluR567
E15
D
E15

Figure 4. Immunostaining of ventral diencephalic sections for anti-GluR567 at different stages. These were the horizontal sections; rostral was to the top and the midline was indicated by the arrows. GluR5/6/7 was highly expressed in the cells that are arranged in an inverted V-shape domain in the ventral diencephalon at E13 (n=8; Fig. A-B). At E14 (n=5), the immunoreactive GluR5/6/7 was detected in the optic stalk (OS) and the optic tract (OT); extensively in the whole ventral diencephalon (Fig. C-D). At E15 (n=6), There was distinct staining in the OS and OT, and extensively in the other regions of ventral diencephalon (Fig. E). In high magnification, the immunoreactive GluR5/6/7 was preferentially detected in the beginning of chiasm and OT (Fig. F). Scale bars = 200μm in A (also applies to B-C); 200μm in D (also applies to E-F).

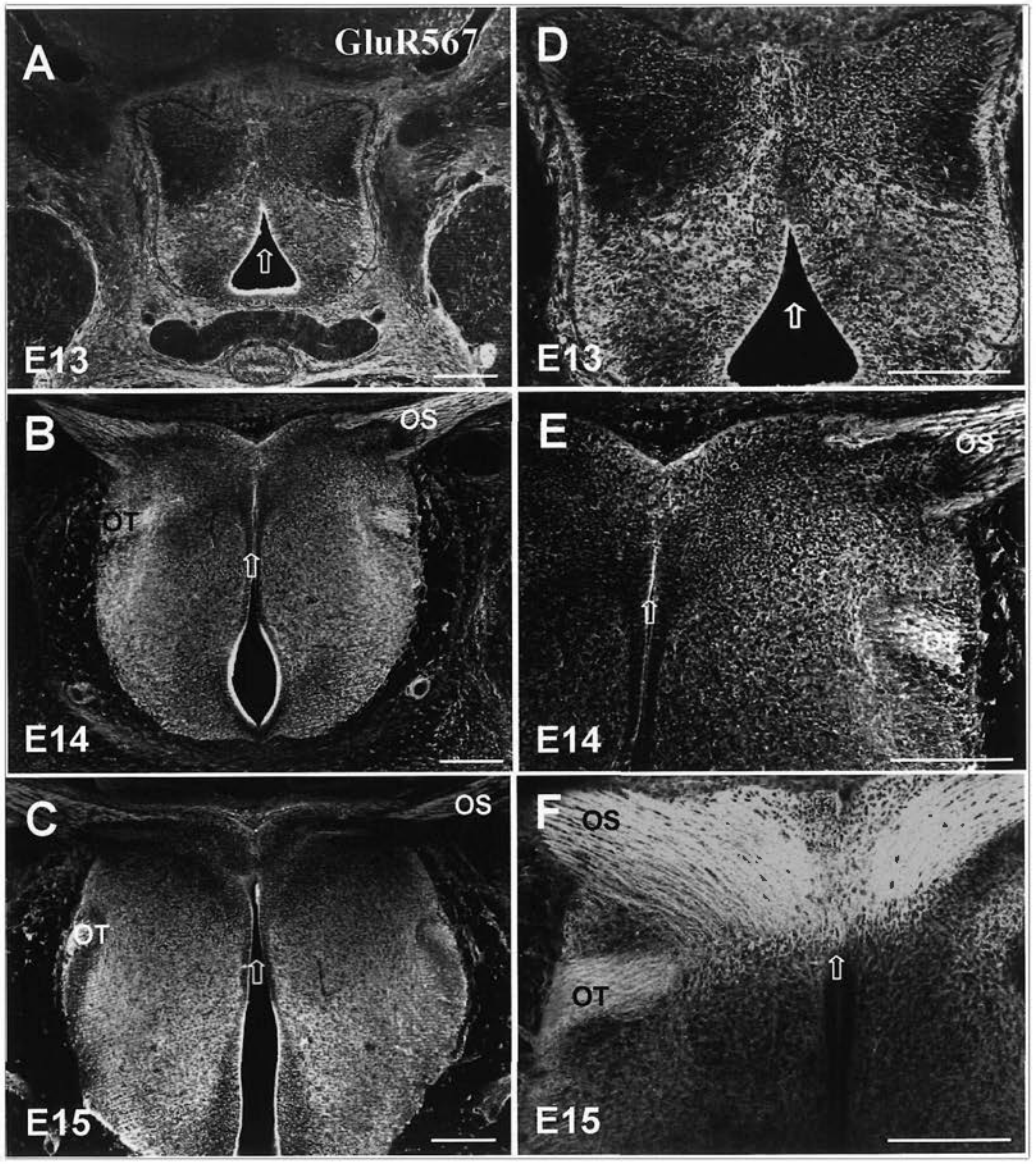
A
GluR567
E13
D
E13
B
OS
OT
E14
E
OS
E14
C
OS
OT
E15
F
OS
OT
E15

Figure 5. Immunostaining of including chiasm sections for anti-GluR567. There were frontal sections of E14; the arrow points to the midline of the brain, and rostral is up. Obvious expression of GluR5/6/7 was localized in the optic fibers in the beginning of the chiasm, glial-like cells in ventricular zone and some cells (arrowheads) at the midline anterior to the optic fibers in the chiasm (n=4; Fig. A-C). At the midlevel of the chiasm, the staining was strongly found in the optic fibers in the chiasm (Fig. D-E). In the optic tract, the intense staining of GluR5/6/7 was observed (Fig. F). Scale bars = 100μm in A (also applies to B-F).

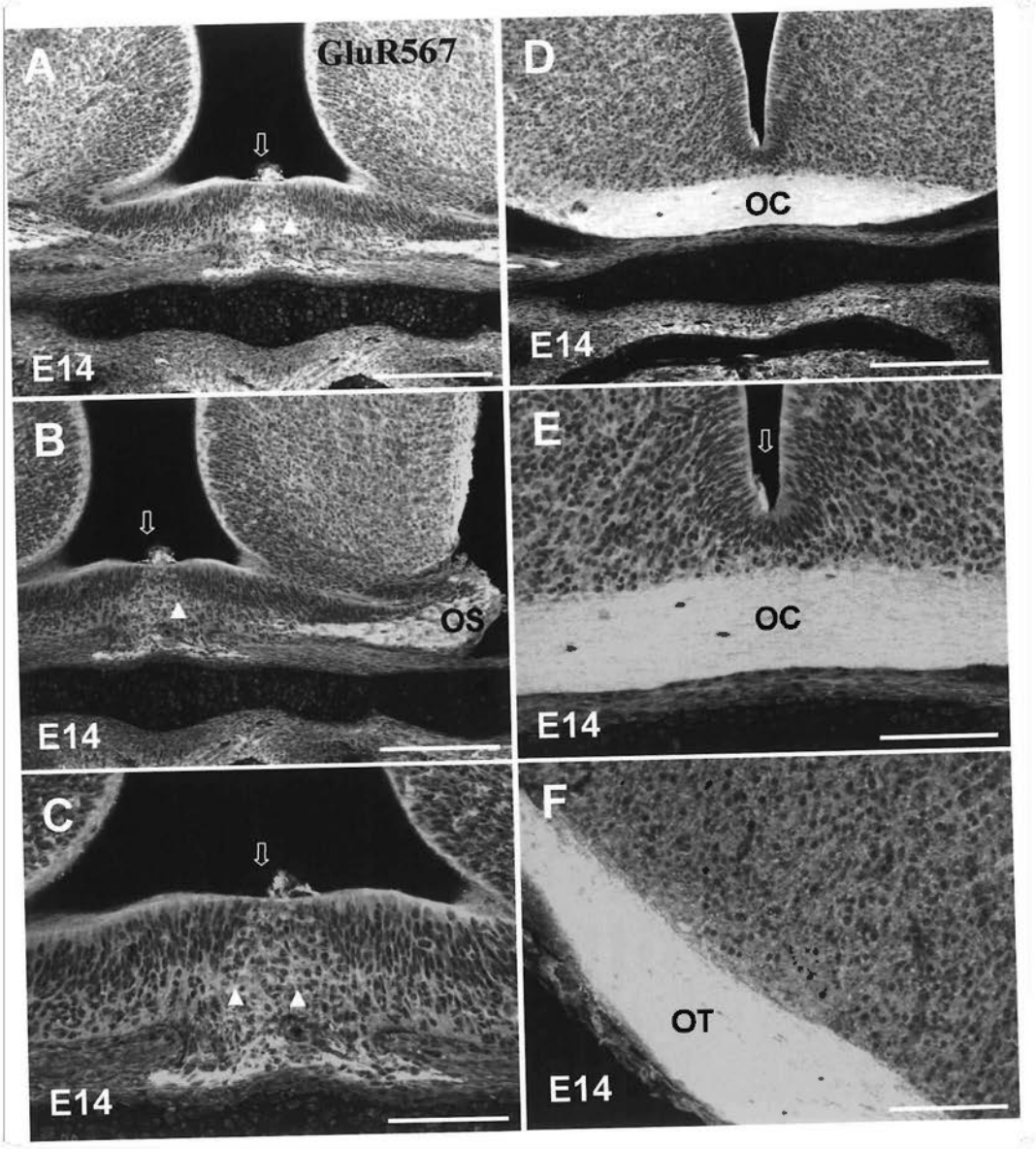
A
GluR567
E14
B
OS
E14
C
E14
D
OC
E14
E
OC
E14
F
OT
E14

Figure 6. Immunostaining of ventral diencephalic sections for (IM7) CD44 and anti-GluR567. This was the horizontal section; rostral was to the top and the midline was indicated by the arrows. At E14, the immunopositive GluR5/6/7 was intensely expressed in the optic tract (OT) and extensively distributed in the whole ventral diencephalon, where merged with CD44 positive chiasmatic neurons (n=3; Fig. A). In high magnification, GluR5/6/7 was localized on the surface of the cells, some of the GluR5/6/7 positive cells could coincide with the cells which were immunoreactive for CD44 (Fig. B-G). However, there were still other GluR5/6/7 positive cells that could not be stained by anti-CD44 (Fig. A, D). Scale bars = 200μm in A; 100μm in B (also applies to C-D); 50μm in E (also applies to F-G).

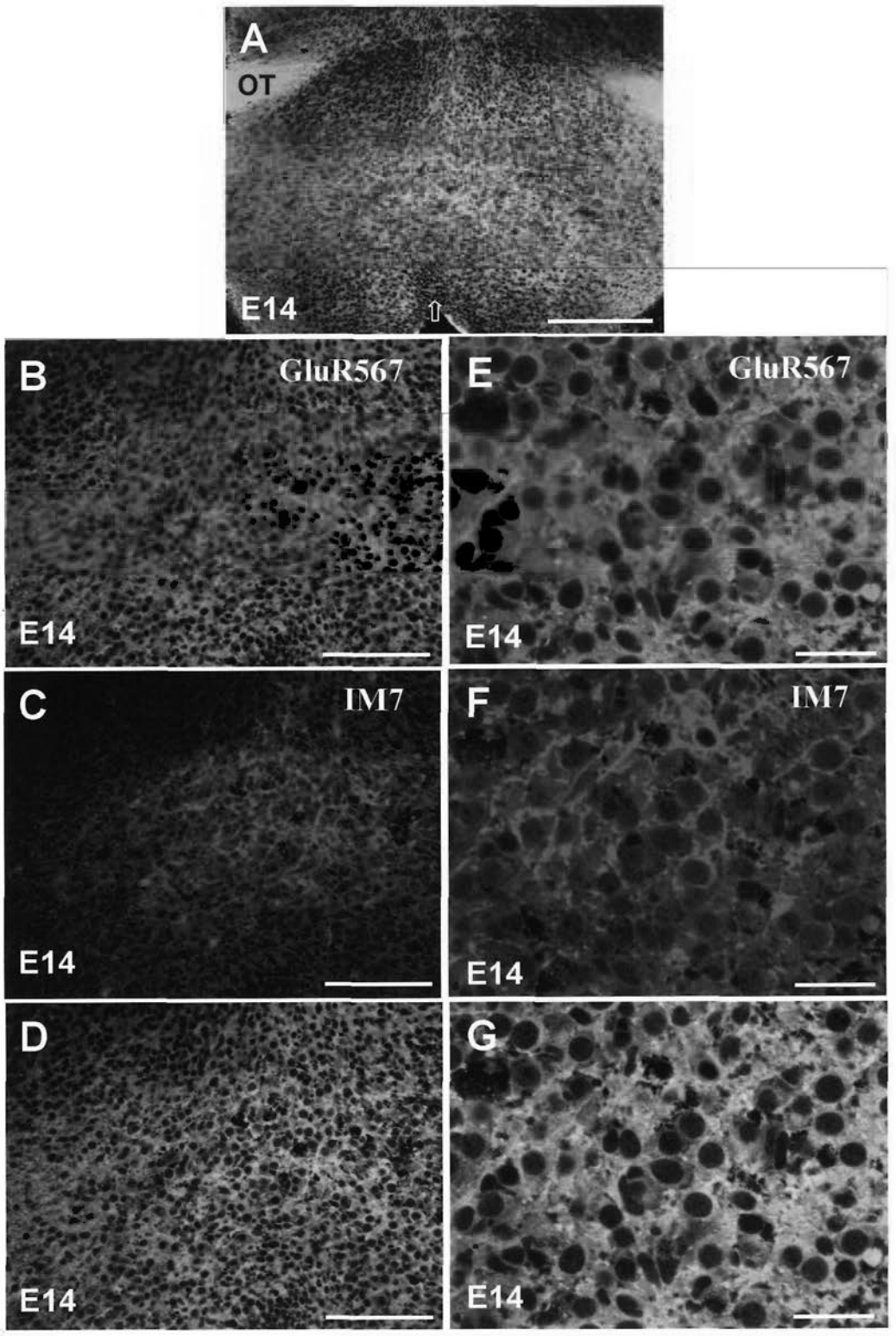
A
OT
E14
B
GluR567
E14
E
GluR567
E14
C
IM7
E14
F
IM7
E14
D
E14
G
E14

Figure 7. Effect of UBP301 on retinal neurite outgrowth in cultured retinal explants. In control preparations at E14, neurites from the retinal explants grew normally (Fig. A). In the presence of the UBP301 with different concentration (5μM, 10μM and 20μM; a potent noncompetitive KAR antagonist), neurites from the retinal explants also grew normally (Fig. B-D). Plot showed that there was no statistical significance to the neurite outgrowth in the UBP301 treated groups compared with that of the control one (Fig. E). Scale bars = 500μm.

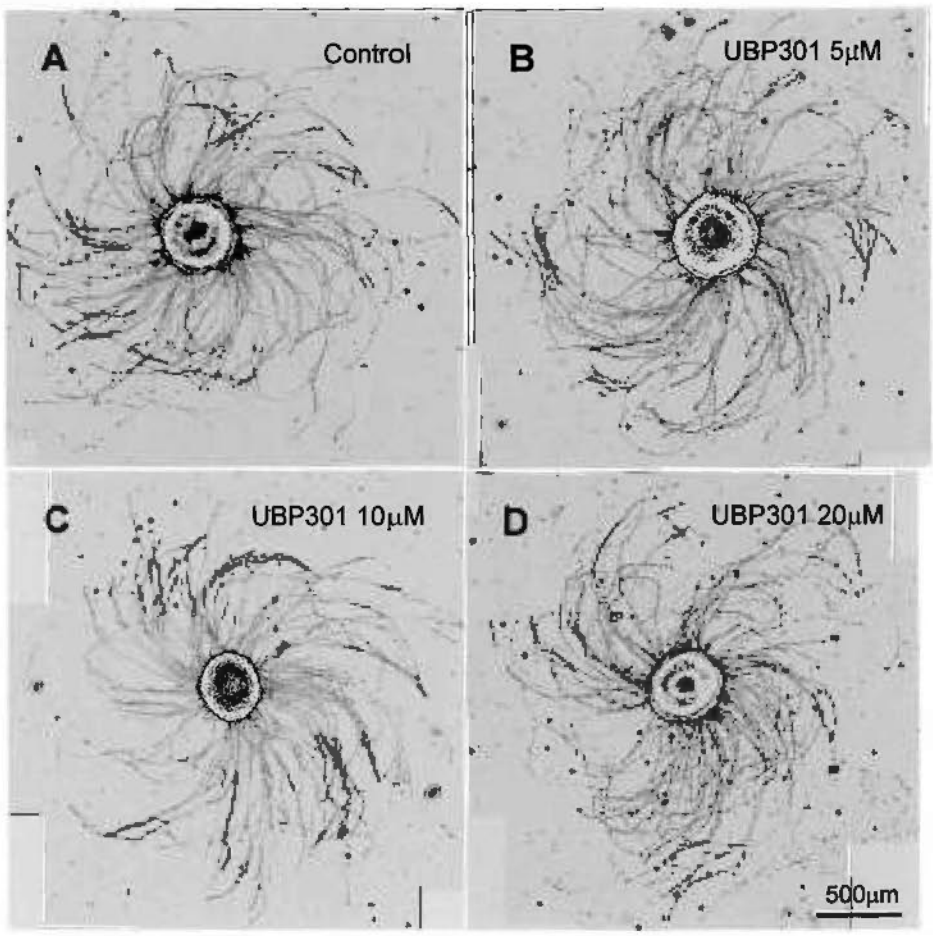
A
Control
B
UBP301 5μM
C
UBP301 10μM
D
UBP301 20μM
500μm

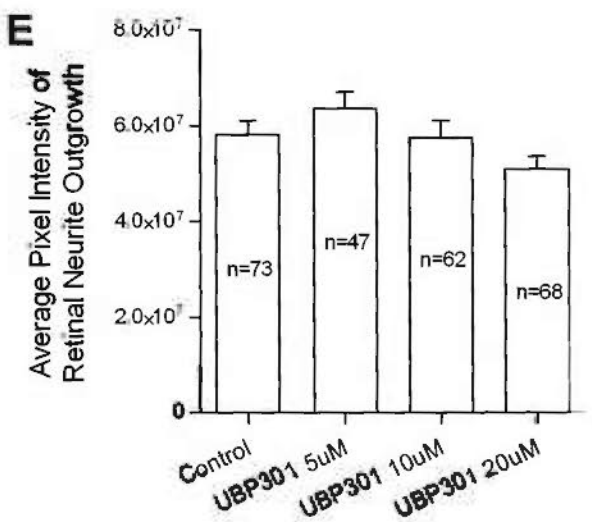
E
Average Pixel Intensity of Retinal Neurite Outgrowth
8.0x10⁷
6.0x10⁷
4.0x10⁷
2.0x10⁷
0
n=73
n=47
n=62
n=68
Control
UBP301 5uM
UBP301 10uM
UBP301 20uM

Figure 8. Effect of CNQX on retinal neurite outgrowth in cultured retinal explants. In control preparations at E14, neurites from the retinal explants grew normally (Fig. A). In the presence of the CNQX with different concentration (50μM, 100μM, 200μM and 500μM; a competitive AMPAR and KAR antagonist), neurites from the retinal explants also grew normally (Fig. B-E). Plot showed that there was no statistical significance to neurites outgrowth in the CNQX treated groups compared with that of the control one (Fig. F). Scale bars = 500μm.

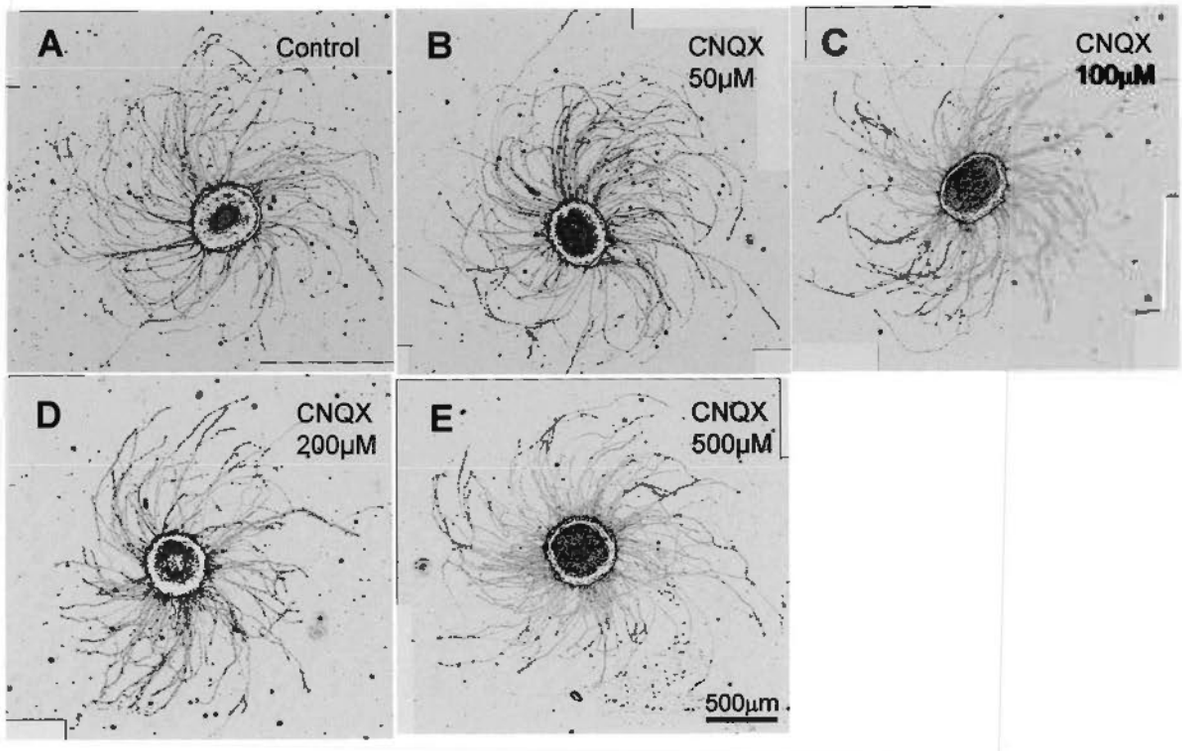
A
Control
B
CNQX
50μM
C
CNQX
100μM
D
CNQX
200μM
E
CNQX
500μM
500μm

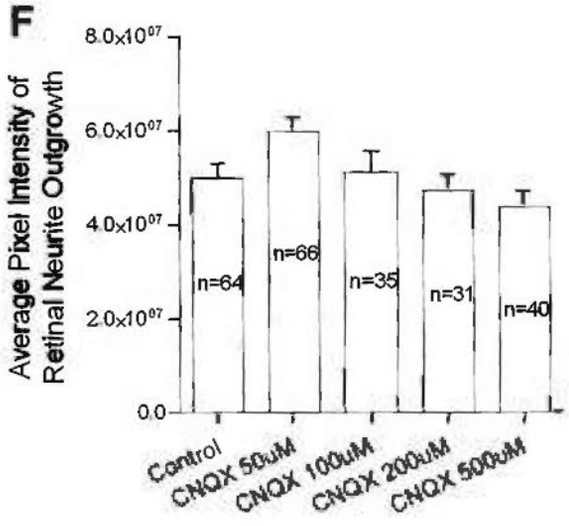
F
Average Pixel Intensity of Retinal Neurite Outgrowth
8.0x10^07
6.0x10^07
4.0x10^07
2.0x10^07
0.0
n=64
n=66
n=35
n=31
n=40
Control
CNQX 50uM
CNQX 100uM
CNQX 200uM
CNQX 500uM

CHAPTER 5

Glutamate and its ionotropic receptors control the retinal axon growth at the mouse optic pathway

Introduction

Glutamate toxicity is attenuated in the highly glutamatergic developing retina (Haberecht et al., 1997; Haberecht and Redburn, 1996), which has also been shown by our study in the retinal explants culture. Application of 0.5-2mM glutamate to retinal explant culture will promote retinal axon outgrowth (Chapter 2); Nichol et al, have also reported that application of glutamate to rat retinal ganglion cell cultures will show to be neurotropic (Nichol et al., 1995). Extracellular levels of endogenous glutamate are relatively high in the developing retina; and glutamatergic pools can be observed by immunocytochemistry (Haberecht and Redburn, 1996). The highly glutamatergic environment in the retina appears to promote cell survival and developmental processes, but this concentration is considered as toxic in the adult.

During development of the retinofugal pathway, optic fibers in the optic nerve will be sorted at the optic chiasm to form the two optic tracts. Fibers from nasal retina cross the midline and project to contralateral side, whereas fibers from temporal retina do

not cross and turn to the ipsilateral side (Jeffery and Erskine, 2005; Marcus et al., 1995). This process is controlled by a population of early generated neurons (SSEA-1 or CD44 positive neurons) and glial cells (RC2 positive neurons), which release or express some signaling molecules (Chan et al., 1998; Marcus et al., 1995). Most of the neurons and glial cells express glutamate receptors both during development and in the adult brain. As glutamate is one of the excitatory neurotransmitters in the mammalian retina and other parts of central nervous system, and previous studies through in situ hybridization show that expression of ionotropic glutamate receptors subunits can be found at as early as embryonic day 14-18 (Zhang et al., 1996). The prominent expression of glutamate and its receptors in the developing retina suggests that glutamate might also play a critical role in the retinal ontogeny and the early pathway formation, although synaptic contacts and most of retina development occur in the postnatal period.

Various evidences show that glutamate takes part in the postsynaptic neuronal morphology at dendritic spines, and there is also increasing evidences of its foundation in shaping axonal structures and regulating axonal outgrowth (Mattson et al., 1988; Muller and Nikonenko, 2003; Pearce et al., 1987). It is possible that glutamate and its receptors may be related to the retina and retinal axon formation. Application of 1mM NMDA at postnatal day 1 in the rabbit retina leads to retinal changes which show a disruption of the outer plexiform layer and cellular organization of the neuroblastic layers (Haberecht et al., 1997); and glutamate and its receptors antagonists induce changes of cell differentiation process in E15 mouse retina (Rorig and Grantyn, 1994). Several studies have shown that the ionotropic receptors appear to participate in the refinement of dendritic contacts in the retina (Bodnarenko and Chalupa, 1993; Bodnarenko et al., 1995).

In our studies, we have shown the localization of glutamate and non-NMDA receptor subunits at E13 to E15. Function of AMPARs and kainate receptors has also been inferred from retinal explant culture in which application of AMPAR or kainate receptor antagonists leads to retinal axon outgrowth changes. Through 1-amino-4-guanidobutane (agmatine; AGB) immunolabelling, it is reported that glutamate ionotropic receptors on the E18 retinal ganglion cells are activated by applying a range of glutamate analogs at E18 (Acosta et al., 2007). The question remains unclear whether the functional ionotropic receptors may work together to affect retinal axon growth and the role of glutamate in the developing mouse retinofugal pathway.

Materials and Methods

Animal preparation

All the preparation was done as described in chapter 2.

Experimental reagents

Stock solutions were prepared by dissolving drugs in water or dimethyl sulfoxide (DMSO) (1% maximal, final concentration) according to the manufacturer's recommendation. Stock solutions were directly used to the working concentration or diluted with 1xPBS immediately before the experiment. The following drugs were used L-glutamate (500μM to 2mM); MK-801 (50-100μM) (RBI Co; USA); CP465022 hydrochloride (2-20μM); GYKI52466 dihydrochloride (25-150μM); CNQX (50-500μM); UBP 301 (5-25μM); Cyclosporine A (csp A) (Tocris Co; UK); KN-93 (5-20μM) (Calbiochem Co; USA).

Preparation of retinal explants and receptor antagonist treatments

The procedure was the same as described in Chapter 2. Various compositions of MK-801 (100μM), CP465022 (10μM), CNQX (50μM), UBP301 (5μM), and KN93 (5μM) were added at the different final concentration before the culture.

Analysis of the retinal explant outgrowth

The procedures were the same as described in chapter 2.

Ventral diencephalon glial cell culture

The pregnant mice were killed by cervical dislocation. Embryos from E14 were taken out and kept in cold Dulbecco's modified Eagle's medium (DMEM)/F12 (high glucose) medium containing penicillin (1000U/ml) and streptomycin (1000μg/ml). Ventral diencephalic cells were dissociated and digested by 0.1% trypsin for 3 min at 37°C, plated at a density of 60,000/ cm^2 directly on the culture dish and maintained in the culture medium with 15% FBS (Invitrogen, USA) in a 5% CO_2 incubator at 37°C for 10 d. During these days, the medium was changed every 3 for two passages, plated on the Poly-DL-ornithine coated coverslips after the last passage.

Immunostaining

Cultures were fixed with 4% paraformaldehyde for 30 min at 4°C and double labeled with primary antibodies against either GluR1 (Genscript, rabbit polyclonal; 1:100), or GluR2/3 (Abcam, rabbit monoclonal; 1:300), or GluR4 (Millipore, rabbit polyclonal; 1:60), and antibody against RC2 (DSHB, mouse supernatant; 1:10) at 4°C overnight. After three wash steps with 1xPBS, cultures were incubated with secondary antibodies conjugated to Alexa Fluor 488 and Alexa Fluor 568 (1:200; Molecular Probes, USA), respectively for 1 h at RT.

Preparation of brain slices

The experiment procedures in this study were approved by the Animal Ethic Committee of the Chinese University of Hong Kong. Pregnant pigmented C57 mice

were killed by cervical dislocation and embryos at E13 or E15 were taken out. The embryos were decapitated and kept in chilled Dulbecco's modified Eagle's medium (DMEM)/F12 medium containing penicillin (1000 U/ml) and streptomycin (1000 μg/ml). Brain slice preparations of the retinofugal pathway that contained the eyes, optic stalks, chiasm and proximal parts of the optic tract were prepared as described in our earlier studies (Chan et al., 1998).The brain slice was cultured in DMEM/F12 with 10% fetal bovine serum (Invitrogen Co, USA) at 37°C in a rolling incubator for 5 hr. Within this period, the culture was supplied with pure oxygen three times each lasts 50 sec, by directing a jet of oxygen into the air space above the culture medium. In some brain slices, (1) MK-801 was added at final concentrations of 200μM or 500μM before the incubation; this drug is a noncompetitive antagonist to NMDARs; (2) CP465022 was added at the final concentrations of 100μM, 150μM or 200μM before the incubation; this drug was a noncompetitive antagonist to AMPARs; (3) Both MK-801 (500μM) and CP465022 (100μM, 150μM or 200μM) were added at the final concentration before the incubation; to simultaneously block NMDARs and AMPARs; (4) Both CP465022 and KN93 were added at the final concentration of 150μM and 20μM before the incubation, respectively, to block AMPARs and its possible downstream activation, KN93 was a CaMKI/II/IV inhibitor. The control cultures were maintained in the same medium for 5 hr but without addition of drugs, but with the same volume of DMSO.

After the 5 hr culture, the brain slices were fixed with 4% paraformaldehyde in 0.1M phosphate buffer (PB) at 4°C overnight. Then the next day, a small granule of DiI (1, 1′-dioctadecyl-3, 3, 3′, 3′-tetramethylindocarbocyanine perchlorate, Molecular Probes; USA) was put into the optic disk. The embryos were then stored in a dark place at room temperature in 2% buffered formalin. After 5 d for E13 brain slices, 18 d

for E15 brain slices, when there had been sufficient diffusion of the dye, the retinofugal pathway was dissected, whole-mounted on a slide, coverslipped and examined under the confocal microscope (FV300, Olympus Co, Japan). Images of individual growth cones labeled by DiI at different regions of the retinofugal pathway were collected using a 40 × objective.

Analysis of the retinal crossed axons in the ventral diencephalon

Pixel intensity of all retinal axons and growth cones within defined areas flanking both sides of the midline was measured in MetaMorph software (Universal Imaging Co, USA). The ratio of readings obtained from each side of the midline (post-/pre-) was used as an index for the extent of the midline crossing. The uncrossed pathway was represented by the total pixel intensity of retinal axons and growth cones in the initial segment of the ipsilateral optic tract. The data obtained were compared by Mann-Whitney nonparametric tests (GraphPad Inc, USA).

Results

1. GluR1, GluR2/3, and GluR4 expressed on E14 radial glial cells

Cultured cells were examined by anti-GFAP, and could not be labeled by anti-SSEA-1, indicating that these cultured cells were GFAP-positive glial cells (Fig. 1A-C). Cultured cells were also labeled by the radial glial marker RC2 (Fig. 1D, G, J); and the antibodies to all four AMPAR subunits (Fig. 1E, H, K). Only the GluR2/3 subunit was intensely stained in the cell nucleus and weakly in the cell membrane; the GluR1 subunit staining was weak in the cell nucleus; and GluR4 subunit was observed on the whole cell membrane (Fig. 1F, I, L).

2. Glutamate ionotropic receptor antagonists produced reduction in the crossed projection in the optic chiasm at E13

In the control E13 chiasm, a number of dye-filled optic fibers had already entered the chiasm (Fig. 2A-B). In the 200μM CP465022 treated brain slices, the crossed projection appeared to be reduced, although this reduction has no statistically significance compared with the controls (P>0.05) (Fig. 2C-D, Q). In the 500μM MK801 treated brain slices; the crossed projection was not obviously affected compared with the controls, although in some the crossed projection was reduced (P>0.05) (Fig. 2E-F, Q). In the 100μM CP465022+200uM MK801 treated brain slices, the crossed projection was reduced, although this reduction has no statistically significance compared with the controls (P>0.05) (Fig. 2G-H, Q). In the 150μM CP465022+200μM MK801, 200μM CP465022+20μM KN93 and 200μM CP465022+500μM MK801 treated brain slices, the crossed projection was dramatically reduced; furthermore, these reductions has significant differences when compared with the crossed projection of the controls (P<0.05, 0.01, and 0.001, respectively) (Fig. 2I-N, Q). The lower rows showed the magnified view of the axons and their growth cones at the midline (Fig. 2O-P).

3. Glutamate ionotropic receptor antagonists had no effects on the uncrossed projection in the optic chiasm at E15

In the control E15 chiasm, a number of dye-filled optic fibers could be divided into two groups: one was the crossed optic axons that formed the contralateral optic tract; the other was the uncrossed optic axons that formed the ipsilateral optic tract (Fig. 3A-B). B was the higher magnification to view the uncrossed optic fibers (Fig. 3B). In the 150μM CP465022+200μM MK801 treated brain slices, the uncrossed projection showed no obvious change compared with the controls (P>0.05) (Fig. 3C-F, G), and the same was observed with the crossed axons at the midline (P>0.05)

(Fig. 3H). D and F were the higher magnification to view the uncrossed optic fibers (Fig. 3D, F).

4. Blockage of glutamate ionotropic receptors (AMPARs, KARs and NMDARs) had inhibitory effect on neurite outgrowth in the retinal explants

In the control E14 retinal explants, neurites grew normally and densely (Fig. 4A, 5A). When treated with 50μM CNQX+10μM CP465022, 50μM CNQX+10μM CP465022+100μM MK801, 5μM UBP301+5μM KN93, 5μM UBP301+ 10μM CP465022, 5μM UBP301+100μM MK801, and 5μM UBP301+10μM CP465022+100μM MK801, neurites grew shorter and sparser compared with those of control groups, and neurites from these groups had statistical significance from the control ones (Fig. 4B, D, F, 5B-E, G). Application of 50μM CNQX+5μM UBP301 to the retinal explants groups, neurites grew normally and densely; they showed no difference to that of control groups (Fig. 4E, 5F). Application of 50μM CNQX+100μM MK801 to the retinal explant groups, they showed no difference to that of control groups (Fig. 4C, F).

Discussion

This investigation has tried to resolve whether retinal axon path-finding is regulated by glutamate. Our results show that retinal axons respond to glutamate activation that promotes the axonal growth. This activation is likely involved activation of both NMDA and AMPA receptors. The kainate receptor activation may inhibit slightly axon growth or some unknown function which needs to be continued to explore, but its function is apparently different from NMDA and AMPA receptors. Such a glutamate evoked effect on retinal axonal growth and receptor-dependent responses have not been described. Furthermore, glutamate and its ionotropic receptors may

play an important role in the retinofugal pathway development. We observed that the combined blockage of AMPA and NMDA receptors induced a reduction in the crossed retinal axons in E13 pathway, but had no effects on the uncrossed retinal axons at E15.

1. Glutamate ionotropic receptors express in the prenatal period

We have described the expression pattern of different AMPAR subunits and KAR subunits in horizontal or frontal sections of mouse optic pathway; here we put the emphasis on their expression in the developing cells. This idea originates from the GluR2/3 staining that is localized in the cell nucleus but not on the cell body; and analyzing the frontal sections stained with AMPAR and kainate receptor subunit antibodies show that GluR5/6/7 is obviously stained in the cell body of glial-like cells near the ventricular zone. All of the AMPAR subunits except GluR4 are found in the nucleus of these cells. We propose that it may be another phenomenon that some glutamate ionotropic receptor subunits may be expressed first in the nucleus of some cells at the early stages of prenatal period and later become restricted to the somatodendritic compartments, where GluR1 subunit expression has been reported (Craig et al., 1993).

In the glial cell culture of diencephalon, glial cells will be spread in the culture dish and easily detected by their morphology. The GluR2/3 staining is obviously found in the glial cell nucleus and the organelles surrounding the nucleus, weak on the cell membrane. For GluR1 staining, it is not so typical compared with GluR2/3 staining, but the intense staining is also found in the glial cell nucleus. For the GluR4 staining, it is spread throughout the whole glial cells especially on the membrane of the cells, corresponding with its positive staining in the frontal chiasm sections. Although our previous study demonstrates that GluR1 and GluR4 are localized in

retinal neurites and growth cones, their localization may be varied in different cell types or tissues. To our knowledge, physiological evidence for AMPA receptors expressed in the cell nucleus in immature brain or neuronal cultures has not been reported. In the adult brain, AMPA receptor subunits are found almost exclusively in the somatodendritic compartment (Craig et al., 1993; Martin et al., 1993), only rare examples show GluR1 found in the axons (Martin et al., 1993). In immature brain, GluR1 immunoreactive neuronal processes show ultrastructural characteristics in accord to axonal and dendritic growth cones (Martin et al., 1998; Vaughn, 1989).

The expression of AMPAR subunits in development is region-dependent. Previous study shows that GluR1 is lower in newborns than in adults in the neocortex and hippocampus; the case is reverse in the striatum (Martin et al., 1998). They also display a transient expression in some population of neurons (cerebellar granule and Purkinje cells) at specific developmental times (Martin et al., 1993; Martin et al., 1998). For immunoreactive GluR2/3, it displays a whole cell expression in E13 diencephalon and restricts to cell body and short processes in E15 diencephalon; and in the retina, it is localized in the cell nucleus from E13 to E18. These data provide the first evidence for in vivo and in vitro existence of AMPAR subunits clustering in different regions and cellular structures in developing mouse retina and diencephalon.

The significance of both GluR2/3 staining in retinal cell nucleus and GluR1-4 in diencephalic glial cells, and whether these receptors are functional, remains to be clarified. The possible function may regulate expression of some stage specific genes for neuronal maturation during CNS development (Sugiura et al., 2001). They may elicit a cellular Ca^{2+} pool response accompanying an increase of c-fos, c-jun and nerve growth factor inducible factor A (NGFI-A) (Gudehithlu et al., 1993; Mack et

al., 1994). Some growth factors (PDGF, bFGF) modulate the expression of glutamate receptor channels to control the cell proliferation and differentiation (McKinnon et al., 1990). However, their possible function remains unravel, but they may function in regulating early neuronal activity during development.

2. Glutamate ionotropic receptors and retinofugal pathway

2.1. Glutamate ionotropic receptors affect the crossed projection in the midline at early stage

The crossing of retinal axons in the midline displays obvious changes after treatment with different combination of glutamate receptor antagonists at E13. The quantitative comparison of ratios of the pixel intensity in the post-midline to pre-midline region reveals significant difference between the treatment groups (appropriate concentration or combination of antagonists) and the control ones.

Glutamate may promote retinal axon growth, and the localization of its ionotropic receptor AMPAR and kainate receptor subunits shows that they are localized on RGCs and their axons, radial glial cells, and chiasmatic neurons, which have been shown to contribute to the correct formation of retinofugal pathway (Chan et al., 1999). However, glutamate is widely expressed in the retina and diencephalon. Glutamate transporters GLAST, GLT1, and EAAC1 are also expressed in the embryonic mouse CNS, which are essential for the maintenance of glutamate extracellular concentration (Matsugami et al., 2006; Tanaka et al., 1997). With the use of combination of different NMDAR and AMPAR antagonists with a relative high concentration, the data demonstrates that blocking the glutamatergic activity will reduce the crossing retinal axons at E13.

Previous studies demonstrate that the glutamate receptor-dependent acceleration of axon growth acts through a calcium-dependent signaling pathway (Schmitz et al.,

2009; Wen et al., 2004). With the experiment combining CP465022 with KN93 (a CaMKI/II/IV inhibitor) that block the calcium-dependent pathway, which enhances the antagonist inhibition and reduces the controlateral projection at E13. The positive effect of glutamate promotion to retinal axon growth appears to be mediated by a calcium-dependent pathway involving CaMKs.

2.2. Glutamate ionotropic receptors have no effect in the uncrossed projection

Using the combination of antagonists, which is effective to affect axon growth in E13 brain slices, treats E15 brain slices; there is no statistical significance in the ipsilateral projection at E15. Exogenous glutamate has effect in neurites from DN retina but not in those from VT retina, leading to the suggestion that glutamate is not mediating the retinal axon divergence in the mouse optic chiasm.

Previous evidence suggests that in glutamatergic neurons, glutamate released by the advancing growth cone itself may provide a feedback signal which determines the growth cone whether to grow or to halt based on developmental age and the glutamate concentration achieved (Chang and De Camilli, 2001; Ibarretxe et al., 2007; Schmitz et al., 2009; Tashiro et al., 2003). It may also be working in the retina, which has a high concentration of extracellular glutamate in the neonatal retina (Haberecht and Redburn, 1996), and in the prenatal retina. Some papers report that AMPA receptor activation at the cell body induced calcium waves traveling down the axon, leading to growth cone collapse (Chang and De Camilli, 2001; Yamada et al., 2008). Our immunostaining data shows that AMPA receptor subunits GluR1, GluR4 and kainate receptor subunits GluR5/6/7 express in the retinal axons and growth cones, and these staining patterns may be stage-dependent or region-dependent; thus their function will also be different from previous reports.

3. Simultaneous blockage of AMPARs, NMDARs and KARs has an inhibitory effect on neurite outgrowth in retinal explant culture

Although glutamate promotes retinal axon growth by activating a combination of AMPA/kainate and NMDA receptors, the function of individual activation of these receptors is different. Blocking AMPA receptor will inhibit the neurite outgrowth from the retinal explants, but inhibiting kainate receptor will not generate such an effect. Previous study shows that activation of AMPA/kainate receptor will lead to growth cone collapse in hippocampus neurons (Chang and De Camilli, 2001; Yamada et al., 2008); and transient activation of kainate receptors will induce a fast and reversible growth cone stalling (Ibarretxe et al., 2007).

Our experimental data demonstrates that combination of AMPA/kainate and NMDA receptor antagonists displays an obvious effect of inhibiting neurite outgrowth and their growth distance. Although low concentration of kainate receptor antagonists shows a tendency to slightly promote retinal axon growth, it cannot reverse the positive effects of other receptor antagonist. It needs to mention that CNQX is a competitive antagonist to AMPA/kainate receptor; however, it has a different effect compared with AMPA receptor antagonists and has a similar effect as UBP301 a potent kainate receptor antagonist. This may suggest that CNQX may have a higher affinity to kainate receptor in mouse embryonic retina. Previous study shows that low concentration of kainate (0.5μM) will decrease the rate of axonal outgrowth by a mechanism involving metabotropic signaling cascades (Lerma, 2003; Pinheiro and Mulle, 2006). It also produces an effect to induce growth cone motility (Ibarretxe et al., 2007). Thus the function of different concentration of kainate to retinal axons needs further investigation.

With the experiment combining CP465022/MK801 with KN93 (a CaMKI/II/IV inhibitor) which is used to block the calcium-dependent pathway, this will enhance the antagonist inhibition and reduce the neurite outgrowth from retinal explants. KN93 alone at the concentration used shows little effect on the neurites. The glutamate induced promotion to retinal axon growth appears to be mediated by a calcium-dependent pathway involving CaMKs (Schmitz et al., 2009). It has been known that neurotransmitters involve intracellular calcium changes affecting neurite growth (Gomez and Zheng, 2006; Schmitz et al., 2009), and different calcium amplitudes can evoke attraction or repulsion of growth cone (Robles et al., 2003; Wen et al., 2004). In the developing retinal axons, this direct effect of calcium-dependent pathway inducing by glutamate needs continuous exploration.

As a summary, the findings in this chapter show that 1). The staining pattern of AMPA receptor subunits will change in a stage-dependent and a tissue-dependent manner in the embryonic period. This change may be an indispensible factor for glutamate function in prenatal stages. 2). Glutamate may act as an attractor to retinal axons, blocking its ionotropic receptors will lead to a reduced crossed pathway at the mouse chiasm; but this will not affect the uncrossed fibers, as suggested by the results that exogenous glutamate promotes DN retinal neurites, but not the VT ones. 3). Blocking individual or a combination of ionotropic receptors shows that NMDA/AMPA or kainate receptors display a different function: the former one is to promote retinal neurite outgrowth, the later one to inhibit or regulate growth cone motility.

Figures:

Figure 1. Immunostaining of E14 ventral diencephalic cells for GFAP, SSEA-1, RC2, GluR1, GluR2/3, and GluR4. Cultured cells were examined by anti-GFAP, and could not be labeled by anti-SSEA-1, indicating that these cells were GFAP-positive glial cells (Fig. A-C). Culture cells were also labeled by anti-RC2 (Fig. D, G, J), and the antibodies to all four AMPAR subunits (Fig. E, H, K). Only GluR2/3 subunit was intensely stained in the cell nucleus and weakly in the cell membrane; GluR1 subunit was weak in cell nucleus; and GluR4 subunit was observed intensely on cell membrane (Fig. D-L). Scale bars = 100μm in A (also applies to B-C); 50μm in D (also applies to E-L).

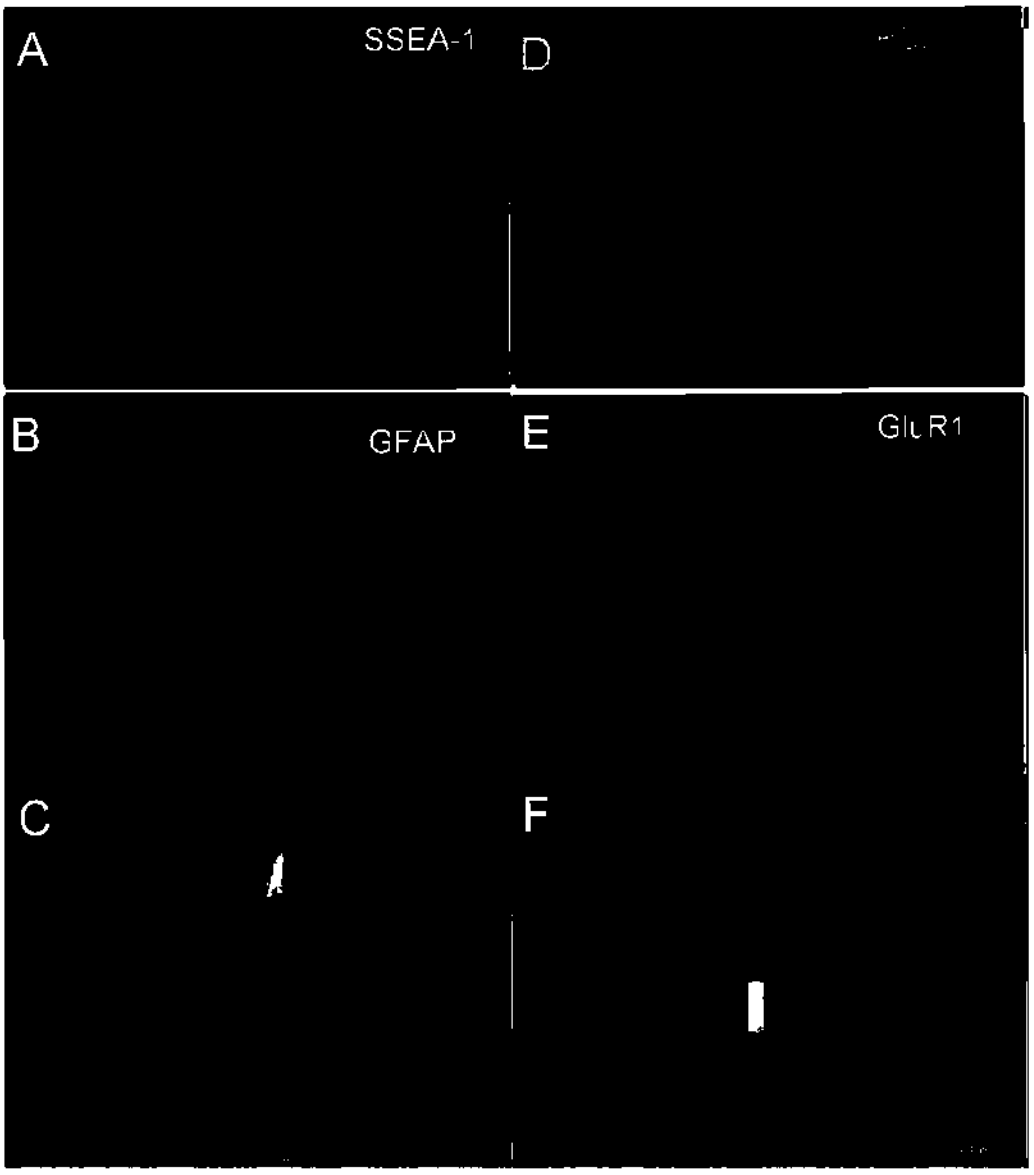
A
SSEA-1
D
B
GFAP
E
GluR1
C
F

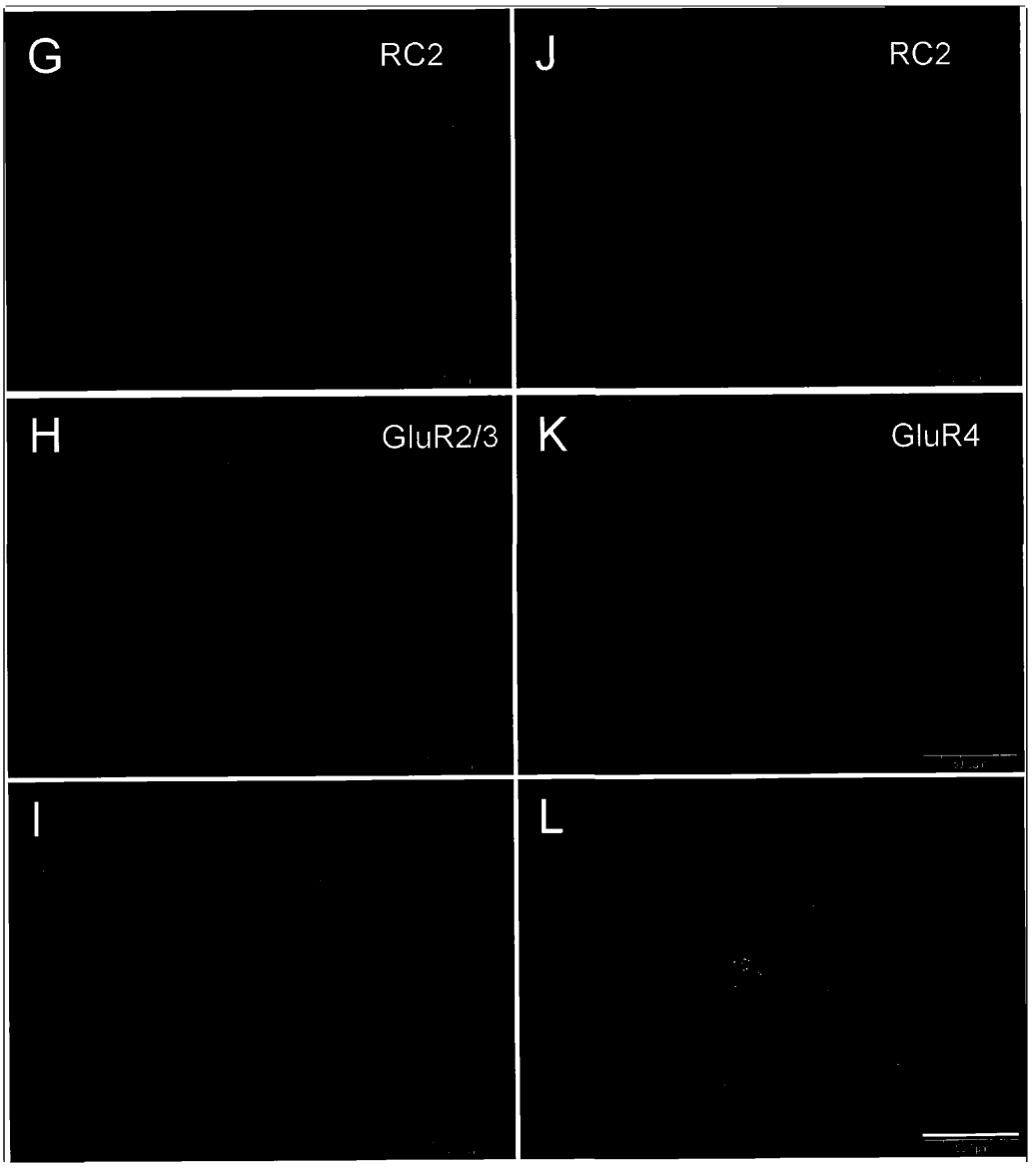
G
RC2
J
RC2
H
GluR2/3
K
GluR4
I
L

Figure 2. Glutamate ionotropic receptor antagonists produce reduction in the crossed projection in the optic chiasm at E13. In these whole-mounted preparations of the optic chiasm, rostral is to the top, the middle is showed by the white arrow. In the control E13 chiasm, a number of dye-filled early arrived optic fibers had already entered the chiasm (Fig. A-B). In the 200μM CP465022 treated brain slices, the crossed projection appeared to be reduced, although this reduction has no statistically significance compared with the controls ($P>0.05$) (Fig. C-D, Q). In the 500μM MK801 treated brain slices, the crossed projection was not obviously affected compared with the controls, although some of the crossed projection was reduced ($P>0.05$) (Fig. E-F, Q). Scale bars = 200μm in A (also applies to B-F).

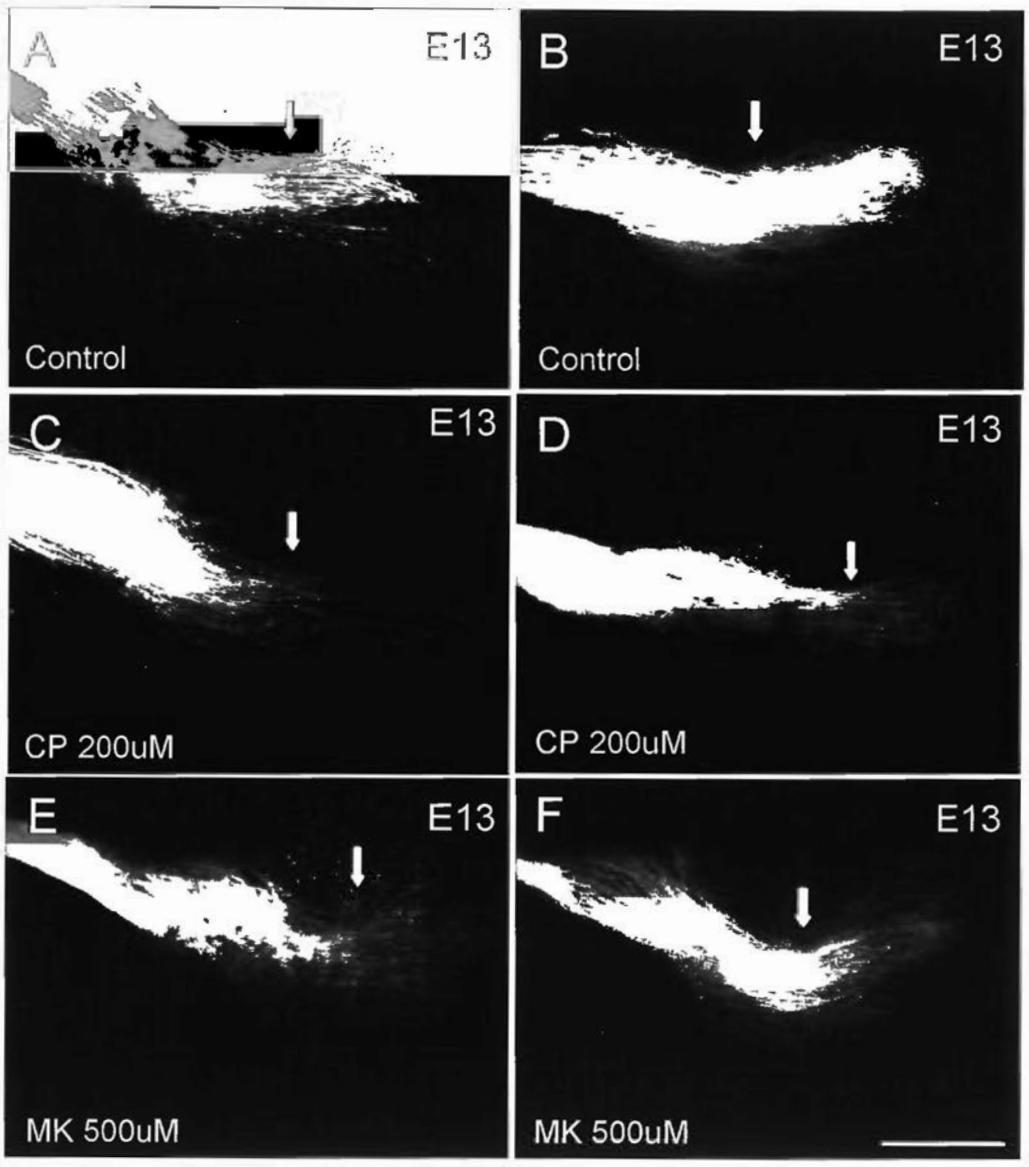
A
E13
Control
B
E13
Control
C
E13
CP 200uM
D
E13
CP 200uM
E
E13
MK 500uM
F
E13
MK 500uM

Figure 2. Glutamate ionotropic receptor antagonists produce reduction in the crossed projection in the optic chiasm at E13. In these whole-mounted preparations of the optic chiasm, rostral is to the top, the middle is showed by the white arrow. In the 100μM CP465022+200μM MK801 treated brain slices, the crossed projection was reduced, although this reduction has no statistically significance compared with the controls ($P>0.05$) (Fig G-H, Q). In the 150μM CP465022+200μM MK801 (Fig. I-F), 200μM CP465022+20μM KN93 (Fig. K) and 200μM CP465022+500μM MK801 (Fig. L) treated brain slices, the crossed projection was dramatically reduced, furthermore these reduction has significant differences from the controls ($P<0.05$, 0.01, and 0.001, respectively) (Fig. Q). Scale bars = 200μm in G (also applies to H-L).

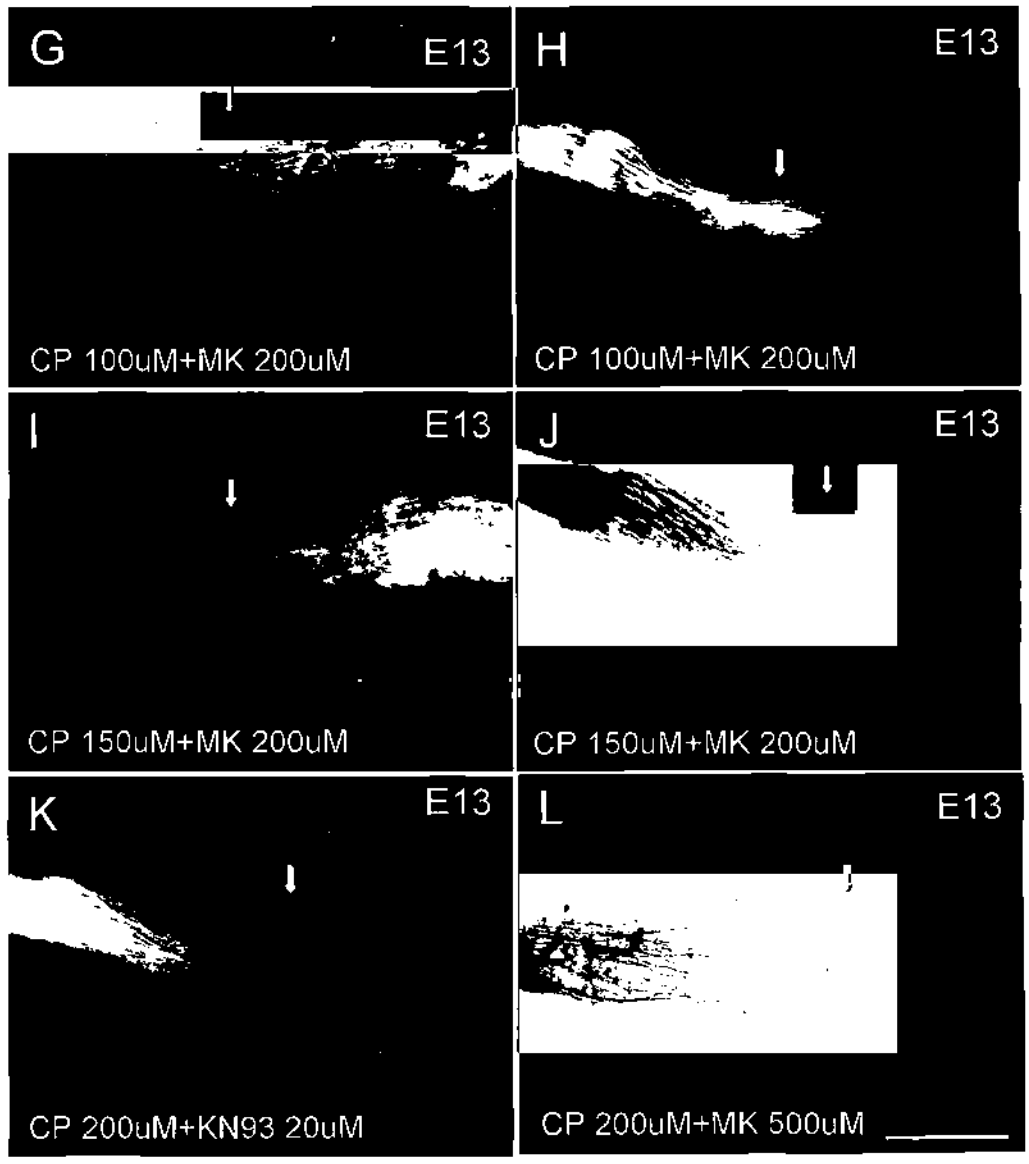
G
E13
CP 100uM+MK 200uM
H
E13
CP 100uM+MK 200uM
I
E13
CP 150uM+MK 200uM
J
E13
CP 150uM+MK 200uM
K
E13
CP 200uM+KN93 20uM
L
E13
CP 200uM+MK 500uM

Figure 2. Glutamate ionotropic receptor antagonists produce reduction in the crossed projection in the optic chiasm at E13. In these whole-mounted preparations of the optic chiasm, rostral is to the top, the middle is showed by the white arrow. In the 200μM CP465022+20μM KN93 (Fig. M) and 200μM CP465022+500μM MK801 (Fig. N) treated brain slices, the crossed projection was dramatically reduced compared with the controls ($P<0.01$, and 0.001, respectively) (Fig. Q); the lower rows showed the magnified view of the axons and their growth cones at the midline (Fig. O-P). Scale bars = 200μm in M (also applies to N); 100μm in O (also applies to P).

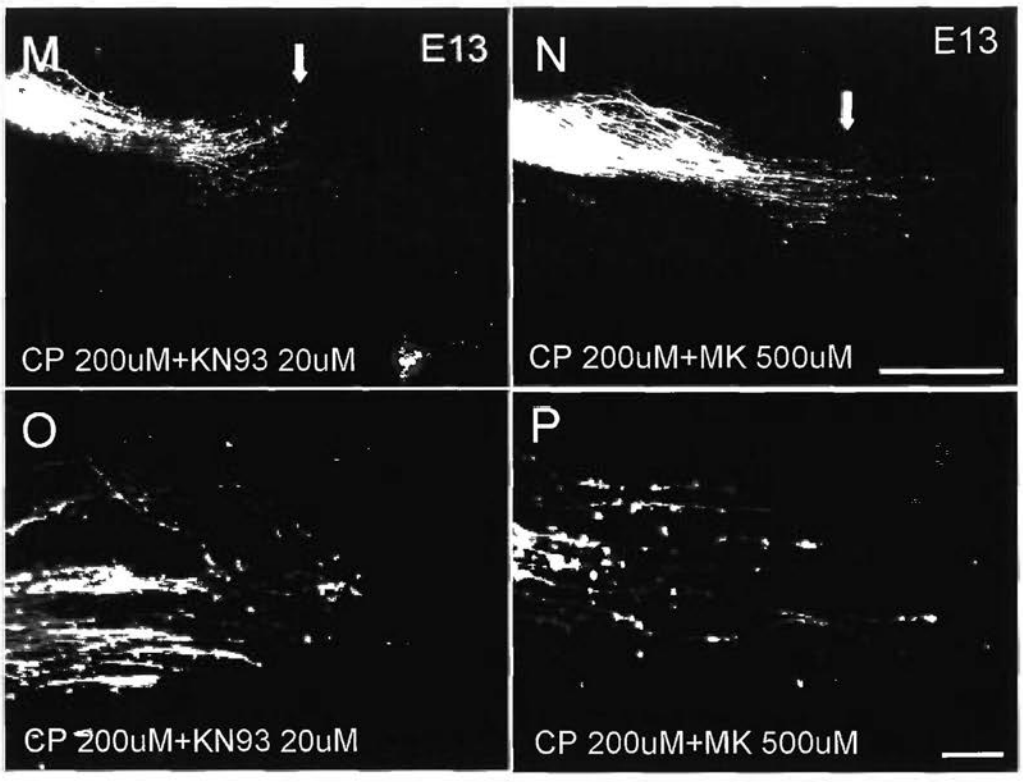
M
E13
CP 200uM+KN93 20uM
N
E13
CP 200uM+MK 500uM
O
CP 200uM+KN93 20uM
P
CP 200uM+MK 500uM

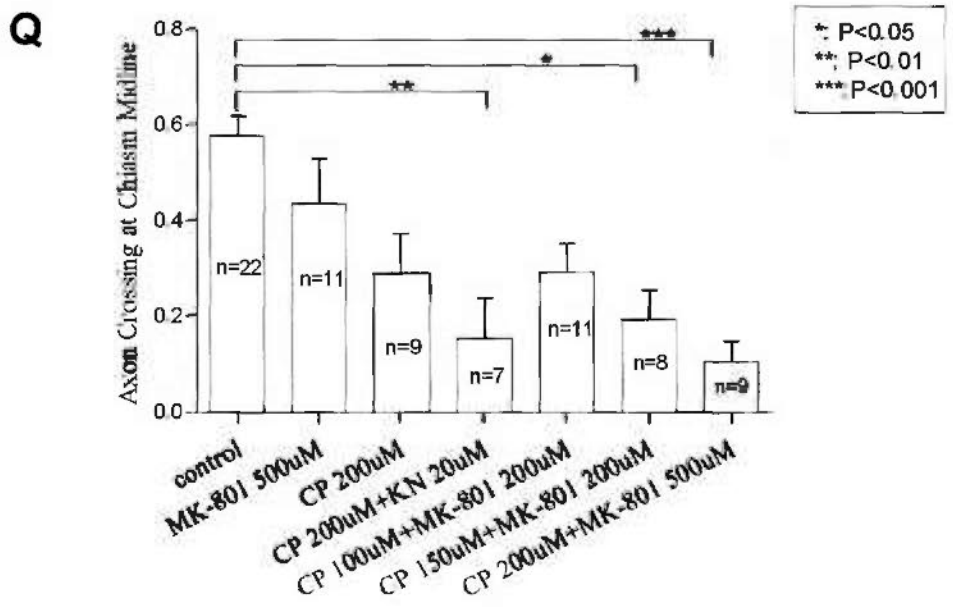
Q
*: P<0.05
**: P<0.01
***: P<0.001
Axon Crossing at Chiasm Midline
0.0
0.2
0.4
0.6
0.8
n=22
n=11
n=9
n=7
n=11
n=8
n=9
control
MK-801 500uM
CP 200uM
CP 200uM+KN 20uM
CP 100uM+MK-801 200uM
CP 150uM+MK-801 200uM
CP 200uM+MK-801 500uM

Figure 3. Glutamate ionotropic receptor antagonists had no effects on the uncrossed projection in the optic chiasm at E15. In these whole-mounted preparations of the optic chiasm, rostral is to the top; the midline is showed by the white arrow. In the control E15 chiasm, a number of dye-filled optic fibers could be divided into two groups: one was the crossed optic axons that formed the contralateral optic tract; the other was the uncrossed optic axons and formed the ipsilateral optic tract (Fig. A-B). B was the higher magnification to view the uncrossed optic fibers (Fig. B). In the 150μM CP465022+200μM MK801 treated brain slices, the uncrossed projection showed no obvious change compared with the controls ($P>0.05$) (Fig. C-F, G), and the same was observed with the crossed axons at the midline ($P>0.05$) (Fig. H). D and F were the higher magnification to view the uncrossed optic fibers (Fig. D, F). Scale bars = 200μm in A (also applies to C, E); 100μm in B (also applies to D, F).

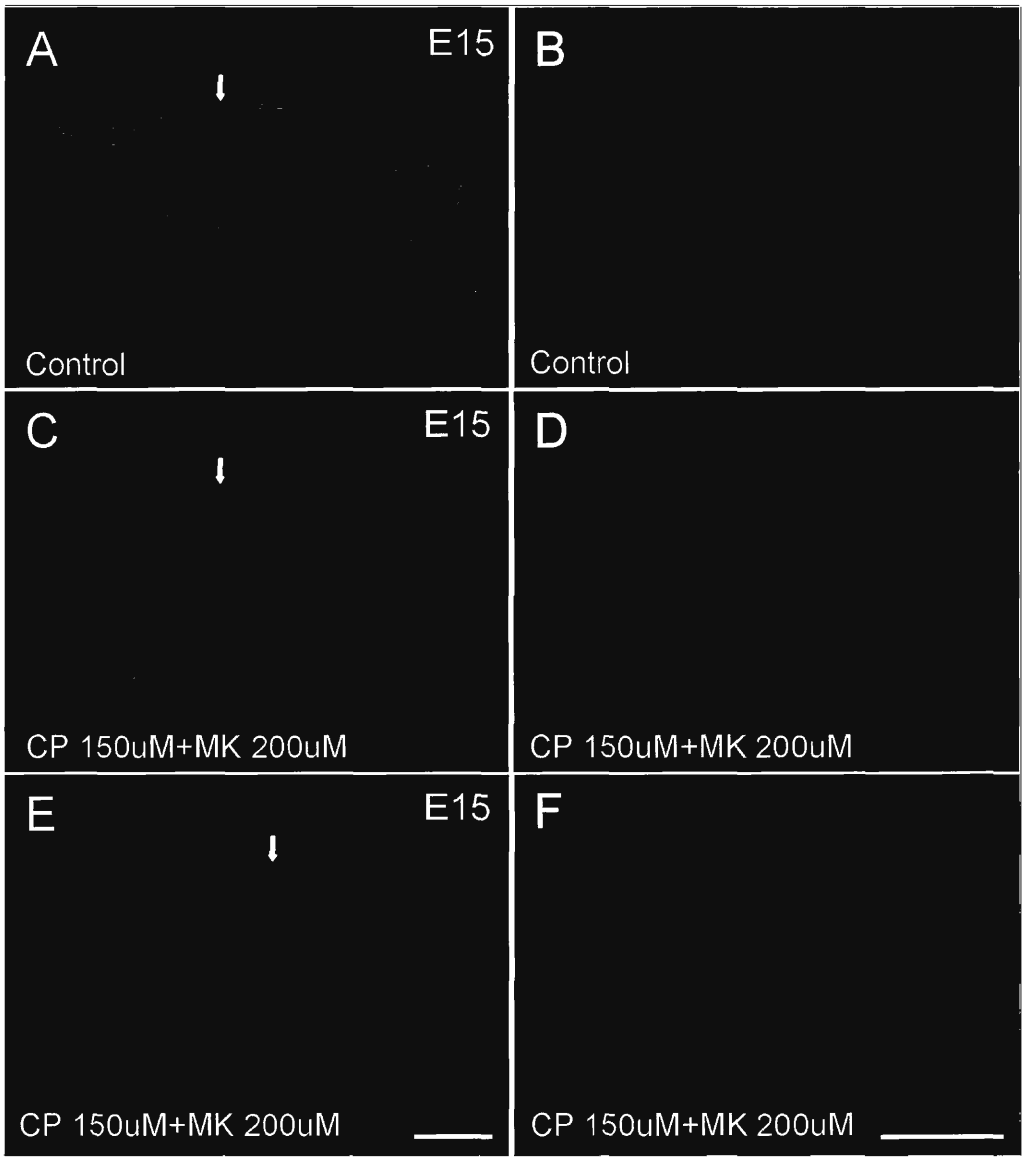
A
E15
Control
B
Control
C
E15
CP 150uM+MK 200uM
D
CP 150uM+MK 200uM
E
E15
CP 150uM+MK 200uM
F
CP 150uM+MK 200uM

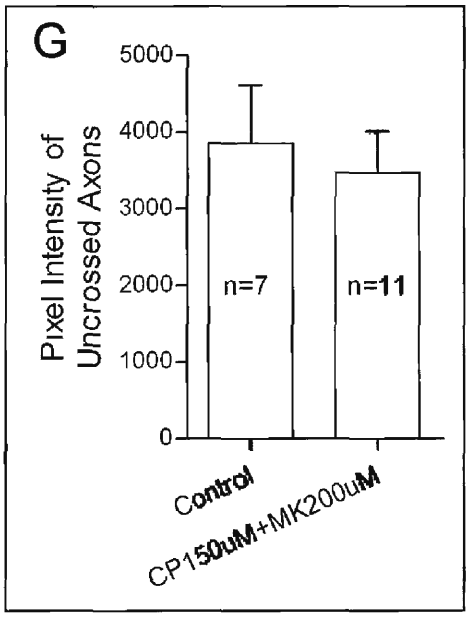
G
Pixel Intensity of Uncrossed Axons
5000
4000
3000
2000
1000
0
n=7
n=11
Control
CP150uM+MK200uM

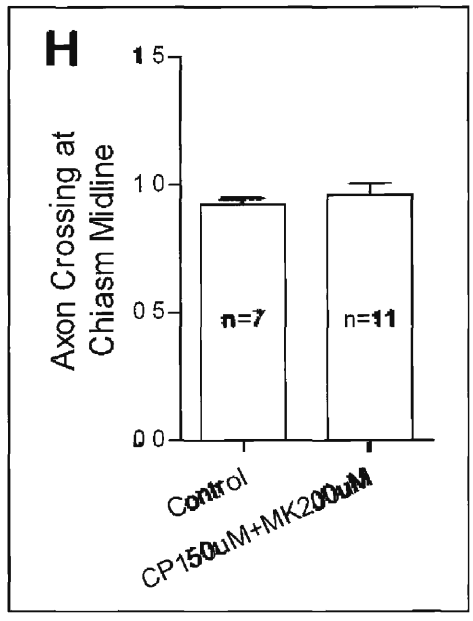
H
Axon Crossing at Chiasm Midline
1.5
1.0
0.5
0.0
n=7
n=11
Control
CP150uM+MK200uM

Figure 4. Blockage of glutamate ionotropic receptors (AMPARs, KARs and NMDARs) had inhibitory effect on neurite outgrowth in the retinal explants. In the control retinal explants from E14 mice, neurites grew normally and densely (Fig. A). When treated with 50μM CNQX+10μM CP465022 (Fig. B), 50μM CNQX+10μM CP465022+100μM MK80 (Fig. D), neurites from these two groups grew shorter and sparser compared with those from the control group, and the plot showed that the inhibition had significant difference (Fig. F). Application of 50μM CNQX+100μM MK801 to the retinal explant group, neurites from this group showed no difference from the control group (Fig. C). Application of 50μM CNQX+5μM UBP301 to the retinal explants group, the morphology of neurites showed no difference from control group (Fig. E). Scale bars = 500μm in A (also applies to B-E).

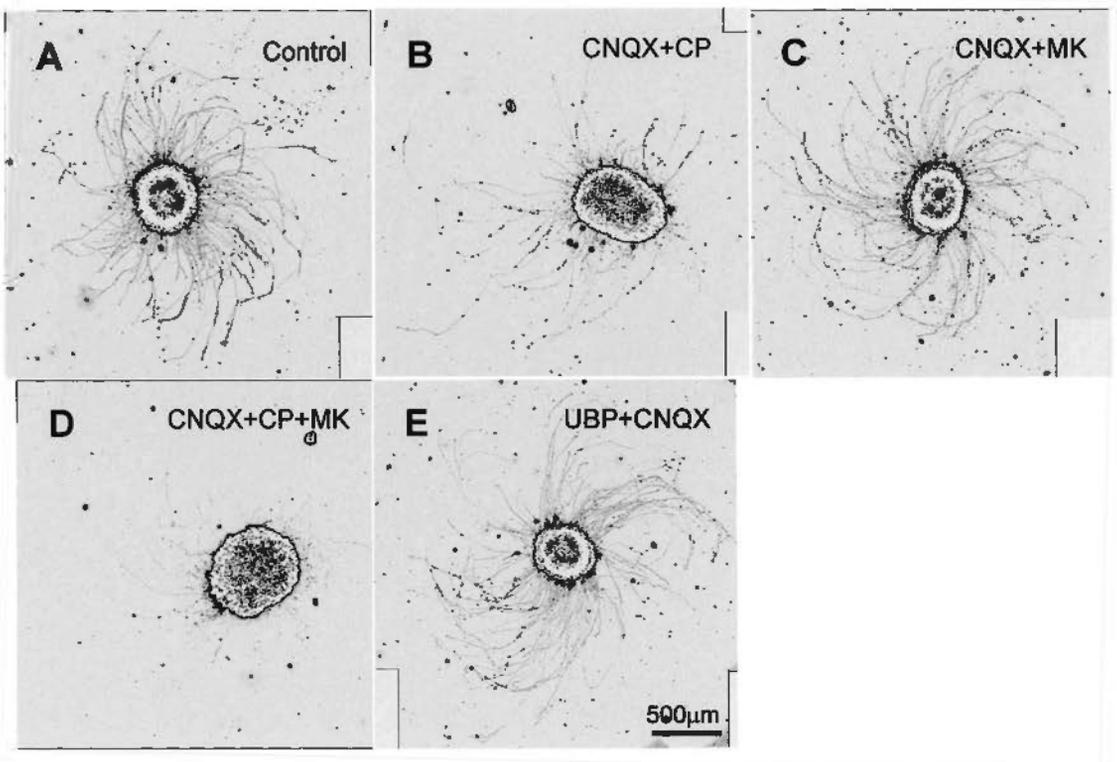
A
Control
B
CNQX+CP
C
CNQX+MK
D
CNQX+CP+MK
E
UBP+CNQX
500μm

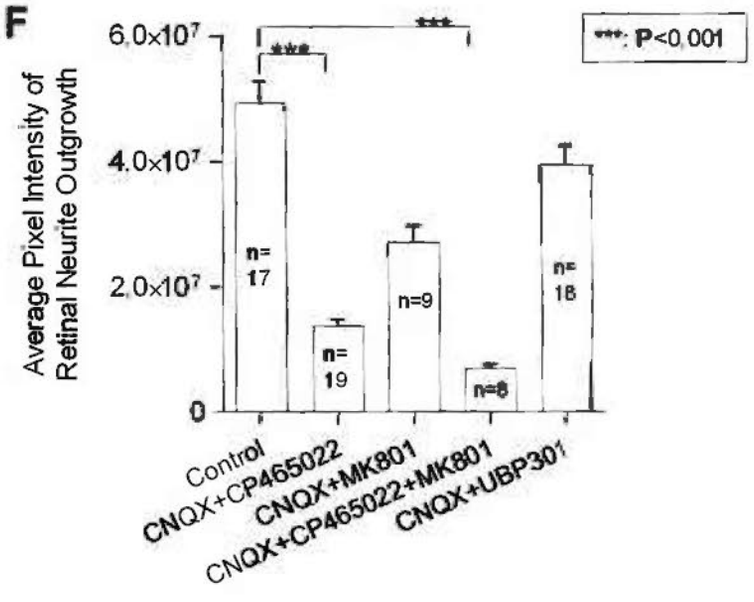
F
Average Pixel Intensity of Retinal Neurite Outgrowth
6.0x10⁷
4.0x10⁷
2.0x10⁷
0
***
***
***: P<0.001
n= 17
n= 19
n=9
n=8
n= 18
Control
CNQX+CP465022
CNQX+MK801
CNQX+CP465022+MK801
CNQX+UBP301

Figure 5. Blockage of glutamate ionotropic receptors (AMPARs, KARs and NMDARs) had an inhibitory effect on neurite outgrowth in the retinal explants. In the control retinal explants from E14 mice, neurites grew normally and densely (Fig. A). When treated with 5μM UBP301+5μM KN93 (Fig. B), 5μM UBP301+ 10μM CP465022 (Fig. C), 5μM UBP301+100μM MK801 (Fig. D), and 5μM UBP301+10μM CP465022+100μM MK801 (Fig. E), neurites from these four groups grew shorter and sparser compared with those from the control group (Fig. B-E). The plot showed these inhibitions had significant differences from the control one (Fig. G). Application of 50μM CNQX+5μM UBP301 to the retinal explants group, the morphology of neurites showed no difference from the control one (Fig. F). Scale bars = 500μm in A (also applies to B-E).

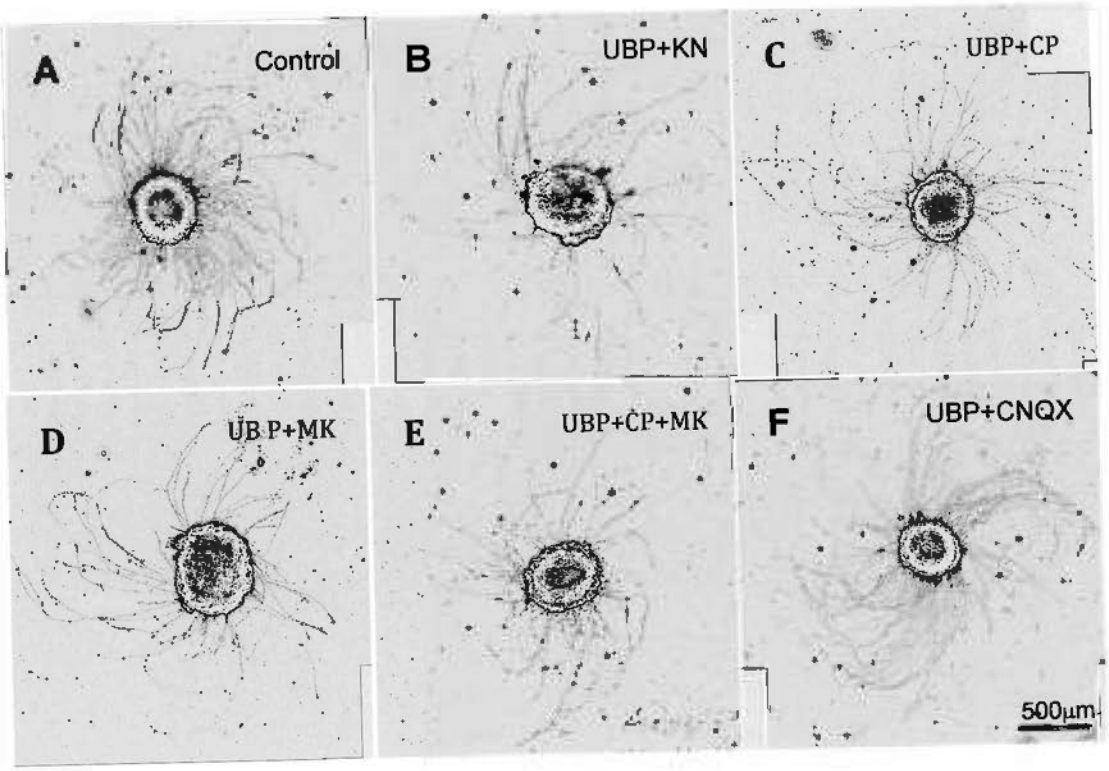
A
Control
B
UBP+KN
C
UBP+CP
D
UB P+MK
E
UBP+CP+MK
F
UBP+CNQX
500μm

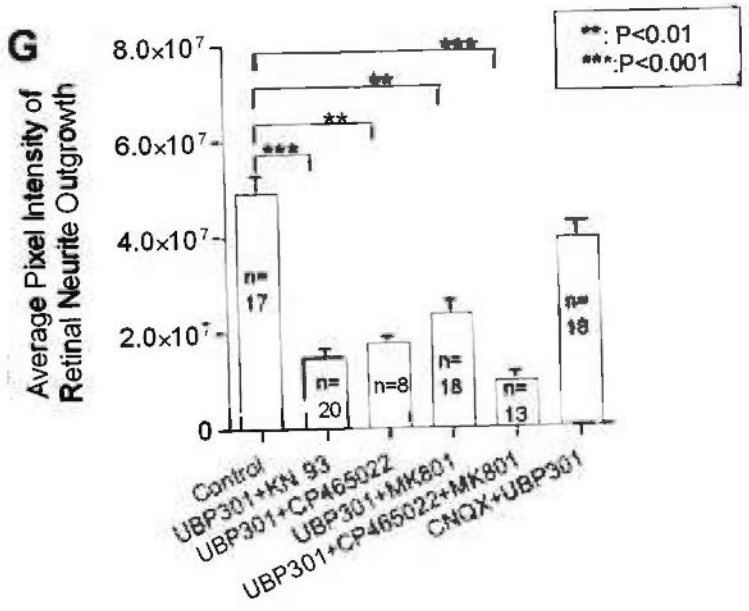
G
Average Pixel Intensity of Retinal Neurite Outgrowth
8.0x10⁷
6.0x10⁷
4.0x10⁷
2.0x10⁷
0
**: P<0.01
***:P<0.001
***
**
**
***
n= 17
n= 20
n=8
n= 18
n= 13
n= 18
Control
UBP301+KN 93
UBP301+CP465022
UBP301+MK801
UBP301+CP465022+MK801
CNQX+UBP301

CHAPTER 6

General discussion

Recent investigations propose that glutamate releases by the glutamatergic neuron growth cone provide a feed back signal which determines whether a growth cone should to grow or to halt based on developmental age and the achieved glutamate concentration (Chang and De Camilli, 2001; Ibarretxe et al., 2007; Schmitz et al., 2009; Tashiro et al., 2003); and the released glutamate from the nearby neurons or glial cells may act as a diffusible molecule that directly affects axon growth. We want to test this phenomenon by studying the glutamate and its ionotropic receptors in the developing mouse retinofugal pathway. As retinal axons undergo several changes in fiber order along their course in the retinofugal pathways (Chan and Chung, 1999), our study emphasizes on the changes from the optic nerve to the optic tract, especially the segregation of the crossed and uncrossed axons in the optic chiasm that is essential to binocular vision in mammals.

High concentration of extracellular glutamate is found in neonatal retina, and is reduced to low levels in the adult retina (Haberecht and Redburn, 1996). Previous study shows that application of high concentration of glutamate (5mM) to rat neonatal retinal ganglion cell cultures demonstrates to be neurotropic to the cells, which can regulate their survive in the serum free defined medium culture (Nichol et al., 1995). Similarly, in our retinal explant culture, the high concentration of

glutamate is needed to promote neurite outgrowth from the retinal explants. Our immunohistochemistry data reveal that the immunoreactive glutamate is detected in E13 mouse retina and ventral diencephalon, especially in the inner region of the retina, and the optic stalk entering the chiasm. At later stages, glutamate is widely detected in the diencephalon, the retinal ganglion cells and retinal axons. It is proposed that retinal ganglion cells are able to store and release glutamate. It may regulate its axon growth in an autocrine way or affecting other axons nearby. Moreover, at early embryonic stages, neurotransmitters can mediate long-range interactions as a diffusible factor or short-range communications through the axon neurites or processes in neurons or glial cells (Behar et al., 1996; Metin et al., 2000; Zheng et al., 1994). These mechanisms may also exist in the retinofugal pathway to modulate retinal axon guidance.

Glutamate is expressed in the mouse embryonic period; we therefore have characterized its ionotropic receptors localization using immunohistochemistry. We show that GluR1 and GluR5/6/7 subunits are highly detected in the retinal axons in the retina, the optic nerve, the optic chiasm and optic tract. GluR2/3 subunit is obviously labeled in the cell nucleus in the retina and diencephalon at the early stage staining supporting cells in the optic nerve and optic chiasm; but this staining pattern will shift to the cell body and processes of diencephalic cells at later stage. GluR4 subunit staining is restricted to the glial cells near the ventricular zone and cells in the midline region near the chiasm. All of these AMPA and kainate receptor subunits are expressed on the radial glial cells whose processes interdigitating with retinal growth cones, and on the chiasmatic neurons which form the posterior border and a rostral raphe at the midline of the chiasm to restrict growth of early arriving retinal axons (Jeffery and Erskine, 2005; Lin and Chan, 2003; Marcus et al., 1995).

AMPA receptors are expressed in both neurons and glia throughout the CNS (Wisden and Seeburg, 1993). The majority of AMPA receptors are GluR2-containing heteromers, other AMPA receptor subunits are determined by their location in the brain of the mature CNS (Craig et al., 1993; Wenthold et al., 1996). During early postnatal development, expression of GluR2 is low and will increase rapidly at the first postnatal week (Monyer et al., 1991; Wisden and Seeburg, 1993). Compared with our data, blocking AMPA receptor will induce inhibition of neurite outgrowth from the retinal explants and also reduce the crossed axons in E13 brain slices. We propose that GluR2/3 staining is restricted largely to the cell nucleus, which is different from that in the mature CNS, which may relate to their function in the mouse embryonic development. GluR2-free AMPA receptors will elicit inward calcium currents, which are now known to exist in a wide variety of neuronal types and neurons during development. They may play a pivotal role like NMDA receptors having permeability to Ca^{2+}.

In the early embryonic retina and diencephalon, our data show that GluR2-free AMPA receptors distribute in the cell body and its axon growth cones to form Ca^{2+}-permeable channels that participate in the neuronal activity. The distribution of GluR2/3 is interesting and needs to further investigate. In the glial cell culture of ventral diencephalon, it shows that not only GluR2/3 has such a phenomenon of localizing in the cell nucleus, but GluR1 and GluR4 (its staining is localized in the whole cell except for the nuclear) show similar distribution as well. It demonstrates that region-dependent and stage-dependent localization pattern may exist in the developmental regulation of AMPA receptor subunits, even in the individual cellular level. For example, GluR1 expression in the retinal ganglion cells and the glial cells in the chiasm and its mRNA expression level varied in the E13 retina and ventral

diencephalon are region-dependent; GluR2/3 expression in the diencephalic cells at E13 and E18 is stage dependent. Previous study has shown that GluR1 protein expression exist such a region-dependent localization pattern (Martin et al., 1998).

These staining patterns in the glial cells may relate to their proliferation or migration in the development. Glutamate may activate its receptors to induce some immediate gene expression, such as c-fos, c-jun and nerve growth factor inducible factor A (NGFI-A) (Gudehithlu et al., 1993). Previous studies show that Ca^{2+} influx mediated by activation of glutamate will affect gene transcription in glia; and a common glutamate receptor mediated signal transduction pathway involving Ras and mitogen-activated protein (MAP) kinase has emerged in different glial cell types (Liu et al., 1999; Pende et al., 1997). But the function of these receptors found in the diencephalic glial cells has been unraveled.

Although we can not neglect the function of glutamate metabotropic receptors, AMPA and NMDA receptors antagonists can obviously reduce the neurite outgrowth from the retinal explants and inhibit the crossed axons in the E13 brain slices. Glutamate activation will promote neurite outgrowth; this mechanism may at least mediated partly by AMPA/NMDA receptors. In the presence of kainate receptor antagonists, it will not affect the neurite outgrowth from the retinal explants. On the contrary, low concentration of antagonists will show a tendency to promote neurite outgrowth. Such a different effect on AMPA/NMDA and kainate receptors has not been reported, suggesting that they will play a different function if glutamate is released by the retinal axons and their growth cones.

In retinal explant culture experiment, the presence of KN93, a CaMKI/II/IV inhibitor used to block the calcium-dependent pathway, will enhance the antagonist inhibition and reduce neurite outgrowth. It has been known that neurotransmitters

involve intracellular calcium changes to affect neurite growth (Gomez and Zheng, 2006; Schmitz et al., 2009); and different calcium amplitudes can evoke attraction or repulsion of growth cones (Robles et al., 2003; Wen et al., 2004). In the developing retinal axons, this direct effect of calcium-dependent pathway induced by glutamate needs further exploration. Other evidence shows that AMPA receptors distributed in the cell body will induce calcium waves traveling down the axon and lead to growth cone collapse, which may be mediated by a calcineurin-dependent pathway (Schmitz et al., 2009; Wen et al., 2004; Yamada et al., 2008). In our data, AMPA receptors are distributed on the retinal ganglion cell axon and growth cone. They can be blocked by antagonists that lead to reduction in retinal neurite outgrowth. Kainate receptors are also distributed on retinal axons and growth cones and have a different function compared with AMPA receptors. It is still unclear if the different localization of AMPA/kainate receptor determines different calcium amplitudes to evoke growth cone attraction or repulsion.

For glutamate and the developing retinofugal pathway, glutamate and its ionotropic receptor subunits are expressed widely in the retina and the ventral diencephalon, and in cells that are known to be involved in chiasm formation, the function of glutamate may depend on which receptors are activated and whether it plays as a communicator or an attractor to regulate embryonic neurons and glial cells in the pathway. Like GABA receptors, activation of different GABA receptor subtypes will lead to cell motility or movement arresting in rat cortical plate (Behar et al., 1998). This mechanism may also exist in the glutamate ionotropic receptors. Some receptors promote axon growth, and then activate a second class of receptors to attenuate this, providing a stop signal to notify the axons approaching their final positions (Behar et al., 1999; Metin et al., 2000). Although there is a complicated

network in the chiasm formation, glutamate may play as a communicator or attractor to coordinate with other factors to affect retinal growth cones from retina to their terminal sites in the brain, as glutamate promotes retinal neurite growth from DN retina and blockage of glutamate ionotropic receptors will inhibit the E13 crossed axons.

The summary of glutamate and its ionotropic receptors localization and function is as follows (Table 1):

Table 1:

Glutamate ionotropic receptors		Localization	Function
Glutamate		Staining is intense in retinal ganglion cells and their axons; also in chiasmatic neurons.	Promote retinal neurite outgrowth
AMPA receptors	GluR1	Staining is strong in retinal ganglion cells and their axons, Müller glial cells; also found in chiasmatic neurons.	Promote retinal neurite growth
	GluR2/3	Staining is observed in the retinal ganglion cell nuclei and Müller glial cell nuclei, but almost no staining is detected in their axons. It is also found in nucleus of chiasmatic neuron and radial glial cell in early embryonic stage, but changes to somatodendritic compartment of cells in diencephalon at E18.	
	GluR4	Staining is prominent in retinal ganglion cells and weak in their axons, and Müller glial cells; also localized in chiasmatic neurons and radial glial cells, it is also strongly found in the midline region of the chiasm.	
KA receptors	GluR5/6/7	Staining is strong in retinal ganglion cells and their axons, also found in chiasmatic neurons.	Have no effect in retinal neurite growth
Blockage of all of Glutamate ionotropic receptors			Inhibit retinal neurite growth

References:

Acosta, M.L., Bumsted O'Brien, K.M., Tan, S.S., and Kalloniatis, M. (2008). Emergence of cellular markers and functional ionotropic glutamate receptors on tangentially dispersed cells in the developing mouse retina. J Comp Neurol *506*, 506-523.

Acosta, M.L., Chua, J., and Kalloniatis, M. (2007). Functional activation of glutamate ionotropic receptors in the developing mouse retina. J Comp Neurol *500*, 923-941.

Bahn, S., Volk, B., and Wisden, W. (1994). Kainate receptor gene expression in the developing rat brain. J Neurosci *14*, 5525-5547.

Barbieri, A.M., Broccoli, V., Bovolenta, P., Alfano, G., Marchitiello, A., Mocchetti, C., Crippa, L., Bulfone, A., Marigo, V., Ballabio, A., *et al.* (2002). Vax2 inactivation in mouse determines alteration of the eye dorsal-ventral axis, misrouting of the optic fibres and eye coloboma. Development *129*, 805-813.

Bardoul, M., Drain, M.J., and Konig, N. (1998a). Modulation of intracellular calcium in early neural cells by non-NMDA ionotropic glutamate receptors. Perspect Dev Neurobiol 5, 353-371.

Bardoul, M., Levallois, C., and Konig, N. (1998b). Functional AMPA/kainate receptors in human embryonic and foetal central nervous system. J Chem Neuroanat 14, 79-85.

Barnstable, C.J. (1993). Glutamate and GABA in retinal circuitry. Curr Opin Neurobiol *3*, 520-525.

Behar, T.N., Li, Y.X., Tran, H.T., Ma, W., Dunlap, V., Scott, C., and Barker, J.L. (1996). GABA stimulates chemotaxis and chemokinesis of embryonic cortical neurons via calcium-dependent mechanisms. J Neurosci *16*, 1808-1818.

Behar, T.N., Schaffner, A.E., Scott, C.A., O'Connell, C., and Barker, J.L. (1998). Differential response of cortical plate and ventricular zone cells to GABA as a migration stimulus. J Neurosci 18, 6378-6387.

Behar, T.N., Scott, C.A., Greene, C.L., Wen, X., Smith, S.V., Maric, D., Liu, Q.Y., Colton, C.A., and Barker, J.L. (1999). Glutamate acting at NMDA receptors stimulates embryonic cortical neuronal migration. J Neurosci *19*, 4449-4461.

Belachew, S., and Gallo, V. (2004). Synaptic and extrasynaptic neurotransmitter receptors in glial precursors' quest for identity. Glia *48*, 185-196.

Bernardos, R.L., Barthel, L.K., Meyers, J.R., and Raymond, P.A. (2007). Late-stage neuronal progenitors in the retina are radial Muller glia that function as retinal stem cells. J Neurosci *27*, 7028-7040.

Ben-Ari, Y. (2002). Excitatory actions of gaba during development: the nature of the nurture. Nat Rev Neurosci 3, 728-739.

Bezzi, P., Carmignoto, G., Pasti, L., Vesce, S., Rossi, D., Rizzini, B.L., Pozzan, T., and Volterra, A. (1998). Prostaglandins stimulate calcium-dependent glutamate release in astrocytes. Nature 391, 281-285.

Bhattacharjee, J., and Sanyal, S. (1975). Developmental origin and early differentiation of retinal Muller cells in mice. J Anat *120*, 367-372.

Birgbauer, E., Cowan, C.A., Sretavan, D.W., and Henkemeyer, M. (2000). Kinase independent function of EphB receptors in retinal axon pathfinding to the optic disc from dorsal but not ventral retina. Development *127*, 1231-1241.

Birgbauer, E., Oster, S.F., Severin, C.G., and Sretavan, D.W. (2001). Retinal axon growth cones respond to EphB extracellular domains as inhibitory axon guidance cues. Development *128*, 3041-3048.

Bloss, E.B., and Hunter, R.G. (2010). Hippocampal kainate receptors. Vitam Horm *82*, 167-184.

Bogaert, E., d'Ydewalle, C., and Van Den Bosch, L. (2010). Amyotrophic lateral sclerosis and excitotoxicity: from pathological mechanism to therapeutic target. CNS Neurol Disord Drug Targets *9*, 297-304.

Bortolotto, Z.A., Clarke, V.R., Delany, C.M., Parry, M.C., Smolders, I., Vignes, M., Ho, K.H., Miu, P., Brinton, B.T., Fantaske, R., *et al.* (1999). Kainate receptors are involved in synaptic plasticity. Nature *402*, 297-301.

Brandstatter, J.H., Koulen, P., and Wassle, H. (1998). Diversity of glutamate receptors in the mammalian retina. Vision Res 38, 1385-1397.

Bringmann, A., Pannicke, T., Grosche, J., Francke, M., Wiedemann, P., Skatchkov, S.N., Osborne, N.N., and Reichenbach, A. (2006). Muller cells in the healthy and diseased retina. Prog Retin Eye Res *25*, 397-424.

Brittis, P.A., and Silver, J. (1994). EXOGENOUS GLYCOSAMINOGLYCANS INDUCE COMPLETE INVERSION OF RETINAL GANGLION-CELL BODIES AND THEIR AXONS WITHIN THE RETINAL NEUROEPITHELIUM. Proceedings of the National Academy of Sciences of the United States of America *91*, 7539-7542.

Brusa, R., Zimmermann, F., Koh, D.S., Feldmeyer, D., Gass, P., Seeburg, P.H., and Sprengel, R. (1995). Early-onset epilepsy and postnatal lethality associated with an editing-deficient GluR-B allele in mice. Science *270*, 1677-1680.

Chan, S.O., and Chung, K.Y. (1999). Changes in axon arrangement in the retinofugal [correction of retinofungal] pathway of mouse embryos: confocal microscopy study using single- and double-dye label. J Comp Neurol 406, 251-262.

Chan, S.O., Cheung, W.S., and Lin, L. (2002). Differential responses of temporal and nasal retinal neurites to regional-specific cues in the mouse retinofugal pathway. Cell Tissue Res *309*, 201-208.

Chan, S.O., Wong, K.F., Chung, K.Y., and Yung, W.H. (1998). Changes in morphology and behaviour of retinal growth cones before and after crossing the midline of the mouse chiasm - a confocal microscopy study. Eur J Neurosci *10*, 2511-2522.

Chang, S., and De Camilli, P. (2001). Glutamate regulates actin-based motility in axonal filopodia. Nat Neurosci *4*, 787-793.

Chang, Y.C., and Chiao, C.C. (2008). Localization and functional mapping of AMPA receptor subunits in the developing rabbit retina. Invest Ophthalmol Vis Sci 49, 5619-5628.

Chen, S., and Diamond, J.S. (2002). Synaptically released glutamate activates extrasynaptic NMDA receptors on cells in the ganglion cell layer of rat retina. J Neurosci 22, 2165-2173.

Chew, L.J., Fleck, M.W., Wright, P., Scherer, S.E., Mayer, M.L., and Gallo, V. (1997). Growth factor-induced transcription of GluR1 increases functional AMPA receptor density in glial progenitor cells. J Neurosci 17, 227-240.

Chiu, S.Y., and Kriegler, S. (1994). Neurotransmitter-mediated signaling between axons and glial cells. Glia 11, 191-200.

Clements, J.D., Lester, R.A., Tong, G., Jahr, C.E., and Westbrook, G.L. (1992). The time course of glutamate in the synaptic cleft. Science *258*, 1498-1501.

Cohen-Cory, S. (2002). The developing synapse: construction and modulation of synaptic structures and circuits. Science *298*, 770-776.

Colello, R.J., and Guillery, R.W. (1990). The early development of retinal ganglion cells with uncrossed axons in the mouse: retinal position and axonal course. Development *108*, 515-523.

Collingridge, G.L., Olsen, R.W., Peters, J., and Spedding, M. (2009). A nomenclature for ligand-gated ion channels. Neuropharmacology *56*, 2-5.

Craig, A.M., Blackstone, C.D., Huganir, R.L., and Banker, G. (1993). The distribution of glutamate receptors in cultured rat hippocampal neurons: postsynaptic clustering of AMPA-selective subunits. Neuron *10*, 1055-1068.

Cull-Candy, S., Brickley, S., and Farrant, M. (2001). NMDA receptor subunits: diversity, development and disease. Curr Opin Neurobiol 11, 327-335.

De Cesare, D., and Sassone-Corsi, P. (2000). Transcriptional regulation by cyclic AMP-responsive factors. Prog Nucleic Acid Res Mol Biol 64, 343-369.

Deisseroth, K., Singla, S., Toda, H., Monje, M., Palmer, T.D., and Malenka, R.C. (2004). Excitation-neurogenesis coupling in adult neural stem/progenitor cells. Neuron 42, 535-552.

Demarque, M., Represa, A., Becq, H., Khalilov, I., Ben-Ari, Y., and Aniksztejn, L. (2002). Paracrine intercellular communication by a Ca2+- and SNARE-independent release of GABA and glutamate prior to synapse formation. Neuron 36, 1051-1061.

De Paola, V., Arber, S., and Caroni, P. (2003). AMPA receptors regulate dynamic equilibrium of presynaptic terminals in mature hippocampal networks. Nat Neurosci *6*, 491-500.

Dingledine, R., Borges, K., Bowie, D., and Traynelis, S.F. (1999). The glutamate receptor ion channels. Pharmacol Rev *51*, 7-61.

Dumitrescu, O.N., Protti, D.A., Majumdar, S., Zeilhofer, H.U., and Wassle, H. (2006). Ionotropic glutamate receptors of amacrine cells of the mouse retina. Vis Neurosci 23, 79-90.
Durand, G.M., and Zukin, R.S. (1993). Developmental regulation of mRNAs encoding rat brain kainate/AMPA receptors: a northern analysis study. J Neurochem 61, 2239-2246.

Eun, S.Y., Hong, Y.H., Kim, E.H., Jeon, H., Suh, Y.H., Lee, J.E., Jo, C., Jo, S.A., and Kim, J. (2004). Glutamate receptor-mediated regulation of c-fos expression in cultured microglia. Biochem Biophys Res Commun 325, 320-327.

Feldmeyer, D., Kask, K., Brusa, R., Kornau, H.C., Kolhekar, R., Rozov, A., Burnashev, N., Jensen, V., Hvalby, O., Sprengel, R., *et al.* (1999). Neurological dysfunctions in mice expressing different levels of the Q/R site-unedited AMPAR subunit GluR-B. Nat Neurosci *2*, 57-64.

Fisahn, A., Contractor, A., Traub, R.D., Buhl, E.H., Heinemann, S.F., and McBain, C.J. (2004). Distinct roles for the kainate receptor subunits GluR5 and GluR6 in kainate-induced hippocampal gamma oscillations. J Neurosci *24*, 9658-9668.

Frerking, M., and Nicoll, R.A. (2000). Synaptic kainate receptors. Curr Opin Neurobiol *10*, 342-351.

Gallo, V., and Ghiani, C.A. (2000). Glutamate receptors in glia: new cells, new inputs and new functions. Trends Pharmacol Sci 21, 252-258.

Gallo, V., Pende, M., Scherer, S., Molne, M., and Wright, P. (1995). Expression and regulation of kainate and AMPA receptors in uncommitted and committed neural progenitors. Neurochem Res 20, 549-560.

Gallo, V., and Russell, J.T. (1995). Excitatory amino acid receptors in glia: different subtypes for distinct functions? J Neurosci Res 42, 1-8.

Gao, X.B., and van den Pol, A.N. (2000). GABA release from mouse axonal growth cones. J Physiol 523 Pt 3, 629-637.

Geiger, J.R., Melcher, T., Koh, D.S., Sakmann, B., Seeburg, P.H., Jonas, P., and Monyer, H. (1995). Relative abundance of subunit mRNAs determines gating and Ca2+ permeability of AMPA receptors in principal neurons and interneurons in rat CNS. Neuron 15, 193-204.

Goldberg, J.L., Vargas, M.E., Wang, J.T., Mandemakers, W., Oster, S.F., Sretavan, D.W., and Barres, B.A. (2004). An oligodendrocyte lineage-specific semaphorin, Sema5A, inhibits axon growth by retinal ganglion cells. J Neurosci *24*, 4989-4999.

Gomez, T.M., and Zheng, J.Q. (2006). The molecular basis for calcium-dependent axon pathfinding. Nat Rev Neurosci 7, 115-125.

Grunder, T., Kohler, K., Kaletta, A., and Guenther, E. (2000). The distribution and developmental regulation of NMDA receptor subunit proteins in the outer and inner retina of the rat. J Neurobiol *44*, 333-342.

Gudehithlu, K.P., Neff, N.H., and Hadjiconstantinou, M. (1993). c-fos and NGFI-A mRNA of rat retina: evidence for light-induced augmentation and a role for cholinergic and glutamate receptors. Brain Res 631, 77-82.

Guillery, R.W., and Walsh, C. (1987). Changing glial organization relates to changing fiber order in the developing optic nerve of ferrets. J Comp Neurol *265*, 203-217.

Haberecht, M.F., Mitchell, C.K., Lo, G.J., and Redburn, D.A. (1997). N-methyl-D-aspartate-mediated glutamate toxicity in the developing rabbit retina. J Neurosci Res 47, 416-426.

Haberecht, M.F., and Redburn, D.A. (1996). High levels of extracellular glutamate are present in retina during neonatal development. Neurochem Res 21, 285-291.

Hamassaki-Britto, D.E., Hermans-Borgmeyer, I., Heinemann, S., and Hughes, T.E. (1993). Expression of glutamate receptor genes in the mammalian retina: the localization of GluR1 through GluR7 mRNAs. J Neurosci 13, 1888-1898.

Hartmann, B., Ahmadi, S., Heppenstall, P.A., Lewin, G.R., Schott, C., Borchardt, T., Seeburg, P.H., Zeilhofer, H.U., Sprengel, R., and Kuner, R. (2004). The AMPA receptor subunits GluR-A and GluR-B reciprocally modulate spinal synaptic plasticity and inflammatory pain. Neuron *44*, 637-650.

Herrmann, K. (1996). Differential distribution of AMPA receptors and glutamate during pre- and postnatal development in the visual cortex of ferrets. J Comp Neurol *375*, 1-17.

Hestrin, S. (1992). Activation and desensitization of glutamate-activated channels mediating fast excitatory synaptic currents in the visual cortex. Neuron *9*, 991-999.

Higuchi, M., Maas, S., Single, F.N., Hartner, J., Rozov, A., Burnashev, N., Feldmeyer, D., Sprengel, R., and Seeburg, P.H. (2000). Point mutation in an AMPA receptor gene rescues lethality in mice deficient in the RNA-editing enzyme ADAR2. Nature *406*, 78-81.

Hollmann, M., Hartley, M., and Heinemann, S. (1991). Ca2+ permeability of KA-AMPA--gated glutamate receptor channels depends on subunit composition. Science *252*, 851-853.

Hollmann, M., and Heinemann, S. (1994). Cloned glutamate receptors. Annu Rev Neurosci *17*, 31-108.

Hynd, M.R., Scott, H.L., and Dodd, P.R. (2004). Glutamate-mediated excitotoxicity and neurodegeneration in Alzheimer's disease. Neurochem Int *45*, 583-595.

Ibarretxe, G., Perrais, D., Jaskolski, F., Vimeney, A., and Mulle, C. (2007). Fast regulation of axonal growth cone motility by electrical activity. J Neurosci *27*, 7684-7695.

Isaac, J.T., Ashby, M., and McBain, C.J. (2007). The role of the GluR2 subunit in AMPA receptor function and synaptic plasticity. Neuron *54*, 859-871.

Isaac, J.T., Mellor, J., Hurtado, D., and Roche, K.W. (2004). Kainate receptor trafficking: physiological roles and molecular mechanisms. Pharmacol Ther *104*, 163-172.

Jakobs, T.C., Ben, Y., and Masland, R.H. (2007). Expression of mRNA for glutamate receptor subunits distinguishes the major classes of retinal neurons, but is less specific for individual cell types. Mol Vis *13*, 933-948.

Jane, D.E., Lodge, D., and Collingridge, G.L. (2009). Kainate receptors: pharmacology, function and therapeutic potential. Neuropharmacology *56*, 90-113.

Jeffery, G., and Erskine, L. (2005). Variations in the architecture and development of the vertebrate optic chiasm. Prog Retin Eye Res 24, 721-753.

Jonas, P., and Spruston, N. (1994). Mechanisms shaping glutamate-mediated excitatory postsynaptic currents in the CNS. Curr Opin Neurobiol 4, 366-372.

Kater, S.B., and Lipton, S.A. (1995). Neurotransmitter regulation of neuronal outgrowth, plasticity and survival in the year 2001. Trends Neurosci 18, 71-72.

Kidd, F.L., and Isaac, J.T. (1999). Developmental and activity-dependent regulation of kainate receptors at thalamocortical synapses. Nature *400*, 569-573.

Komuro, H., and Rakic, P. (1993). Modulation of neuronal migration by NMDA receptors. Science *260*, 95-97.

Kumar, S.S., Bacci, A., Kharazia, V., and Huguenard, J.R. (2002). A developmental switch of AMPA receptor subunits in neocortical pyramidal neurons. J Neurosci *22*, 3005-3015.

Lazzaro, J.T., Paternain, A.V., Lerma, J., Chenard, B.L., Ewing, F.E., Huang, J., Welch, W.M., Ganong, A.H., and Menniti, F.S. (2002). Functional characterization of CP-465,022, a selective, noncompetitive AMPA receptor antagonist. Neuropharmacology *42*, 143-153.

Lerma, J. (2003). Roles and rules of kainate receptors in synaptic transmission. Nat Rev Neurosci *4*, 481-495.

Lerma, J., Paternain, A.V., Rodriguez-Moreno, A., and Lopez-Garcia, J.C. (2001). Molecular physiology of kainate receptors. Physiol Rev *81*, 971-998.

Leung, K.M., Margolis, R.U., and Chan, S.O. (2004). Expression of phosphacan and neurocan during early development of mouse retinofugal pathway. Brain Res Dev Brain Res *152*, 1-10.

Lin, L., and Chan, S.O. (2003). Perturbation of CD44 function affects chiasmatic routing of retinal axons in brain slice preparations of the mouse retinofugal pathway. Eur J Neurosci *17*, 2299-2312.

Liu, H.N., Larocca, J.N., and Almazan, G. (1999). Molecular pathways mediating activation by kainate of mitogen-activated protein kinase in oligodendrocyte progenitors. Brain Res Mol Brain Res 66, 50-61.

Liu, L.O., Laabich, A., Hardison, A., and Cooper, N.G. (2001). Expression of ionotropic glutamate receptors in the retina of the rdta transgenic mouse. BMC Neurosci *2*, 7.

Livesey, F.J., and Hunt, S.P. (1997). Netrin and netrin receptor expression in the embryonic mammalian nervous system suggests roles in retinal, striatal, nigral, and cerebellar development. Mol Cell Neurosci *8*, 417-429.

LoTurco, J.J., Owens, D.F., Heath, M.J., Davis, M.B., and Kriegstein, A.R. (1995). GABA and glutamate depolarize cortical progenitor cells and inhibit DNA synthesis. Neuron *15*, 1287-1298.

Lujan, R., Shigemoto, R., and Lopez-Bendito, G. (2005). Glutamate and GABA receptor signalling in the developing brain. Neuroscience 130, 567-580.

Mack, K.J., Kriegler, S., Chang, S., and Chiu, S.Y. (1994). Transcription factor expression is induced by axonal stimulation and glutamate in the glia of the developing optic nerve. Brain Res Mol Brain Res 23, 73-80.

Marcus, R.C., Blazeski, R., Godement, P., and Mason, C.A. (1995). Retinal axon divergence in the optic chiasm: uncrossed axons diverge from crossed axons within a midline glial specialization. J Neurosci *15*, 3716-3729.

Marcus, R.C., and Mason, C.A. (1995). The first retinal axon growth in the mouse optic chiasm: axon patterning and the cellular environment. J Neurosci *15*, 6389-6402.

Maric, D., Liu, Q.Y., Grant, G.M., Andreadis, J.D., Hu, Q., Chang, Y.H., Barker, J.L., Joseph, J., Stenger, D.A., and Ma, W. (2000). Functional ionotropic glutamate receptors emerge during terminal cell division and early neuronal differentiation of rat neuroepithelial cells. J Neurosci Res 61, 652-662.

Marquardt, T., Ashery-Padan, R., Andrejewski, N., Scardigli, R., Guillemot, F., and Gruss, P. (2001). Pax6 is required for the multipotent state of retinal progenitor cells. Cell 105, 43-55.

Martin, L.J., Blackstone, C.D., Levey, A.I., Huganir, R.L., and Price, D.L. (1993). Cellular localizations of AMPA glutamate receptors within the basal forebrain magnocellular complex of rat and monkey. J Neurosci *13*, 2249-2263.

Martin, L.J., Furuta, A., and Blackstone, C.D. (1998). AMPA receptor protein in developing rat brain: glutamate receptor-1 expression and localization change at regional, cellular, and subcellular levels with maturation. Neuroscience *83*, 917-928.

Martins, R.A., Linden, R., and Dyer, M.A. (2006). Glutamate regulates retinal progenitors cells proliferation during development. Eur J Neurosci 24, 969-980.

Mason, C.A., and Sretavan, D.W. (1997). Glia, neurons, and axon pathfinding during optic chiasm development. Curr Opin Neurobiol 7, 647-653.

Massey, S.C., and Miller, R.F. (1988). Glutamate receptors of ganglion cells in the rabbit retina: evidence for glutamate as a bipolar cell transmitter. J Physiol *405*, 635-655.

Matsugami, T.R., Tanemura, K., Mieda, M., Nakatomi, R., Yamada, K., Kondo, T., Ogawa, M., Obata, K., Watanabe, M., Hashikawa, T., *et al.* (2006). From the Cover: Indispensability of the glutamate transporters GLAST and GLT1 to brain development. Proc Natl Acad Sci U S A *103*, 12161-12166.

Mattson, M.P., Dou, P., and Kater, S.B. (1988). Outgrowth-regulating actions of glutamate in isolated hippocampal pyramidal neurons. J Neurosci *8*, 2087-2100.

Mayer, M.L. (2006). Glutamate receptors at atomic resolution. Nature 440, 456-462.

McKinney, R.A., Luthi, A., Bandtlow, C.E., Gahwiler, B.H., and Thompson, S.M. (1999). Selective glutamate receptor antagonists can induce or prevent axonal sprouting in rat hippocampal slice cultures. Proc Natl Acad Sci U S A *96*, 11631-11636.

McKinnon, R.D., Matsui, T., Dubois-Dalcq, M., and Aaronson, S.A. (1990). FGF modulates the PDGF-driven pathway of oligodendrocyte development. Neuron 5, 603-614.

Metin, C., Denizot, J.P., and Ropert, N. (2000). Intermediate zone cells express calcium-permeable AMPA receptors and establish close contact with growing axons. J Neurosci *20*, 696-708.

Miller, R.F. (2008). Cell communication mechanisms in the vertebrate retina the proctor lecture. Invest Ophthalmol Vis Sci 49, 5184-5198.

Monyer, H., Seeburg, P.H., and Wisden, W. (1991). Glutamate-operated channels: developmentally early and mature forms arise by alternative splicing. Neuron *6*, 799-810.

Morgan, J.I., and Curran, T. (1988). Calcium as a modulator of the immediate-early gene cascade in neurons. Cell Calcium 9, 303-311.

Muller, F., Greferath, U., Wassle, H., Wisden, W., and Seeburg, P. (1992). Glutamate receptor expression in the rat retina. Neurosci Lett *138*, 179-182.

Nichol, K.A., Schulz, M.W., and Bennett, M.R. (1995). Nitric oxide-mediated death of cultured neonatal retinal ganglion cells: neuroprotective properties of glutamate and chondroitin sulfate proteoglycan. Brain Res 697, 1-16.

Niclou, S.P., Jia, L., and Raper, J.A. (2000). Slit2 is a repellent for retinal ganglion cell axons. J Neurosci 20, 4962-4974.

Nguyen, L., Rigo, J.M., Rocher, V., Belachew, S., Malgrange, B., Rogister, B., Leprince, P., and Moonen, G. (2001). Neurotransmitters as early signals for central nervous system development. Cell Tissue Res 305, 187-202.

Noctor, S.C., Flint, A.C., Weissman, T.A., Wong, W.S., Clinton, B.K., and Kriegstein, A.R. (2002). Dividing precursor cells of the embryonic cortical ventricular zone have morphological and molecular characteristics of radial glia. J Neurosci *22*, 3161-3173.

Oster, S.F., Bodeker, M.O., He, F., and Sretavan, D.W. (2003). Invariant Sema5A inhibition serves an ensheathing function during optic nerve development. Development *130*, 775-784.

Park, Y., Jo, J., Isaac, J.T., and Cho, K. (2006). Long-term depression of kainate receptor-mediated synaptic transmission. Neuron *49*, 95-106.

Paternain, A.V., Morales, M., and Lerma, J. (1995). Selective antagonism of AMPA receptors unmasks kainate receptor-mediated responses in hippocampal neurons. Neuron *14*, 185-189.

Pearce, I.A., Cambray-Deakin, M.A., and Burgoyne, R.D. (1987). Glutamate acting on NMDA receptors stimulates neurite outgrowth from cerebellar granule cells. FEBS Lett *223*, 143-147.

Pellegrini-Giampietro, D.E., Bennett, M.V., and Zukin, R.S. (1991). Differential expression of three glutamate receptor genes in developing rat brain: an in situ hybridization study. Proc Natl Acad Sci U S A 88, 4157-4161.

Pende, M., Fisher, T.L., Simpson, P.B., Russell, J.T., Blenis, J., and Gallo, V. (1997). Neurotransmitter- and growth factor-induced cAMP response element binding protein

phosphorylation in glial cell progenitors: role of calcium ions, protein kinase C, and mitogen-activated protein kinase/ribosomal S6 kinase pathway. J Neurosci 17, 1291-1301.

Petralia, R.S., and Wenthold, R.J. (1992). Light and electron immunocytochemical localization of AMPA-selective glutamate receptors in the rat brain. J Comp Neurol *318*, 329-354.

Pickard, L., Noel, J., Henley, J.M., Collingridge, G.L., and Molnar, E. (2000). Developmental changes in synaptic AMPA and NMDA receptor distribution and AMPA receptor subunit composition in living hippocampal neurons. J Neurosci *20*, 7922-7931.

Pinheiro, P., and Mulle, C. (2006). Kainate receptors. Cell Tissue Res *326*, 457-482.

Plachez, C., Andrews, W., Liapi, A., Knoell, B., Drescher, U., Mankoo, B., Zhe, L., Mambetisaeva, E., Annan, A., Bannister, L., *et al.* (2008). Robos are required for the correct targeting of retinal ganglion cell axons in the visual pathway of the brain. Mol Cell Neurosci *37*, 719-730.

Rakic, P. (1972). Mode of cell migration to the superficial layers of fetal monkey neocortex. J Comp Neurol *145*, 61-83.

Rakic, P., and Komuro, H. (1995). The role of receptor/channel activity in neuronal cell migration. J Neurobiol 26, 299-315.

Rasband, K., Hardy, M., and Chien, C.B. (2003). Generating X: formation of the optic chiasm. Neuron 39, 885-888.

Reese, B.E., Maynard, T.M., and Hocking, D.R. (1994). Glial domains and axonal reordering in the chiasmatic region of the developing ferret. J Comp Neurol *349*, 303-324.

Ren, Z., Riley, N.J., Garcia, E.P., Sanders, J.M., Swanson, G.T., and Marshall, J. (2003a). Multiple trafficking signals regulate kainate receptor KA2 subunit surface expression. J Neurosci *23*, 6608-6616.

Ren, Z., Riley, N.J., Needleman, L.A., Sanders, J.M., Swanson, G.T., and Marshall, J. (2003b). Cell surface expression of GluR5 kainate receptors is regulated by an endoplasmic reticulum retention signal. J Biol Chem *278*, 52700-52709.

Ringstedt, T., Braisted, J.E., Brose, K., Kidd, T., Goodman, C., Tessier-Lavigne, M., and O'Leary, D.D. (2000). Slit inhibition of retinal axon growth and its role in retinal axon pathfinding and innervation patterns in the diencephalon. J Neurosci 20, 4983-4991.

Robles, E., Huttenlocher, A., and Gomez, T.M. (2003). Filopodial calcium transients regulate growth cone motility and guidance through local activation of calpain. Neuron 38, 597-609.

Rorig, B., and Grantyn, R. (1994). Ligand- and voltage-gated ion channels are expressed by embryonic mouse retinal neurones. Neuroreport 5, 1197-1200.

Rosenmund, C., Stern-Bach, Y., and Stevens, C.F. (1998). The tetrameric structure of a glutamate receptor channel. Science *280*, 1596-1599.

Schenk, U., Verderio, C., Benfenati, F., and Matteoli, M. (2003). Regulated delivery of AMPA receptor subunits to the presynaptic membrane. EMBO J *22*, 558-568.

Schmitz, Y., Luccarelli, J., Kim, M., Wang, M., and Sulzer, D. (2009). Glutamate controls growth rate and branching of dopaminergic axons. J Neurosci *29*, 11973-11981.

Schulte, D., Furukawa, T., Peters, M.A., Kozak, C.A., and Cepko, C.L. (1999). Misexpression of the Emx-related homeobox genes cVax and mVax2 ventralizes the retina and perturbs the retinotectal map. Neuron 24, 541-553.

Shewan, D., Dwivedy, A., Anderson, R., and Holt, C.E. (2002). Age-related changes underlie switch in netrin-1 responsiveness as growth cones advance along visual pathway. Nat Neurosci 5, 955-962.

Shimshek, D.R., Bus, T., Grinevich, V., Single, F.N., Mack, V., Sprengel, R., Spergel, D.J., and Seeburg, P.H. (2006a). Impaired reproductive behavior by lack of GluR-B containing AMPA receptors but not of NMDA receptors in hypothalamic and septal neurons. Mol Endocrinol *20*, 219-231.

Shimshek, D.R., Jensen, V., Celikel, T., Geng, Y., Schupp, B., Bus, T., Mack, V., Marx, V., Hvalby, O., Seeburg, P.H., *et al.* (2006b). Forebrain-specific glutamate receptor B deletion impairs spatial memory but not hippocampal field long-term potentiation. J Neurosci *26*, 8428-8440.

Soeda, H., Tatsumi, H., and Katayama, Y. (1997). Neurotransmitter release from growth cones of rat dorsal root ganglion neurons in culture. Neuroscience *77*, 1187-1199.

Sonnenberg, J.L., Mitchelmore, C., Macgregor-Leon, P.F., Hempstead, J., Morgan, J.I., and Curran, T. (1989). Glutamate receptor agonists increase the expression of Fos, Fra, and AP-1 DNA binding activity in the mammalian brain. J Neurosci Res 24, 72-80.

Sretavan, D.W. (1990). Specific routing of retinal ganglion cell axons at the mammalian optic chiasm during embryonic development. J Neurosci *10*, 1995-2007.

Sretavan, D.W., Feng, L., Pure, E., and Reichardt, L.F. (1994). Embryonic neurons of the developing optic chiasm express L1 and CD44, cell surface molecules with opposing effects on retinal axon growth. Neuron *12*, 957-975.

Sretavan, D.W., Pure, E., Siegel, M.W., and Reichardt, L.F. (1995). Disruption of retinal axon ingrowth by ablation of embryonic mouse optic chiasm neurons. Science *269*, 98-101.

Steinhauser, C., and Gallo, V. (1996). News on glutamate receptors in glial cells. Trends Neurosci 19, 339-345.

Sucher, N.J., Kohler, K., Tenneti, L., Wong, H.K., Grunder, T., Fauser, S., Wheeler-Schilling, T., Nakanishi, N., Lipton, S.A., and Guenther, E. (2003). N-methyl-D-aspartate receptor subunit NR3A in the retina: developmental expression, cellular localization, and functional aspects. Invest Ophthalmol Vis Sci *44*, 4451-4456.

Sugiura, N., Patel, R.G., and Corriveau, R.A. (2001). N-methyl-D-aspartate receptors regulate a group of transiently expressed genes in the developing brain. J Biol Chem 276, 14257-14263.

Tashiro, A., Dunaevsky, A., Blazeski, R., Mason, C.A., and Yuste, R. (2003). Bidirectional regulation of hippocampal mossy fiber filopodial motility by kainate receptors: a two-step model of synaptogenesis. Neuron *38*, 773-784.

Taylor, W.R., Chen, E., and Copenhagen, D.R. (1995). Characterization of spontaneous excitatory synaptic currents in salamander retinal ganglion cells. J Physiol 486 (Pt 1), 207-221.

Thompson, H., Camand, O., Barker, D., and Erskine, L. (2006). Slit proteins regulate distinct aspects of retinal ganglion cell axon guidance within dorsal and ventral retina. J Neurosci *26*, 8082-8091.

Vaughn, J.E. (1989). Fine structure of synaptogenesis in the vertebrate central nervous system. Synapse *3*, 255-285.

Vincent, P., and Mulle, C. (2009). Kainate receptors in epilepsy and excitotoxicity. Neuroscience *158*, 309-323.

Vitanova, L. (2007). AMPA and kainate receptors in turtle retina: an immunocytochemical study. Cell Mol Neurobiol *27*, 407-421.

Wang, J., Chan, C.K., Taylor, J.S., and Chan, S.O. (2008). The growth-inhibitory protein Nogo is involved in midline routing of axons in the mouse optic chiasm. J Neurosci Res *86*, 2581-2590.

Watanabe, M., Mishina, M., and Inoue, Y. (1994). Differential distributions of the NMDA receptor channel subunit mRNAs in the mouse retina. Brain Res 634, 328-332.

Watkins, J.C., and Evans, R.H. (1981). Excitatory amino acid transmitters. Annu Rev Pharmacol Toxicol *21*, 165-204.

Wen, Z., Guirland, C., Ming, G.L., and Zheng, J.Q. (2004). A CaMKII/calcineurin switch controls the direction of Ca(2+)-dependent growth cone guidance. Neuron 43, 835-846.

Wenthold, R.J., Petralia, R.S., Blahos, J., II, and Niedzielski, A.S. (1996). Evidence for multiple AMPA receptor complexes in hippocampal CA1/CA2 neurons. J Neurosci *16*, 1982-1989.

Williams, S.E., Mann, F., Erskine, L., Sakurai, T., Wei, S., Rossi, D.J., Gale, N.W., Holt, C.E., Mason, C.A., and Henkemeyer, M. (2003). Ephrin-B2 and EphB1 mediate retinal axon divergence at the optic chiasm. Neuron 39, 919-935.

Wisden, W., and Seeburg, P.H. (1993a). A complex mosaic of high-affinity kainate receptors in rat brain. J Neurosci *13*, 3582-3598.

Wisden, W., and Seeburg, P.H. (1993b). Mammalian ionotropic glutamate receptors. Curr Opin Neurobiol *3*, 291-298.

Wong, W.T., Faulkner-Jones, B.E., Sanes, J.R., and Wong, R.O. (2000a). Rapid dendritic remodeling in the developing retina: dependence on neurotransmission and reciprocal regulation by Rac and Rho. J Neurosci 20, 5024-5036.

Wong, W.T., Myhr, K.L., Miller, E.D., and Wong, R.O. (2000b). Developmental changes in the neurotransmitter regulation of correlated spontaneous retinal activity. J Neurosci 20, 351-360.

Woo, T.U., Shrestha, K., Amstrong, C., Minns, M.M., Walsh, J.P., and Benes, F.M. (2007). Differential alterations of kainate receptor subunits in inhibitory interneurons in the anterior cingulate cortex in schizophrenia and bipolar disorder. Schizophr Res *96*, 46-61.

Yamada, R.X., Sasaki, T., Ichikawa, J., Koyama, R., Matsuki, N., and Ikegaya, Y. (2008). Long-range axonal calcium sweep induces axon retraction. J Neurosci 28, 4613-4618.

Yaqub, A., Guimaraes, M., and Eldred, W.D. (1995). Neurotransmitter modulation of Fos- and Jun-like proteins in the turtle retina. J Comp Neurol 354, 481-500.

Young, R.W. (1984). Cell death during differentiation of the retina in the mouse. J Comp Neurol 229, 362-373.

Zhang, L.I., and Poo, M.M. (2001). Electrical activity and development of neural circuits. Nat Neurosci 4 Suppl, 1207-1214.

Zhang, C., Hammassaki-Britto, D.E., Britto, L.R., and Duvoisin, R.M. (1996). Expression of glutamate receptor subunit genes during development of the mouse retina. Neuroreport *8*, 335-340.

Zheng, J.Q., Felder, M., Connor, J.A., and Poo, M.M. (1994). Turning of nerve growth cones induced by neurotransmitters. Nature *368*, 140-144.

Zheng, J.Q., Wan, J.J., and Poo, M.M. (1996). Essential role of filopodia in chemotropic turning of nerve growth cone induced by a glutamate gradient. J Neurosci *16*, 1140-1149